Appendix 1

The trachea: The first tissue-engineered organ?

Pierre R. Delaere, MD, PhD,[a] and Dirk Van Raemdonck, MD, PhD[b]

Major medical breakthroughs deserve the necessary press attention to inform the medical community and public of the news. Unfortunately, misrepresentation of medical information can occur and is particularly problematic when members of the professional and public press are misled to believe unrealistic medical breakthroughs.

In 2008 and 2011, 2 revolutionary articles were published in *The Lancet* reporting on regeneration of a tracheal transplant.[1,2] The tracheal transplant procedure used stem cells extracted from the patient's bone marrow in conjunction with a synthetic scaffold to create the artificial organ. In September 2012, an article printed in *The New York Times*, "A First: Organs Tailor-Made With Body's Own Cells,"[3] recognized tracheal regeneration as the first regenerative medicine procedure designed to implant "bioartificial" organs. This achievement was touted as the beginning of complex organ engineering for the heart, liver, and kidneys, and it was suggested that allotransplantation along with immunosuppression might become problems of the past.[3]

Two questions, however, remain: (1) How does a synthetic tube transform into a viable airway tube? (2) Is the trachea really the first bioengineered organ?

REGENERATION VERSUS SECONDARY WOUND HEALING

In reports on bioengineered tracheas, it is frequently stated that the trachea is well suited to tissue engineering because it consists of a hollow, relatively simple structure. In reality, however, the trachea has an ingenious morphology that allows it to fulfill its function (Figure 1, *A*). It is thus one of the most difficult organs of the human body to replace.[4] To date, regeneration within the airway tract is only possible for epithelial defects above the basement membrane. If a tissue injury is severe and involves damage to both epithelial cells and the submucosal layer, healing will be accomplished by secondary intention, leading to stenosis of the airway (Figure 1, *B*). The current challenge for regenerative medicine is to overcome barriers to regeneration of the epithelial lining in full-thickness mucosal defects, which is not yet possible (Figure 1, *C*).

PROSTHETIC VERSUS REGENERATED TRACHEA

Tracheal regeneration for airway repair with bioengineered constructs typically consists of a cartilaginous tube lined with viable respiratory mucosa.[1,2] These constructs are created with bone marrow stem cells and growth factors (of which the clinical value for tissue healing is unknown) that are applied to a nonvascularized scaffold. The mechanism behind the transformation from nonviable construct to viable airway cannot be explained with our current knowledge of tissue healing, tissue transplantation, and tissue regeneration. In fact, cells have never been observed to adhere, grow, and regenerate into complex tissues when applied to an avascular or synthetic scaffold. Moreover, this advanced form of tissue regeneration has never been observed in laboratory-based research.

Of the 14 patients who have received bioengineered tracheas,[5] 3 have been described in case reports in 4 different articles (the first patient was described after both 6-month and 5-year follow-ups).[1,2,6,7] In these articles, 2 different scaffolds (2 cases with an enzymatically decellularized tracheal allotransplant[1,6,7] and 1 case with a synthetic nanocomposite[2]) were reported as being used, along with 2 different techniques of applying bone marrow cells to the scaffold (2 cases with a bioreactor for "ex vivo" use[1,2,7] and 1 case where the bone marrow cells were applied "in vivo"[6]). Production of the bioengineered trachea in all cases produced similar results, and the different approaches worked in comparable ways. Information gathered from published reports on these 3 patients and unpublished reports on an additional 11 patients suggests that mortality and morbidity were very high.[5] More than half of the patients died within a 3-month period, and the patients who survived longer functioned with an airway stent that preserved the airway lumen.

From this information, it can be concluded that the bioengineered tracheal replacements were in fact airway replacements that functioned only as scaffolds, behaving in a similar way to synthetic tracheal prostheses. In recent years, most synthetic materials used for tracheal replacement have been tested in experimental animal research. From these studies, it became clear that definitive prosthetic replacement of the airway wall is not possible.[8] To date, nearly all surgical prostheses that have been successful were observed in potentially sterile

From the Departments of Otolaryngology Head & Neck Surgery[a] and Thoracic Surgery,[b] University Hospital Leuven, Leuven, Belgium.

Disclosures: Authors have nothing to disclose with regard to commercial support.
Received for publication Nov 3, 2013; revisions received Nov 24, 2013; accepted for publication Dec 20, 2013; available ahead of print Feb 4, 2014.

Address for reprints: Pierre R. Delaere, MD, PhD, Department of ENT, Head & Neck Surgery, University Hospital Leuven, Kapucijnenvoer 33, 3000 Leuven, Belgium (E-mail: Pierre.Delaere@uzleuven.be).

J Thorac Cardiovasc Surg 2014;147:1128-32
0022-5223/$36.00

http://dx.doi.org/10.1016/j.jtcvs.2013.12.024

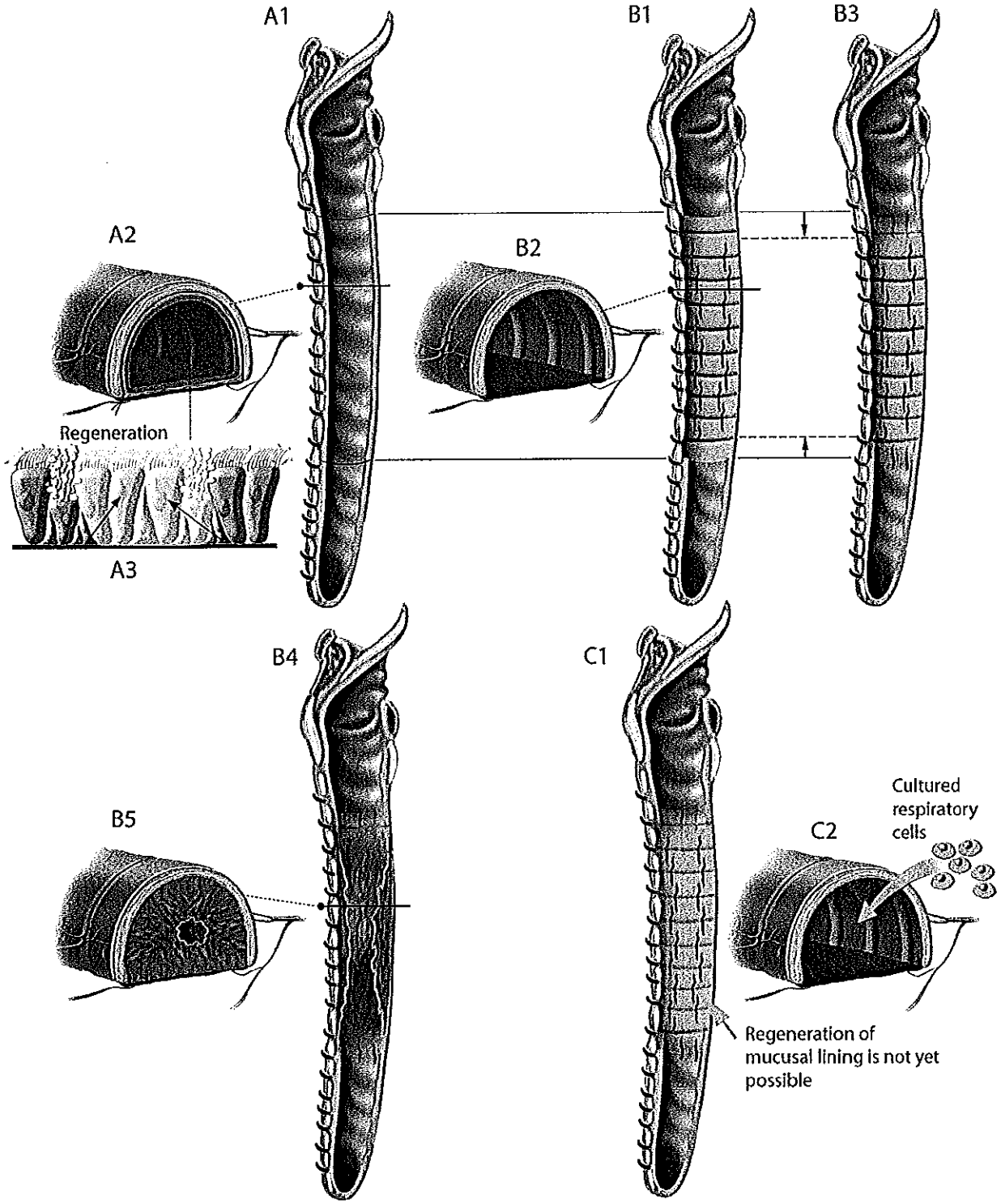

FIGURE 1. Wound healing of a tracheal mucosal defect. A, The trachea has a segmental blood supply that reaches the mucosal lining through the intercartilaginous ligaments and the membranous trachea (A1 and A2). The basement membrane of the mucosal layer supports a pseudostratified epithelium, the surface layer of which is columnar and ciliated, with deeper layers of basal cells. A superficial epithelial wound can heal through regeneration of the surface epithelium (A3). B, The healing pattern of a circumferential full-thickness mucosal defect (B1 and B2) is shown. Healing of full-thickness mucosal wounds combines granulation tissue formation, wound contraction, and reepithelialization from the wound edges (*arrows*). Airway stenosis in the middle part of the denuded segment can develop from circumferential wounds. Healing of anastomotic sites can enable several millimeters of respiratory epithelium to grow into the wound margins (B3) while the remaining tissue between those margins is left as uncovered granular tissue (B4 and B5). C, Research in tracheal tissue engineering should concentrate on attempts to regenerate the mucosal lining by applying epithelial stem cells (C1 and C2) to a tracheal segment with a preserved blood supply and cartilaginous support.

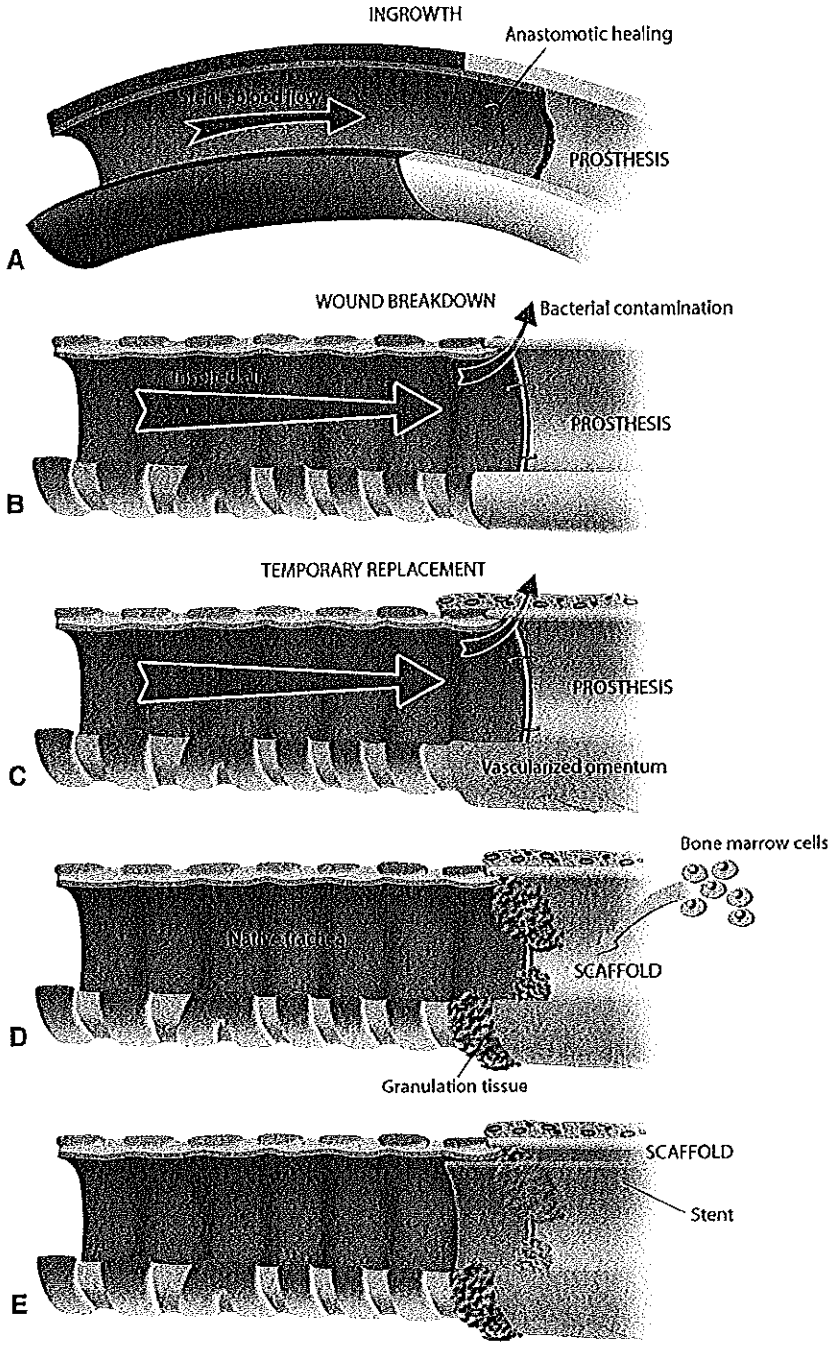

FIGURE 2. Prosthetic versus regenerated trachea A, Blood vessel prosthesis. Endothelialization of the luminal surface of vascular grafts occurs only 1 to 2 cm into the graft from the anastomotic site. These endothelial cells are derived from adjacent, native arterial endothelium, and they enable the anastomosis to heal. B, In the respiratory tract, the flow of inspired air will lead to bacterial contamination and wound breakdown at the anastomoses. The respiratory epithelium will not grow over the prosthesis-airway anastomosis. C, Airway prosthesis wrapped in vascularized tissue. A prosthesis may act as a temporary airway stent when it is wrapped by well-vascularized tissue (eg, omentum). The vascularized tissue around the prosthesis can temporary avoid the complications of wound breakdown at the anastomotic sites. D, A scaffold soaked in bone marrow cells will behave in similarly to a prosthesis. Granulation tissue at the anastomoses will be formed in patients surviving for longer periods. E, A stent can be placed as a temporary airway.

mesenchymal tissues. No example of successful prosthetic repair can be cited in the respiratory, gastrointestinal, or genitourinary tract. The internal site of the airway tract belongs to the outside world, and bacterial contamination at the interface between the airway and prosthesis prevent its ingrowth (Figure 2). The complications of

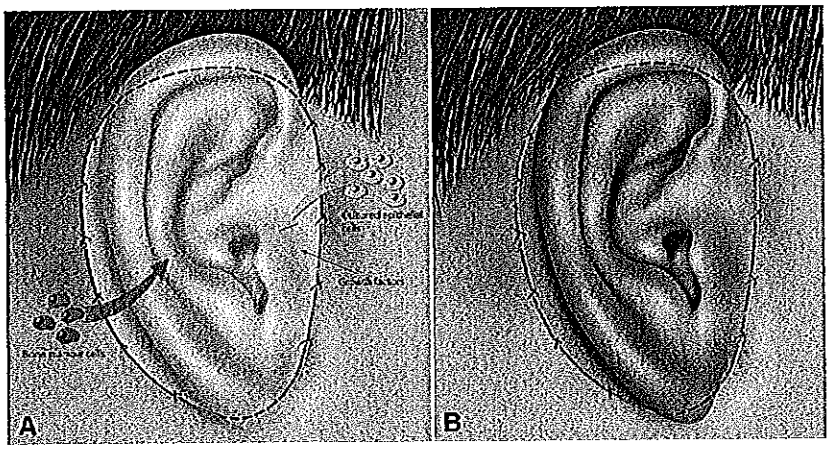

FIGURE 3. Visualization of the bioengineered tissue approach when applied to an external ear (theoretic example). A, The external ear has a comparable tissue composition (cartilage framework and epithelial lining) to the trachea. Here, an enzymatically decellularized allograft treated with bone marrow cells and cultured epithelial cells is attached to a recipient area without restoration of the blood supply. B, Direct visualization of the healing and revascularization of the bioengineered ear should be mandatory to prove (the hypothetical) success of the bioengineering process.

wound breakdown at the anastomoses can be temporarily delayed by wrapping the prosthesis in vascularized tissue, mostly transposed omentum. This is exactly what occurred in nearly all cases of the supposedly bioengineered tracheal replacements. The scaffolds were wrapped in vascularized omentum so that inevitable complications could be delayed. In patients who survive for longer periods, granulation tissue will form at the suture lines, a complication that necessitates placement of a stent to preserve the airway lumen temporarily (Figure 2, *E*).

VISUALIZATION OF BIOENGINEERED TISSUE

It seems contradictory that one of the most difficult organs to replace has been reported as being the first bioengineered organ. How can a synthetic tracheal replacement, destined to fail, be described as a major breakthrough in organ tissue engineering?

The dissemination of misleading information regarding bioengineering of complex tissues would not be possible in tissues that can be directly visualized (Figure 3). For a tracheal replacement, direct visualization of the transplant and subsequent healing is only possible in an experimental setting and during autopsy. Neither of these methods, however, were used to document the tissue-engineered tracheas in the 14 previous patients. Tracheal bioengineering was not tested in animal models, and despite the fact that several patients died after having received the bioengineered tracheal replacement, no postmortem histologic data have been published. Although in vivo visualization of tracheal transplants and their healing process is possible with serial computed tomographic scanning and endoscopic imaging performed at regular intervals after implantation, clear visualization of the transplant is lacking in all reports regarding the bioengineered trachea. Published computed tomographic images and endoscopic views show only images produced shortly after transplantation and either do not allow the clear visualization of the transplant or were obtained with an airway stent in place.[1,2,6,7] In an editorial in *Science* discussing the controversy of this topic,[5] the main scientist behind the bioengineering approach acknowledged that "it was difficult to tell what exactly had happened inside the implanted tracheas," which is remarkable when considering the high-quality computed tomographic scans and endoscopic approaches that are currently available.

The media hype regarding "stem cells" and the work done on an airway that is less accessible for direct visualization are key elements that explain publication of these papers in highly ranked medical journals.[1,2,6,7,9]

In conclusion, the ethical justification of tracheal replacement with a synthetic prosthesis or with a decellularized allograft in humans is questionable, because there are no available experimental data describing a possible successful outcome. The currently available published articles on bioengineered tracheas and the resulting media attention endanger the field of tracheal replacement and the field of tissue engineering as a whole. For patient safety, tracheal bioengineering must be demonstrated as being efficacious and safe before further transplants.

References

1. Macchiarini P, Jungebluth P, Go T, Asnaghi MA, Rees LE, Cogan T, et al. Clinical transplantation of a tissue-engineered airway. *Lancet*. 2008;372:2023-30. Erratum in: Lancet, 2009 Lancet. 2009;373:462.
2. Jungebluth P, Alici E, Baiguera S, Le Blanc K, Blomberg P, Bozóky B, et al. Tracheobronchial transplantation with a stem-cell-seeded bioartificial nanocomposite: a proof-of-concept study. *Lancet*. 2011;379:1997-2004.
3. Fountain H. A first: organs tailor-made with body's own cells. *The New York Times*. September 15, 2012:A1. Available at: http://www.nytimes.com/2012/09/16/health/research/scientists-make-progress-in-tailor-made-organs.html?_r=0. Accessed September 15, 2012.

4. Delaere P, Vranckx J, Verleden G, De Leyn P, Van Raemdonck D, Leuven Tracheal Transplant Group. Tracheal allotransplantation after withdrawal of immunosuppressive therapy. *N Engl J Med*. 2010;362:138-45.
5. Vogel G. Trachea transplants test the limits. *Science*. 2013;340:266-8.
6. Elliott MJ, De Coppi P, Speggiorin S, Roebuck D, Butler CR, Samuel E, et al. Stem-cell-based, tissue engineered tracheal replacement in a child: a 2-year follow-up study. *Lancet*. 2012;380:994-1000.
7. Gonfiotti A, Jaus MO, Barale S, Baiguera S, Comin C, Lavorini F, et al. The first tissue-engineered airway transplantation: 5-year follow-up results. *Lancet*. 2014;383:238-44.
8. Grillo HC. Tracheal replacement: a critical review. *Ann Thorac Surg*. 2002;73: 1995-2004.
9. Jungebluth P, Moll G, Baiguera S, Macchiarini P. Tissue-engineered airway: a regenerative solution. *Clin Pharmacol Ther*. 2012;91:81-93.

performed.[4] Soppa and colleagues might, therefore, achieve even better surgical results using the sutureless technique with significant improvement in patient outcomes.[5]

We fully agree with Dr Soppa that sutureless aortic valve replacement is an ideal option for redo surgery, such as was recently suggested by our preliminary data in this patient subset.[6]

We believe that sutureless aortic valve prostheses have the potential to shorten the surgical time, and future research will determine whether this advantage will also translate into better outcomes in high-risk patients. Sutureless aortic valve replacement has been shown to be associated with improved survival compared with transcatheter aortic valve implantation, owing to the lower or no rates of residual aortic regurgitation. Only randomized prospective studies comparing the 2 surgical techniques will allow definite conclusions to be drawn regarding this issue.

Giuseppe Santarpino, MD
Francesco Pollari, MD
Theodor Fischlein, MD
Department of Cardiac Surgery
Klinikum Nuremberg
Nuremberg, Germany

References

1. Santarpino G, Pfeiffer S, Jessl J, Dell'Aquila AM, Pollari F, Pauschinger M, et al. Sutureless replacement versus transcatheter valve implantation in aortic valve stenosis: a propensity-matched analysis of 2 strategies in high-risk patients. *J Thorac Cardiovasc Surg.* 2014;147:561-7.
2. D'Onofrio A, Messina A, Lorusso R, Alfieri OR, Fusari M, Rubino P, et al. Sutureless aortic valve replacement as an alternative treatment for patients belonging to the "gray zone" between transcatheter aortic valve implantation and conventional surgery: a propensity-matched, multicenter analysis. *J Thorac Cardiovasc Surg.* 2012;144:1010-6.
3. Kodali SK, Williams MR, Smith CR, Svensson LG, Webb JG, Makkar RR, et al. Two-year outcomes after transcatheter or surgical aortic-valve replacement. *N Engl J Med.* 2012;366:1686-95.
4. Santarpino G, Pfeiffer S, Concistré G, Grossmann I, Hinzmann M, Fischlein T. The Perceval S aortic valve has the potential of shortening surgical time: does it also result in improved outcome? *Ann Thorac Surg.* 2013;96:77-81.
5. Ranucci M, Frigiola A, Menicanti L, Castelvecchio S, de Vincentiis C, Pistuddi V. Aortic cross-clamp time, new prostheses, and outcome in aortic valve replacement. *J Heart Valve Dis.* 2012;21:732-9.
6. Santarpino G, Pfeiffer S, Concistrè G, Fischlein T. REDO aortic valve replacement: the sutureless approach. *J Heart Valve Dis.* 2013;22:615-20.

http://dx.doi.org/10.1016/j.jtcvs.2014.03.024

Reply to the Editor:

With all due respect to the clinical competence of Drs Delaere and Van Raemdonck, we would like to address their pointed critique as not only unsubstantiated but also demonstrably false, which is both disturbing and damaging to the field of tracheal transplantation.[1]

The most disturbing comment is "more than half of the patients died within a 3-month period."[1] This is incorrect. Of our first 9 clinical applications using a natural scaffold, only 1 died within the short-term period, and the death was unrelated to the transplantation. A report detailing these cases is under review for publication. We can firmly suggest tissue-engineered tracheal replacement is not "destined to fail" as evidenced by survivors beyond 67 months.[2]

Second, the editorial states "Tracheal bioengineering was not tested in animal models," which is untrue, based on our previous publications. In fact, in 1994, we described the surgical technique for, and revascularization of, tracheal allotransplantations in pigs, published in this Journal.[3] To avoid immunosuppression, several large and small animal models and in vitro airway transplantation studies, not requiring immunosuppression were then completed and published in peer-reviewed journals (the number exceeded the reference limit). All have supported the readiness for ethical clinical application. Additionally, advances in neoangiogenesis, epithelial differentiation, stem cell biology, and systemic and in situ regenerative processes have been reported.[4,5] From this sound preclinical evidence, human airway transplantation has been approved by national and local regulatory bodies in 6 countries, including the US Food and Drug Administration, widely regarded as the world's toughest regulatory body.

Finally, Delaere and Van Raemdonck suggested "dissemination of misinformation" could be avoided with "clear visualization of the trachea." Video endoscopy, high-resolution computed tomography scan images, and photomicrography of the regenerated respiratory epithelium, 5 years after transplantation and without an airway stent in place have, in fact, been published,[2] and whose evidence cannot be disputed.

We value the comments of Delaere and Van Raemdonck and other leaders in this field. We do not expect undisputed acceptance of our approach; however, we would appreciate a certain degree of collegiality and respect for our unceasing efforts to push for an innovative and scientifically sound solution for a vexing clinical problem. The trachea is "one of the most difficult organs in the human body to replace." Rebuilding an identical copy of the native airway might not be possible; however, creating an ideal, nonimmunogenic replacement is. The best strategy for replacement and regeneration has yet to be determined. Tissue-engineered tracheal transplantation is still in its experimental phase, far from routine clinical application, and awaits the results of an ongoing clinical trial (www.clinicaltrials.gov). However, the assertions that our preclinical and translational advances in tracheal transplantation are "misleading and unrealistic" are overreaching, given the extensive published data supporting the cells-to-bioartificial scaffold interactions and documented long-term survival of our own patient series.

Finally, the editorial questions whether the trachea is really the first bioengineered organ. This claim has never been made by us, but rather in

Appendix 2b

a New York Times article describing our work. Dr Anthony Atala has a much better claim to this milestone achievement.

Paolo Macchiarini, MD, PhD
Advanced Center for Translational Regenerative Medicine
Division of Ear, Nose and Throat Department for Clinical Science Intervention and Technology
Karolinska Institutet
Stockholm, Sweden

References

1. Delaere PR, Van Raemdonck D. The trachea: the first tissue-engineered organ? *J Thorac Cardiovasc Surg*. 2014;147:1128-32.
2. Gonfiotti A, Jaus MO, Barale D, Baiguera S, Comin C, Lavorini F, et al. 5-Year follow-up of the first tissue engineered airway transplantation. *Lancet*. 2014;383:238-44.
3. Macchiarini P, Lenot B, de Montpreville V, Dulmet E, Mazmanian GM, Fattal M, et al. Heterotopic pig model for direct revascularization and venous drainage of tracheal allografts. *J Thorac Cardiovasc Surg*. 1994;108:1066-75.
4. Jungebluth P, Bader A, Baiguera S, Möller S, Jaus M, Lim ML, et al. The concept of in vivo airway tissue engineering. *Biomaterials*. 2012;33:4319-26.
5. Jungebluth P, Alici E, Baiguera S, Le Blanck K, Blomberg P, Bozóky B, et al. Tracheobronchial transplantation with a using a stem-cell-seeded bioartificial nanocomposite: a proof-of-concept study. *Lancet*. 2011;378:1997-2004.

http://dx.doi.org/10.1016/j.jtcvs.2014.03.032

Reply to the Editor:

We thank Dr Macchiarini for commenting on our editorial published in the *Journal*, and we acknowledge his team's motivation and efforts to advance tracheal replacement.

In his response to our editorial, Paolo Macchiarini refers to several publications, thus undoubtedly convincing many readers of his views. However, in not one of these articles have mortality rates been published. Furthermore, we cannot follow his suggestion to rely on an unpublished article to obtain this information. Nor indeed can we refer to its content, although we have been in a position to read it. However, the unfortunate results after some of the treatments with "bioengineered" tracheas have reached investigative journalists of *Science*[1] and other media.[2,3]

More important, the purpose of our editorial was to inform the scientific community that regeneration of a viable trachea resulting from applying bone marrow cells to a decellularized or a synthetic scaffold in the absence of any blood supply is based on hope and belief and not on scientific evidence. None of the publications that Macchiarini cites in his response provide scientific evidence for his claims. We therefore strongly warn against further unethical human experimentation. The ongoing clinical trials will show whether or not this warning was justified.

Pierre Delaere, MD, PhD[a]
Dirk Van Raemdonck, MD, PhD[b]
UZ Leuven
[a]*ENT Head and Neck Surgery*
[b]*Thoracic Surgery*
Leuven, Belgium

References

1. Vogel G. Trachea transplants test the limits. *Science*. 2013;340:266-8.
2. Girl dies after groundbreaking trachea transplant. Available at: http://abcnews.go.com/Health/girl-dies-groundbreaking-trachea-transplant/story?id=19604605. Accessed July 8, 2013.
3. Recipient of synthetic trachea dies. Available at: http://articles.baltimoresun.com/2012-03-06/health/bs-hs-trachea-death-20120306_1_cell-research-windpipe-experimental-therapies. Accessed March 6, 2012.

http://dx.doi.org/10.1016/j.jtcvs.2014.03.044

MODIFIABLE RISK FACTORS FOR ACUTE KIDNEY INJURY AFTER CORONARY ARTERY BYPASS GRAFTING

To the Editor:

We read with interest the recent article by Ng and colleagues[1] that identified modifiable risk factors for acute kidney injury (AKI) after coronary artery bypass grafting (CABG) in an Asian population. They showed that preoperative anemia and intraoperative lowest hematocrit were potentially modifiable risk factors independently associated with postoperative AKI. In the design of this study, however, some important data regarding patient perioperative management, such as intraoperative hemodynamic changes, fluid volume, and use of vasoactive medicines, were evidently missing. It has been shown that intraoperative systolic blood pressure decrease relative to baseline is independently associated with postoperative AKI in patients undergoing CABG.[2] Furthermore, the combination of intraoperative hemodilution anemia and hypotension can synergistically act to increase the risk of AKI after cardiac surgery.[3] Campbell and associates[4] have demonstrated that fluid volume before cardiopulmonary bypass can contribute significantly to intraoperative hemodilution anemia and that restricting fluid volume before cardiopulmonary bypass can attenuate intraoperative hemodilution anemia and decrease the need for transfusion in patients undergoing CABG. In addition, perioperative inotropes, vasopressors, antiarrhythmics, and diuretics may also influence development of AKI after cardiac surgery. We therefore argue that optimizing perioperative management, such as intraoperative avoidance of excess fluid volume, hypotension, and renal arterial vasoconstrictive drugs, should be importantly modifiable factors in decreasing the occurrence of postoperative AKI in patients undergoing CABG. We believe that the results of this study would have been more informative had these factors been taken into account.

Ng and colleagues[1] did not mention the specific timing of postoperative creatinine measurements. It was also unclear whether continuous creatinine measurements were performed. It is therefore difficult to determine whether the cases of AKI reported in this study were due to intraoperative or postoperative factors. Although serum creatinine lags behind acute changes in renal function, AKI (defined by serum creatinine >10 mmol/L greater than normal values)

Both epithelial cells and mesenchymal stem cell–derived chondrocytes contribute to the survival of tissue-engineered airway transplants in pigs

Tetsuhiko Go, MD,[a,*] Philipp Jungebluth, MD,[a,*] Silvia Baiguero, PhD,[d] Adelaide Asnaghi, PhD,[e] Jaume Martorell, PhD,[f] Helmut Ostertag, MD, PhD,[g] Sara Mantero, PhD,[e] Martin Birchall, MD, FRCS,[h] Augustinus Bader, PhD,[i] and Paolo Macchiarini, MD, PhD[a,b,c]

Objective: We sought to determine the relative contributions of epithelial cells and mesenchymal stem cell–derived chondrocytes to the survival of tissue-engineered airway transplants in pigs.

Methods: Nonimmunogenic tracheal matrices were obtained by using a detergent-enzymatic method. Major histocompatibility complex–unmatched animals (weighing 65 ± 4 kg) were divided into 4 groups (each n = 5), and 6 cm of their tracheas were orthotopically replaced with decellularized matrix only (group I), decellularized matrix with autologous mesenchymal stem cell–derived chondrocytes externally (group II), decellularized matrix with autologous epithelial cells internally (group III), or decellularized matrix with both cell types (group IV). Autologous cells were recovered, cultured, and expanded. Mesenchymal stem cells were differentiated into chondrocytes by using growth factors. Both cell types were seeded simultaneously with a dual-chamber bioreactor. Animals were not immunosuppressed during the entire study. Biopsy specimens and blood samples were taken from recipients continuously, and animals were observed for a maximum of 60 days.

Results: Matrices were completely covered with both cell types within 72 hours. Survival of the pigs was significantly affected by group ($P < .05$; group I, 11 ± 2 days; group II, 29 ± 4 days; group III, 34 ± 4 days; and group IV, 60 ± 1 days). Cause of death was a combination of airway obstruction and infection (group I), mainly infection (group II), or primarily stenosis (group III). However, pigs in group IV were alive, with no signs of airway collapse or ischemia and healthy epithelium. There were no clinical, immunologic, or histologic signs of rejection despite the lack of immunosuppression.

Conclusions: We confirm the clinical potential of autologous cell– and tissue-engineered tracheal grafts, and suggest that the seeding of both epithelial and mesenchymal stem cell–derived chondrocytes is necessary for optimal graft survival. (J Thorac Cardiovasc Surg 2010;139:437-43)

ET/BS

Long-segment airway stenosis is life-threatening, but present surgical options are not ideal.[1] A tracheal graft suitable for clinical use has to have the biomechanical properties of flexibility, strength to avoid collapse, and formation of airtight seals.[2,3] It should not excite a rejection response and promote cell adhesion and growth, including angiogenesis. Such an ideal construct has proved elusive and difficult to reproduce.[4–7] We recently performed the world's first stem cell–based, fully tissue-engineered tracheal graft, which has been a success to date.[8] However, before we used the graft in human subjects, we evaluated the relative contribution of the autologous biopsy-derived epithelial cells and mesenchymal stem cell (MSC)–derived chondrocytes for the survival of seeded decellularized scaffolds when implanting them orthotopically in pigs. Results are presented here.

MATERIALS AND METHODS

Thirty Yorkshire Duroc pigs (Isoquimen S/L, Barcelona, Spain) weighing 65 ± 4 kg were used. All animals received care in compliance with the "Principles of laboratory animal care" formulated by the National Society for Medical Research and the "Guide for the care and use of laboratory animals" prepared by the Institute of Laboratory Animal Resources, National Research Council, and published by the National Academy Press, revised 1996. This study was approved by the Animal Care and Use Committee and the Bioethics Committee of the University of Barcelona.

From the Departments of General Thoracic Surgery, Hospital Clinic,[a] Institut d'Investigacions Biomèdiques August Pi i Sunyer (IDIBAPS), CIBER Enfermedades Respiratorias,[b] and Universitat de Barcelona,[c] Barcelona, Spain; Pharmaceutical Sciences,[d] University of Padua, Italy; Bioengineering,[e] Politecnico di Milano, Milano, Italy; Immunology,[f] Hospital Clinic, Barcelona, Spain; Pathology,[g] Klinikum Hannover, Hannover, Germany; University College of London Ear Institute,[h] London, United Kingdom; Cell Techniques and Applied Stem Cell Biology,[i] Center of Biotechnology and Biomedicine, University of Leipzig, Leipzig, Germany.

Disclosures: None.

Read at the Eighty-ninth Annual Meeting of The American Association for Thoracic Surgery, Boston, Mass, May 9–13, 2009.

Supported by the Ministerio de Sanidad y Consumo, Instituto de Salud Carlos III, Fondo de Investigación Sanitaria (FIS; PI050987).

* Contributed equally to the work.

Received for publication May 10, 2009; revisions received Sept 14, 2009; accepted for publication Oct 4, 2009; available ahead of print Dec 6, 2009.

Address for reprints: Paolo Macchiarini, MD, PhD, Department of General Thoracic Surgery, Hospital Clinic, University of Barcelona, Villarroel 170, E-08036 Barcelona, Spain (E-mail: pmacchia@ub.edu).

0022-5223/$36.00

doi:10.1016/j.jtcvs.2009.10.002

Abbreviations and Acronyms
DM = decellularized matrix
MHC = major histocompatibility complex
MSC = mesenchymal stem cell
PBS = phosphate-buffered saline

Study Design

The entire trachea (median length, 12 cm) was retrieved from 10 donors. Tracheal matrices were engineered according to our published method.[8–10] Bone marrow–derived MSCs and mucosal epithelial cells were obtained from the intended recipients (n = 20) by means of bone marrow aspiration followed by expansion and differentiation, as previously described, bronchial biopsy, respectively.[8] Recipients were randomly (computer-generated code) divided into 4 groups of 5 animals, and 6 cm of their tracheas was replaced with decellularized matrix (DM) only (group I); DM with external, autologous MSC-derived chondrocytes (group II); DM with internal, autologous epithelial cells (group III); or DM seeded with both cell types (group IV). Biopsy specimens and blood samples were continuously taken from recipients, and animals were observed for a maximum of 60 days. Tracheas were harvested and evaluated postmortem.

Anesthesia: Tracheal Harvesting From Donors and Autologous Cell Isolation From Recipients

Animals (n = 10) were premedicated with azaperone (4 mg/kg administered intramuscularly; Esteve S.A., Barcelona, Spain) and intravenous thiopental injection (10 mg/kg; B. Braun Medical S.A., Rubi, Barcelona, Spain) and relaxed with intravenous vecuronium (Norcuron; 6 mg · kg^{-1} · h^{-1}; Organon S.A., Barcelona, Spain). Orotracheal intubation was obtained with a 7.5F or 8F endotracheal tube. Anesthesia was maintained with fentanyl (1 $\mu g \cdot kg^{-1} \cdot h^{-1}$, B. Braun Medical S.A.) and propofol (3–5 mg · kg^{-1} · h^{-1}, B. Braun Medical S.A.) intravenous infusions. A pulse oximeter (BCI, Inc, Waukesha, Wis) placed at the pig's tail was used to measure the arterial oxygen saturation. For retrieval, a median cervicosternotomy was performed to dissect the trachea in its entirety.[7,8,10] Thereafter, animals were killed with an intravenous bolus of fentanyl, propofol, and potassium chloride (40 mEq; B. Braun, Melsungen, Germany). The entire tracheas were taken (12 cm) and then divided into 2 parts of 6 cm each and stored in a stock solution made of phosphate-buffered saline (PBS; Invitrogen S.A., Barcelona, Spain) containing 1% antibiotic and antimycotic solution (Sigma Chemical Co, Barcelona, Spain). Future graft recipients were anesthetized similarly. Cell populations were obtained by means of a single 80-mL aspiration of bone marrow from the crista iliaca and tracheal endoscopic epithelial biopsy specimens, and maximal attention was paid to isolate cells under completely sterile conditions to avoid cell-culture contamination. After sample harvesting, weaning was induced, and animals were extubated, with time to recover.

Matrix Bioengineering

Matrix bioengineering followed our previously published method.[8–10] Briefly, tracheas were incubated with multiple treatment cycles, including Aqua milliQ (Millipore, Madrid, Spain) storage for 48 hours at 4°C, and then incubated in 4% sodium deoxycholate and 2000 kU DNase-I (Sigma Chemical Co), respectively, for 3 hours. After 17 cycles, which was the previously determined optimum point for loss of antigenicity but preservation of biomechanical strength,[10] samples were examined to check for the absence of intact cells and major histocompatibility complex (MHC) expression. Finally, tracheas were then stored in PBS at 4°C until use.

Autologous Cell Isolation and Culture

MSCs were isolated by purifying the aspirated bone marrow through a previously prepared Percoll (Sigma Chemical Co) gradient (1:9 Percoll/NaCl). Bone marrow was centrifuged at 500*g* (relative centrifugal force) at 4°C, and the thin, bright cell layer was gently removed. Counted cells were seeded at a density of 1.1 × 10^6/mL with complete medium (Dulbecco's modified Eagle's medium containing 1000 mg L-glucose, Sigma-Aldrich), 10% fetal bovine serum (Biological Industries, Beit Haemek, Israel), 100 U/mL penicillin, 100 μg/mL streptomycin, and 2 mmol/L GlutaMax-I (Invitrogen) with 5 ng/mL basic fibroblast growth factor (PeproTech, London, United Kingdom). Cells were used for differentiation, reaching 3 to 4 passages. According to a standard cell-culture protocol, differentiation was induced by adding 10 ng/mL recombinant human transforming growth factor β 3 (R&D Systems, Abingdon, United Kingdom), 10 nmol/L recombinant parathyroid-related peptide (PeproTech), 100 nmol/L dexamethasone, and 10 mg/mL insulin (both Sigma-Aldrich) and incubating for 72 hours. There were no fibroblasts detected before seeding the tracheal matrix.

Epithelial biopsy specimens were incubated with 0.25% trypsin–ethylenediamine tetraacetic acid (Gibco, Prat de Llobregat, Spain) overnight at 4°C and the next morning for 45 minutes at 37°C. The mixture was then neutralized with complete medium (containing fetal bovine serum), and the liquid was removed and transferred to a new tube. Thereafter, liquid was centrifuged at 1000 rpm for 10 minutes, supernatant was removed, and the pellet was resuspended. Obtained cells were then transferred to small flasks and cultured with a specific airway epithelial cell growth medium (PromoCell; Lab S.A., Barcelona, Spain) containing 13 mg/1 mL bovine pituitary extract, 5.0 μg/500 μL human recombinant epidermal growth factor, 250.0 μg/500 μL epinephrine, 250.0 μg/500 μL hydrocortisone, 2.5 mg/500 μL recombinant human insulin, 50.0 ng/500 μL retinoic acid, 5.0 mg/500 μL transferrin, and 3.35 μg/500 μL tri-iodo-L-thyronine in 500 mL. The cell culture was performed according to a standard protocol. However, Hanks buffered salt solution (Sigma) was used when removing cells. Cells were used for seeding at the point at which they reached 4 to 5 passages. Both cell lines were separately seeded on the pre-engineered matrices by using a dedicated, dual-chamber bioreactor. The device provided continuous rotation of the graft, exposing cells to a covering film of alternating gas and liquid phases.

Histology and Immunochemistry

Tracheas were analyzed before transplantation and after harvesting. Samples were washed thoroughly in saline before use. To quantify the remaining cells after each cycle of the detergent-enzymatic method treatment, we analyzed tissues according to our protocol. Briefly, nuclei were visualized with 4′-6-diamidino-2-phenylindole (Vector Laboratories, Inc, Burlingame, Calif), and cell density was determined. Paraffin-embedded tissue sections measuring 5 μm were mounted on slides and stained with hematoxylin and eosin (Merck, Darmstadt, Germany) to evaluate morphologic changes. The presence of MHC markers was evaluated by means of immunostaining with monoclonal anti-MHC class I OX27 and anti-MHC class II OX4 antibodies (Abcam, Cambridge, United Kingdom).

Physical Strain Tests

Bioengineered matrices from each group were tested by using a previously published method[10] based on a tensile-test device (Zwick/Roell, version Z0.5TS; Barcelona, Spain). Each sample was subjected to increasing uniaxial tensile testing until rupture, which was confirmed by the loss of load and the appearance of tears in the tissue. The specimens were clamped into sample holders, a preload (preliminary force) of 2 N was applied, and the trial was started at a constant elongation rate of 1 mm/s at room temperature. The tensile tester recorded the load and elongation to which the tissue was subjected in real time.

Orthotopic Graft Transplantation and Postoperative Observation

The graft transplantation was performed according to our previously described method.[6,7,11] Briefly, after general anesthesia was achieved, recipients' tracheas were exposed through an anterior midline cervical incision.

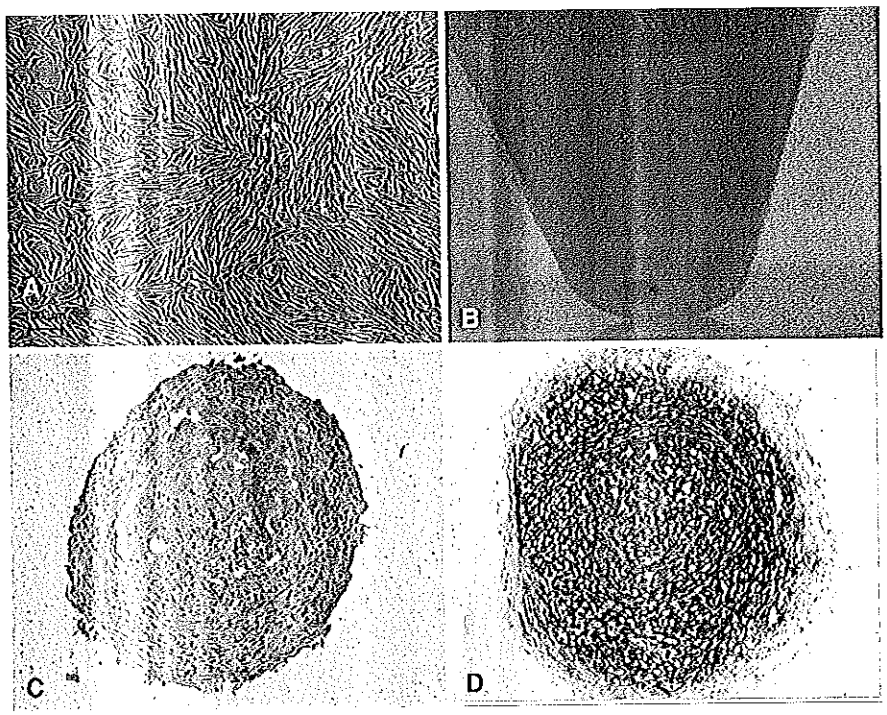

FIGURE 1. A, Mesenchymal stem cells in vitro cultured after isolating with Percoll from bone marrow aspirate. B, Mesenchymal stem cell pellet after centrifugation at 1000 rpm for 5 minutes. Standard method for chondrocyte differentiation: culture cells with 10 ng/mL recombinant human transforming growth factor $\beta 3$. C, Immunohistostaining of mesenchymal stem cells not treated with 10 ng/mL transforming growth factor $\beta 3$ as a negative control. No collagen type II was detected. D, Immunohistostaining for collagen type II detected after 21 days with transforming growth factor $\beta 3$.

Then the sternohyoid muscles were divided and the cervical fat lobe was dissected. We opened the pretracheal fascia, mobilized the intrathoracic trachea, and placed traction sutures to retract it superiorly. The endotracheal tube was pulled back into the subglottic larynx, and 10 to 12 tracheal rings (6 cm) of the recipients' cervical tracheas were excised and replaced with the tissue-engineered graft. At least 2 tracheal rings below the cricoid were left in place to anastomose the tracheal graft. The anastomoses were made with a 4–0 continuous polydiaxone (Ethicon, Inc, Somerville, NJ) parachute sutures of the posterior membranous wall and 5–0 absorbable polygalactin (Vicryl; Ethicon, Inc) interrupted sutures on the anterolateral anastomosis, with knots tied extraluminally. Gas exchange during performance of the anastomoses was through apneic hyperoxygenation. The skin was closed in the usual fashion. Postoperatively, antibiotics (cefazolin, 2 g/d administered intravenously; Lilly, Madrid, Spain) and analgesics (Enantyum [dexketoprofen], 40 mg/12 h; Menarini, Barcelona, Spain) were administered intravenously for the first 7 days. Animals were placed in cages and fed standard laboratory pig food and water ad libitum. They were examined daily for 60 days or until death, if earlier, for clinical signs of inflammation or rejection and for general health. Blood samples were taken weekly to check for the development of antibodies and increased inflammatory response. The presence of bacteria and fungi before and after implantation was determined by means of conventional microbiologic techniques performed on small, fresh tissue biopsy specimens.

Analysis of Tissue From Pig Recipients

Samples were formalin fixed and paraffin embedded before staining with hematoxylin and eosin (Merck). Anti-swine leukocyte antigen antibodies were tested at 7, 15, 23, and 30 days after matrix implantation by using a modification of the standard flow cytometric crossmatch on lymph node cells, as previously described.[10] Briefly, donor pig lymph node cells were incubated for 30 minutes with recipient serum and rinsed 3 times in PBS, and a fluorescein-marked anti-porcine immunoglobulin and phycoerythrin–marked anti-porcine CD3 was added for 30 minutes. A FACS scan (FACS Aria; Becton–Dickinson, Erembodegem, Belgium) was used to evaluate the double fluorescence. The coefficient between the mean channel in test serum in negative control serum for T cells (defined by mentioned double fluorescence) was recorded. We considered a ratio of greater than 2.9 to be positive based on previous samples obtained before implantation. Immunochemistry was performed with a rabbit anti-CD3 antibody (Dako, Glostrup, Denmark) and mouse anti-L1 antibody (Dako), respectively, to identify T lymphocytes, monocytes/macrophages, and polymorphonuclear granulocytes.

Statistical Analysis

Continuous variables were compared by using the independent-samples t test. The odds ratio was calculated to perform comparisons of categorical variables in between groups. Results are presented as the mean ± standard deviation of the mean. SPSS software was used (version 12.0; SPSS, Inc, Chicago, Ill). Statistical significance was accepted at the 5% level.

RESULTS

All bioengineered matrices were negatively stained for both MHC I and II. MSCs could be isolated from bone marrow aspiration and differentiated into chondrocytes (Figure 1). Epithelial cells were easily obtained by means of tracheal biopsy followed by cell culture (Figure 2, *A* and *B*). The bioengineered matrices were seeded through the bioreactor (Figure 2, *D*) to near confluence by 72 hours (Figure 3). There was no evidence of contamination on

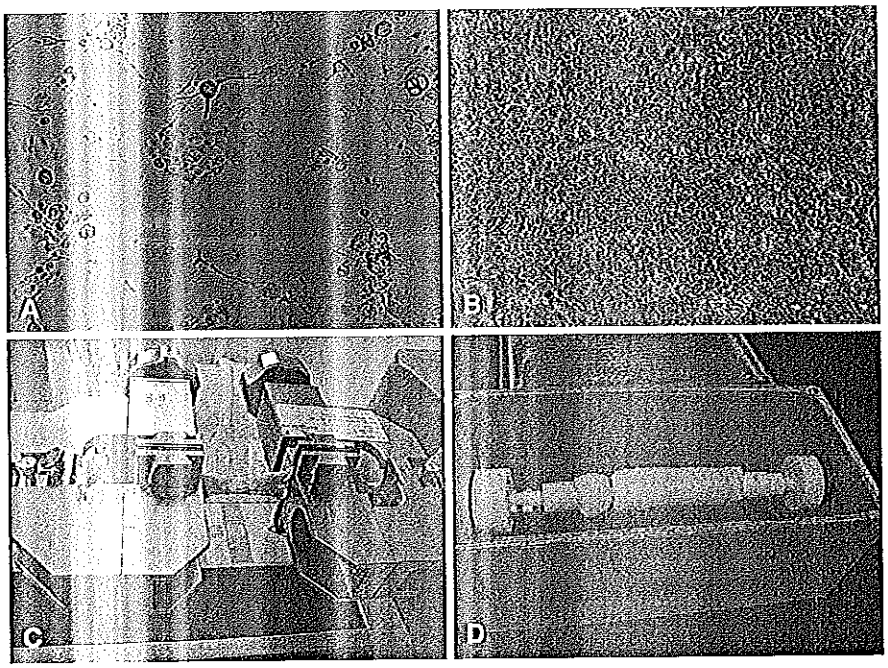

FIGURE 2. A, Epithelial in vitro cell culture after 3 days. B. Epithelial in vitro cell culture after 14 days. C, Tensile-test device evaluating the bioengineered graft. D, Engineered matrix fixed to the bioreactor before starting the seeding process.

bacteriologic analysis before implantation. Over the study period, the implanted graft did not elicit any rejection response, such as swine leukocyte antigen, and this was without immunosuppression. Orthotopically transplanted nonseeded matrices (group I) led to high-grade stenosis (50%–75% decrease in diameter) and bacterium/fungus-contaminated inner surface. The external seeding of MSC-derived chondrocytes (group II) resulted in a quite stable

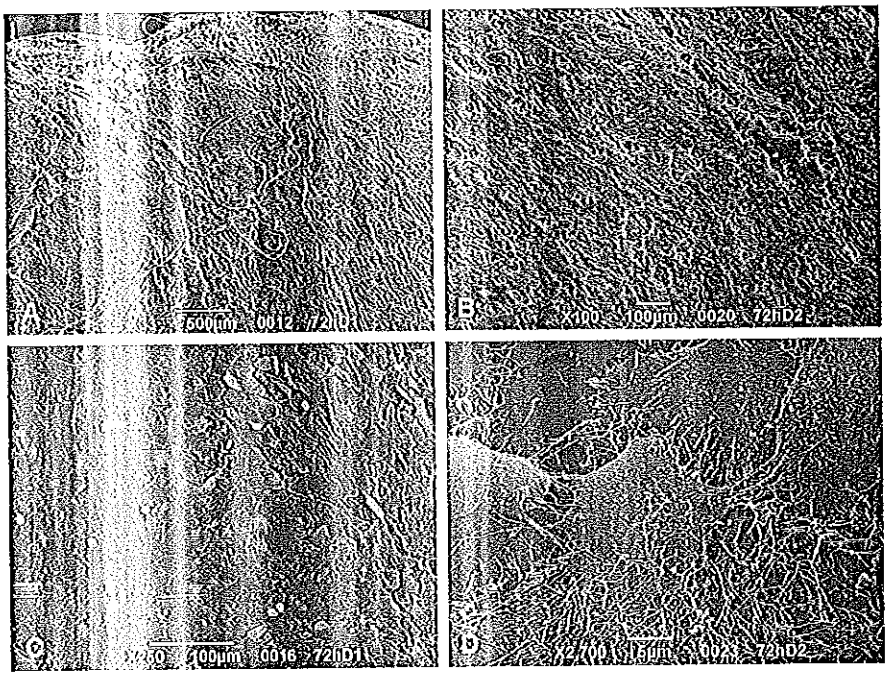

FIGURE 3. Scanning electron microscopic images at different amplifications showing seeded matrices (after 72 hours of seeding time). Different amplifications are shown.

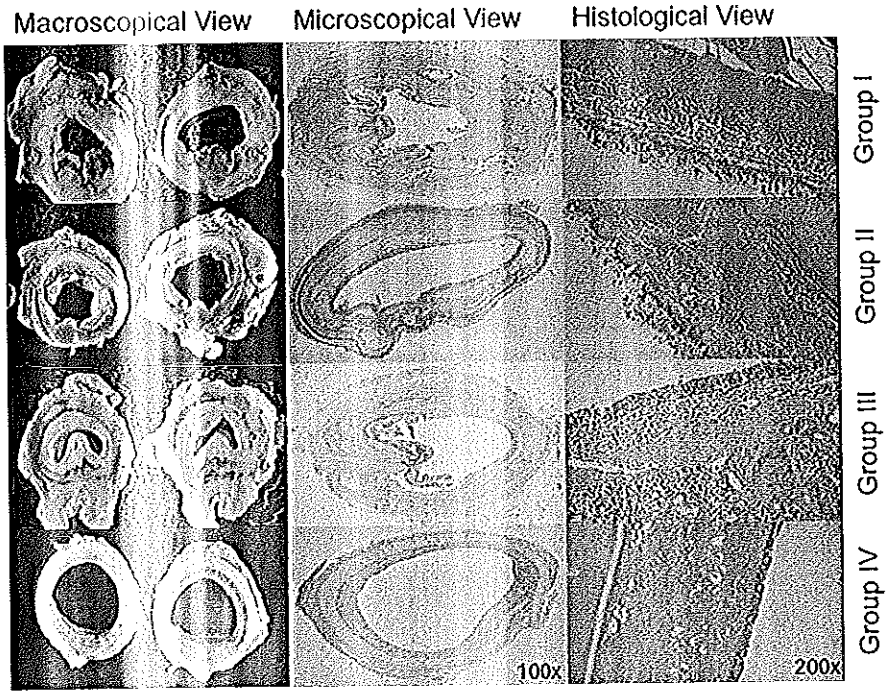

FIGURE 4. The *first column* shows formalin-embedded macroscopic views (transversal sections, group specific). The *second* (100×) and *third* (200×) *columns* display a microscopic view of hematoxylin and eosin histologic transversal sections (group specific). For group I (decellularized matrix only), both stenosis and the inflammatory process are visible. For group II (decellularized matrix with external, autologous mesenchymal stem cell–derived chondrocytes), less stenosis but a high grade of bacterial/fungal contamination is shown. For group III (decellularized matrix with internal, autologous epithelial cells), less inflammatory signs and no bacterial/fungal contamination are shown (high stenosis caused by weakness). For group IV (decellularized matrix with both cell types), no stenosis or contamination is shown.

(25%–50% decrease in diameter) but highly contaminated graft. Grafts seeded only with epithelial cells on the inner surface (group III) also showed high-grade stenosis (>75%), apparently caused by malacia but without bacterial/fungal contamination. Only seeding both sides of the matrices resulted in a healthy functional graft (<25% decrease in diameter, Figure 4), and only slight postoperative inflammatory signs were detected. The histologic and macroscopic findings correlated with the animals' clinical outcome. With respect to the time point of the pigs' death, only group IV animals remained healthy enough to avoid death before the 60-day censor point. All other animals were killed significantly earlier because of signs of marked respiratory distress not amenable to simple treatment measures (group I, 11 ± 2 days; group II, 29 ± 4 days; and group III, 34 ± 4 days). Preimplantation strain tests (Figure 2, *C*) showed no significant difference between the graft and the native trachea, as demonstrated before.[10] However, postoperatively retrieved grafts from groups I to III, but not group IV, showed a statistically lower resilience (Table 1).

DISCUSSION

Our recent first in a human subject experience with a reseeded, decellularized tracheal graft[8] was based on the findings described here. This experimental study explored the biologic mechanisms underlying the success of the

TABLE 1. Comparison of the mechanical characteristics of native and bioengineered tracheas (retrieved postmortem)

Characteristics	Native trachea	Bioengineered grafts (postmortem), groups			
		I	II	III	IV
Mechanical					
Maximum force (N)	182.0 ± 5.1	58.1 ± 8.8*	87.5 ± 6.6*	60.4 ± 8.7*	174.8 ± 7.7†
Rupture force (N)	58.3 ± 2.9	24.4 ± 4.7*	32.7 ± 3.7*	24.2 ± 5.2*	55.6 ± 2.6†
Tracheal rupture point (cm)	12.1 ± 0.4	7.3 ± 0.4*	7.9 ± 0.3 *	7.9 ± 0.9*	11.9 ± 0.4†
Tissue deformation (%)	202 ± 7	121 ± 7*	132 ± 5*	132 ± 14*	198 ± 7†

The term native trachea represents natural untreated tracheas harvested from healthy animals. *Group I*, Decellularized matrix only; *group II*, decellularized matrix with external, autologous mesenchymal stem cell–derived chondrocytes; *group III*, decellularized matrix with internal, autologous epithelial cells; *group IV*, decellularized matrix seeded with both cell types; *Maximum force*, applied maximum force. *$P < .01$ versus native trachea. †$P > .05$ versus native trachea.

transplanted tissue-engineered graft. The first question we wished to answer was as follows: What is the relative contribution of the 2 cell types seeded onto the scaffold, and were both cell types necessary for graft and recipient survival? The study confirmed the applicability of the decellularization, cell preparation, and reseeding techniques, as well as the ease of application of our tracheal bioreactor. However, attention should be paid during cell isolation and culture to avoid contamination caused by fibrocyte proliferation. Notably, no animal demonstrated the development of local or systemic rejection responses to any residual donor antigens, and this was without the administration of immunosuppressive medication. Zani and colleagues[12] demonstrated in 2008 the potential of tissue healing and functional restoration if epithelial and endothelial cells are present at the same time, even with a lack of an ordered architectural relationship. In our model these effects might be provided by residual MSCs in the MSC-derived chondrocyte culture, inducing rapid angiogenesis and making the graft viable. As Genden and associates[13] showed in 2003, the necessity of re-epithelialization is highly important for graft integrity and for protection against a fibroproliferative response of the recipient. Additionally, we showed that long-segment grafts need to be seeded with epithelial cells before orthotopic transplantation to avoid bacterial/fungal contamination. Compared with our previous technically demanding method of direct graft revascularization,[6] the approach described here makes the tracheal reconstruction much more practicable and reproducible but nevertheless with an outstanding outcome.

Gathering knowledge and information regarding the strain abilities of a tracheal graft were disappointing.[14,15] Only a few publications were helpful when designing the tensile test; however, in vitro and in vivo findings did not correlate with each other. Our strain tests showed no difference in biomechanical properties between decellularized scaffolds before implantation, scaffolds seeded with both cell types 60 days after implantation, and normal trachea. Therefore one can assume that there would be no collapse of such grafts. However, our tensile-testing device provided only longitudinal forces, and therefore the true test followed in vivo, when multidirectional forces were applied. Under these conditions, grafts with no cells or only 1 cell type failed to retain functional strength, leading to incompetent airways.

In conclusion, this experimental study demonstrated for the first time the necessity of both MSC-derived chondrocytes and epithelial cells to obtain a functional and proper long-segment tracheal graft with clinical effect. These findings and the applied method of tissue engineering will help forward the reconstruction of the trachea in human subjects. Further studies are required to elucidate the angiogenesis mechanisms and interactions between residual MSCs.

References

1. Grillo HC. Tracheal replacement: a critical review. *Ann Thorac Surg.* 2002;73: 1995-2004.
2. Macchiarini P. Trachea-guided generation: déjà vu all over again? *J Thorac Cardiovasc Surg.* 2004;128:14-6.
3. Birchall M, Macchiarini P. Airway transplantation: a debate worth having? *Transplantation.* 2008;85:1075-80.
4. Macchiarini P, Walles T, Biancosino C, Mertsching H. First human transplantation of a bioengineered airway tissue. *J Thorac Cardiovasc Surg.* 2004;128:638-41.
5. Sekine T, Nakamura T, Matsumoto K, Liu Y, Ueda H, Tamura N, et al. Carinal reconstruction with a Y-shaped collagen-conjugated prosthesis. *J Thorac Cardiovasc Surg.* 2000;119:1162-8.
6. Macchiarini P, Lenot B, de Montpréville VT, Dulmet E, Mazmanian GM, Fattal M, et al. Heterotopic pig model for direct revascularization and venous drainage of tracheal allografts. Paris-Sud University Lung Transplantation Group. *J Thorac Cardiovasc Surg.* 1994;108:1066-75.
7. Macchiarini P, Mazmanian GM, de Montpréville VT, Dulmet E, Fattal M, Lenot B, et al. Experimental tracheal and tracheoesophageal allotransplantation. Paris-Sud University Lung Transplantation Group. *J Thorac Cardiovasc Surg.* 1995;110:1037-46.
8. Macchiarini P, Jungebluth P, Go T, Asnaghi MA, Rees LE, Cogan TA, et al. Clinical transplantation of a tissue-engineered airway. *Lancet.* 2008;372:2023-30.
9. Conconi MT, De Coppi P, Di Liddo R, Vigolo S, Zanon GF, Pamigotto PP, et al. Tracheal matrices, obtained by a detergent-enzymatic method, support in vitro the adhesion of chondrocytes and tracheal epithelial cells. *Transpl Int.* 2005;18:727-34.
10. Jungebluth P, Go T, Asnaghi A, Bellini S, Martorell J, Calore C, et al. Structural and morphological evaluation of a novel detergent-enzymatic tissue engineered tracheal tubular matrix. *J Thorac Cardiovasc Surg.* 2009;138:586-93.
11. Macchiarini P, Dulmet E, de Montpreville V, Mazmanian GM, Chapelier A, Dartevelle P. Tracheal growth after slide tracheoplasty. *J Thorac Cardiovasc Surg.* 1997;113:558-66.
12. Zani BG, Kojima K, Vacanti CA, Edelman ER. Tissue-engineered endothelial and epithelial implants differentially and synergistically regulate airway repair. *Proc Natl Acad Sci U S A.* 2008;105:7046-51.
13. Genden EM, Iskander A, Bromberg JS, Mayer L. The kinetics and pattern of tracheal allograft re-epithelialization. *Am J Respir Cell Mol Biol.* 2003;28:673-81.
14. Behrend M, Kluge E, Von Wasielewski R, Klempnauer J. The mechanical influence of tissue engineering techniques on tracheal strength: an experimental study on sheep trachea. *J Invest Surg.* 2002;15:227-36.
15. Behrend M, Kluge E, Schüttler W, Klempnauer J. The mechanical stability under load of tracheal anastomoses after various phases in vivo. *Laryngoscope.* 2002; 112:364-9.

Discussion

Dr Yolonda Colson *(Boston, Mass).* I have no conflicts.

You are to be congratulated on doing an amazing job in getting this to actually work, and I think that you have defined a very nice clinical problem that currently does not have a great solution. Having said that, I think there are a lot of obvious questions in terms of longer-term follow-up and analysis. I have several questions.

You have 4 different groups that fail for different reasons, except group 4, which does well. Were those groups done sequentially, meaning did you do all the animals in group 1, all the animals in group 2, and so, on so that there is a learning curve in terms of infection and how you do it, or were they randomized?

Dr Go. Yes, it was randomized.

Dr Colson. Therefore there were some in the different groups done after your success in group 4?

Dr Go. Exactly.

Dr Colson. I read the article that you have submitted, and you also talk about there being no evidence of rejection or reaction. What was done to actually know that other than grossly looking at it because you did a lot of biopsies and obtained a lot of blood

samples in the article that you did not talk about here. Second, the animals in group 4 were all killed at 60 days, which is a little less than 1 month after group 3. Is 60 days significant? In terms of longer-term follow-up, does that help us clinically?

Dr Go. To answer the first question, we took blood samples for analysis, as I mentioned in the presentation, to determine, for example, swine leukocyte antigen and other information and the C-reactive protein level. As for the rejection, I just mentioned the swine leukocyte antigen.

Excuse me, what was the second question?

Dr Colson. The animals in group 4 were killed at 60 days routinely rather than seeing what their long-term

Dr Go. To my knowledge, 1 month in the pig is comparable with 6 months in a human subject, which means 60 days in a pig translates to 360 days in a human subject. However, this is just follow-up for the middle term. I would not say this is for the long-term result.

Dr Colson. Have you seen that in your patient whose case was published in *Lancet*?

Dr Go. Yes. Actually, after 3 months of follow-up, she is doing fine.

Dr Frank C. Detterbeck *(New Haven, Conn).* You replaced a 6-cm segment of trachea?

Dr Go. Yes.

Dr Detterbeck. Tell me about the respiratory endothelium. It seems like that has been the problem with longer-segment tracheal replacement. Unless I missed it, you were seeding with chondrocytes primarily, right?

Dr Go. Sorry, I did not hear the question.

Dr Detterbeck. You seeded your bioengineered grafts with chondrocytes.

Dr Colson. On the outside and epithelium on the inside.

Dr Detterbeck. Epithelium on the inside. Okay. I missed that part. Thank you.

Tracheobronchial transplantation with a stem-cell-seeded bioartificial nanocomposite: a proof-of-concept study

Philipp Jungebluth, Evren Alici, Silvia Baiguera, Katarina Le Blanc, Pontus Blomberg, Béla Bozóky, Claire Crowley, Oskar Einarsson, Karl-Henrik Grinnemo, Tomas Gudbjartsson, Sylvie Le Guyader, Gert Henriksson, Ola Hermanson, Jan Erik Juto, Bertil Leidner, Tobias Lilja, Jan Liska, Tom Luedde, Vanessa Lundin, Guido Moll, Bo Nilsson, Christoph Roderburg, Staffan Strömblad, Tolga Sutlu, Ana Isabel Teixeira, Emma Watz, Alexander Seifalian, Paolo Macchiarini

Summary

Background Tracheal tumours can be surgically resected but most are an inoperable size at the time of diagnosis; therefore, new therapeutic options are needed. We report the clinical transplantation of the tracheobronchial airway with a stem-cell-seeded bioartificial nanocomposite.

Methods A 36-year-old male patient, previously treated with debulking surgery and radiation therapy, presented with recurrent primary cancer of the distal trachea and main bronchi. After complete tumour resection, the airway was replaced with a tailored bioartificial nanocomposite previously seeded with autologous bone-marrow mononuclear cells via a bioreactor for 36 h. Postoperative granulocyte colony-stimulating factor filgrastim (10 μg/kg) and epoetin beta (40 000 UI) were given over 14 days. We undertook flow cytometry, scanning electron microscopy, confocal microscopy epigenetics, multiplex, miRNA, and gene expression analyses.

Findings We noted an extracellular matrix-like coating and proliferating cells including a CD105+ subpopulation in the scaffold after the reseeding and bioreactor process. There were no major complications, and the patient was asymptomatic and tumour free 5 months after transplantation. The bioartificial nanocomposite has patent anastomoses, lined with a vascularised neomucosa, and was partly covered by nearly healthy epithelium. Post-operatively, we detected a mobilisation of peripheral cells displaying increased mesenchymal stromal cell phenotype, and upregulation of epoetin receptors, antiapoptotic genes, and miR-34 and miR-449 biomarkers. These findings, together with increased levels of regenerative-associated plasma factors, strongly suggest stem-cell homing and cell-mediated wound repair, extracellular matrix remodelling, and neovascularisation of the graft.

Interpretation Tailor-made bioartificial scaffolds can be used to replace complex airway defects. The bioreactor reseeding process and pharmacological-induced site-specific and graft-specific regeneration and tissue protection are key factors for successful clinical outcome.

Funding European Commission, Knut and Alice Wallenberg Foundation, Swedish Research Council, StratRegen, Vinnova Foundation, Radiumhemmet, Clinigene EU Network of Excellence, Swedish Cancer Society, Centre for Biosciences (The Live Cell imaging Unit), and UCL Business.

Introduction

Primary tracheal cancers are rare neoplastic lesions characterised by a high mortality rate. The gold standard treatment for these lesions is surgical resection with primary reconstruction.[1] However, epidemiological studies have shown that, because of difficulties in the definitive diagnosis, most patients with primary malignant tracheal cancers present with local inoperable disease (exceeding 6 cm or >50% of the total tracheal length) and are, therefore, treated with palliative measures. For these patients, prognosis is poor with a reported 5-year survival rate of about 5%.[2] Moreover, because safe reconstruction of the trachea is not possible, even in patients with operable tumours, the proportion of complete tumour resection is less than 60%.[3] This outcome would be greatly improved if a trachea substitute with similar anatomical, physiological, and biomechanical properties of the native trachea were available.

In 2008, we reported the first fully tissue-engineered tracheal transplantation with a non-immunogenic decellularised human donor trachea reseeded with bone-marrow-derived mesenchymal stem cells (MSCs) and respiratory cells.[4] However, this approach is limited by the shortage of donor organs of an appropriate size and has other disadvantages (webappendix p 9). As a result, an alternative, tailor-made synthetic tracheal scaffold is an urgent clinical need. We report the clinical transplantation of the tracheobronchial airway in a patient with recurrent primary trachea cancer, with use of a tailor-made artificial scaffold reseeded ex vivo with mononuclear cells (MNCs)[5] and a growth factor-induced endogenous stem cells mobilisation.

Methods

The recipient

Webappendix pp 2–9 provides a detailed description of the methods. A 36-year-old man presented in May, 2011,

Lancet 2011; 378: 1997–2004
Published Online November 24, 2011
DOI:10.1016/S0140-6736(11)61715-7

See Comment page 1977

Advanced Center for Translational Regenerative Medicine (P Jungebluth MD, S Baiguera PhD, K-H Grinnemo MD, Prof P Macchiarini MD), Cell and Gene Therapy Centre, Department of Medicine, Division of Hematology (E Alici MD, T Sutlu BSc), Departments of Medicine and Laboratory Medicine (Prof K Le Blanc MD, G Moll MS, E Watz MD), Center for Biosciences, Department of Biosciences and Nutrition (S Le Guyader PhD, Prof S Strömblad PhD), Linnaeus Center in Developmental Biology for Regenerative Medicine, Department of Neuroscience (O Hermanson PhD, T Lilja PhD), Department for Clinical Science, Intervention and Technology (B Leidner MD), Department of Cell and Molecular Biology (V Lundin MS, A I Teixeira PhD), and European Airway Institute (Prof P Macchiarini), Karolinska Institutet, Stockholm, Sweden; Division of Ear, Nose and Throat (P Jungebluth, Prof P Macchiarini, G Henriksson MD, J E Juto MD), Vecura, Clinical Research Center (P Blomberg PhD), Division of Pathology (B Bozóky MD), Department of Cardiothoracic Surgery and Anesthesiology (K-H Grinnemo, J Liska MD), Department of Radiology (Huddinge) (B Leidner MD), and Department of Clinical Immunology and Transfusion Medicine (E Watz), Karolinska University Hospital, Stockholm, Sweden; Centre for Nanotechnology and Regenerative Medicine,

University College London, London, UK (C Crowley MSc, Prof A Seifalian PhD); Department of Pulmonology (O Einarsson MD) and Department of Cardiothoracic Surgery (Prof T Gudbjartsson MD), Landspitali University Hospital, Faculty of Medicine, University of Iceland, Reykjavik, Iceland; Department of Medicine 3, University Hospital RWTH Aachen, Aachen, Germany (T Luedde MD, C Roderburg MD); and Rudbeck Laboratory, Department of Immunology, Genetics and Pathology, Uppsala University, Uppsala, Sweden (Prof B Nilsson MD)

Correspondence to: Prof Paolo Macchiarini, Advanced Center for Translational Regenerative Medicine (ACTREM), European Airway Institute, Division of Ear, Nose and Throat (CLINTEC), Karolinska Institutet, Alfred Nobels Allé 8, Huddinge, SE-141 86 Stockholm, Sweden
paolo.macchiarini@ki.se

See Online for webappendix

See Online for webvideo

at the Karolinska University Hospital (Huddinge, Sweden) with stridor, cough, and respiratory difficulties. The patient, previously treated elsewhere with tumoral debulking surgery and postoperative regional radiation (70 Gy),[6] presented with a recurrence of a primary tracheal mucoepidermoid carcinoma affecting the distal trachea and both main bronchi (figure 1A). The patient underwent an extensive staging,[1] including ^{18}F-fluorodeoxyglucose (^{18}F-FDG) PET scan, multistage biopsies of the respiratory mucosa proximal and distal to the macroscopic tumour burden, and bone marrow biopsy and aspiration. Results showed no local or distant lymphatic or systemic metastasis, and normal stromal cells. The tumour extended from 5 cm above the right tracheobronchial angle into the first 1·3 cm of the right main bronchus, leaving the origins of the upper and intermedius take-offs tumour free, and the first 1·5 cm of the origin of the left main bronchus (webvideo 1). On the basis of surgical standards,[3] this extension was deemed beyond resectability; therefore a transplant procedure, with an artificial biomaterial, was offered to the patient.

We obtained written informed consent from the patient, and the transplant procedure was approved by the local scientific ethics committee.

Pretransplant preparation

We manufactured a tailor-made trachea from the preoperative chest CT and three-dimensional volume rendered images of the patient with a nanocomposite polymer (POSS-PCU; polyhedral oligomericsilsesquioxane [POSS] covalently bonded to poly-[carbonate-urea] urethane [PCU]) processed by an extrusion-phase-inversion method.[7] On the basis of our previous experience with the physical and mechanical properties of human trachea (webappendix p 11)[8] and the patient's preoperative CT scan (figure 1B), we developed a POSS-PCU nanocomposite polymeric airway of appropiate size and morphology, reproducing the exact dimensions of the patient's tracheobronchial structure (webappendix p 12). A Y-shaped three-dimensional glass mandrel was fabricated, and U-shaped rings of POSS-PCU, analogous to the cartilaginous rings of tracheobronchial tissue, were manufactured with casted methodologies and placed around the mandrel. The entire mould was then placed in the POSS-PCU solution to form a coagulated porous scaffold.

A bioreactor to accommodate precisely the maturation requirements of the Y-shaped synthetic windpipe construct used in the transplantation was developed (Hugo Sachs Elektronik-Harvard Apparatus GmbH, March-Hugstetten, Germany; figure 1C, D). The design was based on a sterilisable rotating-construct bioreactor, previously validated but with novel elements to drive a recirculating fluid flow within and around the developing graft,[5] enabling consistent and uniform delivery of cells, nutrients, gases, and hydrodynamic shear forces within the bioreactor. This process is accomplished without external fluid pumps and packaged within the bioreactor assembly so that ease of handling and simplicity of use in good manufacturing practice and clinical environments is not compromised.

Autologous MNCs were obtained 2 days before transplantation from a bone marrow aspirate through density gradient separation. Analyses of white blood cells, mononuclear cells, CD34+ cells, viability, colony-forming unit-fibroblast, flow cytometric characterisation, and sterility were done. To obtain the synthetic bioengineered tracheobronchial construct, cells were resuspended in low-glucose Dulbecco's modified Eagle's medium (Invitrogen, Stockholm, Sweden) and seeded onto the synthetic graft by incubation of the construct in the bioreactor at 37°C for 36 h before transplantation.

Immediately before transplantation, a second bone marrow harvest was done, and MNCs were separated and transferred to the operating theatre. Immediately before implantation, the airway construct was transported to the operating theatre, reseeded with the obtained MNCs, and conditioned with growth and regenerative factors—namely, recombinant human transforming growth factor-β3 (R&D Systems, Minneapolis, MN, USA; 10 μg/cm^2), granulocyte-colony stimulating factor filgrastim (G-CSF, Neupogen; Amgen Europe BV, Breda, Netherlands; 10 μg/kg), and epoetin beta (analogous synthetics of Erythropoietin Roche, Grenzach-Wyhlen, Germany; 40 000 UI). We assessed sections of the graft, surplus to clinical need, by scanning electron microscopy, fluorescence, and bright field light microscopy and confocal live cell imaging (webappendix pp 14–15; webvideo 2).

Transplantation

Under general anaesthesia and orotracheal intubation, a redo sternotomy was done and the tumour-burden area dissected and mobilised, according to the principles of tracheal surgery.[1–3] Because of the previous postsurgical and radiation-induced scar tissue formation, the tumour had to be resected along with the right intrapericardial pulmonary artery, and subsequently revascularised with a Dacron 8F graft (Gelsoft, Vascutek, Terumo, Ann Arbor, MI, USA). The graft was interposed between the retroaortic and the extrapleural origin of the pulmonary artery, clamping both vena cavae for 26 min and without use of cardiopulmonary bypass. Tumour resection included the postlateral and mediastinal aspect of the distal truncus of the superior vena cava via lateral clampage and direct suture. The resected trachea included its distal intrathoracic 6 cm, the entire right main bronchus, and first 2 cm of the left main bronchus. All tumour margins were negative on frozen section, and a complete mediastinal lymph-node dissection was done. The airway was then reconstructed by implantation of the reseeded nanocomposite end-to-end, first to the right and left main bronchi and then to the proximal trachea, with standard techniques.[3] Finally, the omentum major was wrapped around the construct and the median

sternotomy and laparotomy closed in a standard manner. From our past experience with carinal surgery when cough reflex, mucous clearance, and patient's full mobilisation are suboptimal in the early postoperative course, a temporary tracheotomy above the implanted graft was made at the end of the procedure.[9]

Regenerative boosting therapy

To enhance the regenerative process, the patient was treated pharmacologically by subcutaneous injections of G-CSF (10 µg/kg) and epoetin-alpha (40 000 UI), with a loading dose given the day before transplantation and every other day for 2 weeks during the postoperative period.

Follow-up assessment

Control endoscopies were done postoperatively daily for the first 7 days, for inspection of the graft and anastomoses. Bronchoscopies were then done once a week during admission to hospital, and once a month thereafter. Postoperative biopsies of the bioartificial graft were assessed by immunohistochemistry, haematoxylin-eosin stain, periodic acid-Schiff stain, and Masson's trichrome stain. Micro-RNA assessment in serum and analyses of soluble factors in plasma (multiplex cytokine assay and ELISA) were done every second day for 2 weeks after transplantation.

Peripheral blood mononuclear cells (PBMCs) were isolated by gradient centrifugation, with Lymphoprep (Nyegaard, Oslo, Norway) and washed twice with phosphate-buffered saline (Gibco, Grand Island, NY, USA). We assessed cell count and viability assays by Türk and trypan blue dye exclusion or by Nucleocounter NC-100 (ChemoMetec A/S, Allerød, Denmark). We analysed gene expression, chromatin immunoprecipitation, and analyses of PBMC subsets and phenotyping 2 days before surgery, and for 2 weeks postoperatively.

Statistical analysis

We undertook data analysis, preparation of graphs, and statistical comparisons with Prism software (Graphpad Prism version 5.0a) and three-dimensional surface modelling with Microsoft Excel 2010.

Role of the funding source

The sponsors of the study had no role in study design, data collection, data analysis, data interpretation, or writing of the report. The corresponding author had full access to all the data in the study and had final responsibility for the decision to submit for publication.

Results

The patient was awake 24 h after transplantation. The immediate postoperative course was characterised by a right upper lobe pneumonia (day 2); *Candida albicans* (>10 000 CFU/mL) and *Stenotrophomonas maltophilia* (>10 000 CFU/mL) were isolated and treated with broad spectrum antibiotics and intensive physiotherapy. Other than this complication, the patient improved gradually and was weaned from the mechanical ventilation on day 5 postoperatively.

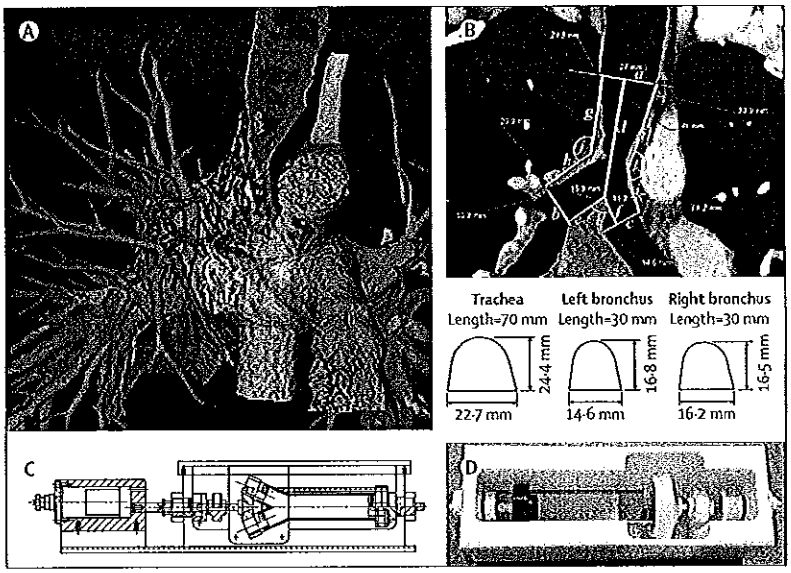

Figure 1: CT scan and three-dimensional volume rendered (VR) images
(A) Preoperative VR frontal plane image. Extension of tumour is shown in green. Tracheal and bronchial tree air space is shown in bright blue. The image shows the relation between tumour and right main pulmonary artery. (B, top) Measurement image. An angulated 2 mm thick CT image is used for measurements for individualised scaffold production. The image was optimised for concurrent visualisation of the tumour involvement of trachea inclusive of carina and proximal bronchi aligned parallel to tracheal longitudinal axis. Yellow lines mark proximal trachea (a) and distal right (b) and left (c) bronchi free from tumour involvement, and measurement of the transverse lumen diameters. Sagittal diameter was calculated from angulated transverse image perpendicular to the central lumen line (not shown). (d) Trachea free from tumour (carina); (e) right bronchus free from tumour (carina); (f) left bronchus free from tumour (carina); (g) trachea free from tumour, angle of trachea and right main bronchus; (h) angle of trachea and right main bronchus, right main bronchus free from tumour; (i) 1+2 corresponding left side measurements; (j) angle of trachea and right bronchus; (k) angle of trachea and left bronchus; (l) carinal angle. (B, bottom) Cross section of mandrel for (a) trachea, (b) left bronchus, and (c) right bronchus. (C) Frontal cutaway view of the improved bioreactor. (D) Macroscopic view showing bioreactor without the lid.

1 week after surgery, the bronchoscopy (webvideo 3, figure 2A) showed a normal and patent airway bleeding from its inner layer at the contact with the scope; the obtained biopsy samples showed the presence of necrotic connective tissue associated with fungi contamination and neoformed vessels (figure 2B). The temporary tracheotomy cannula was removed 18 days later. The patient was then transferred to a normal ward and discharged to the referral hospital 1 month after surgery. The biopsy sample 2 months after transplantation showed large granulation areas with initial signs of epithelialisation and more organised vessel formations, and no bacterial or fungi contamination (figure 2B). The patient was discharged from the referring hospital to start rehabilitation and later resumed his university studies. 5 months after transplantation, the patient is asymptomatic, breathes normally, is tumour free, and has an almost normal airway (figure 2C) and improved lung function compared with preoperatively (table, webappendix p 16).

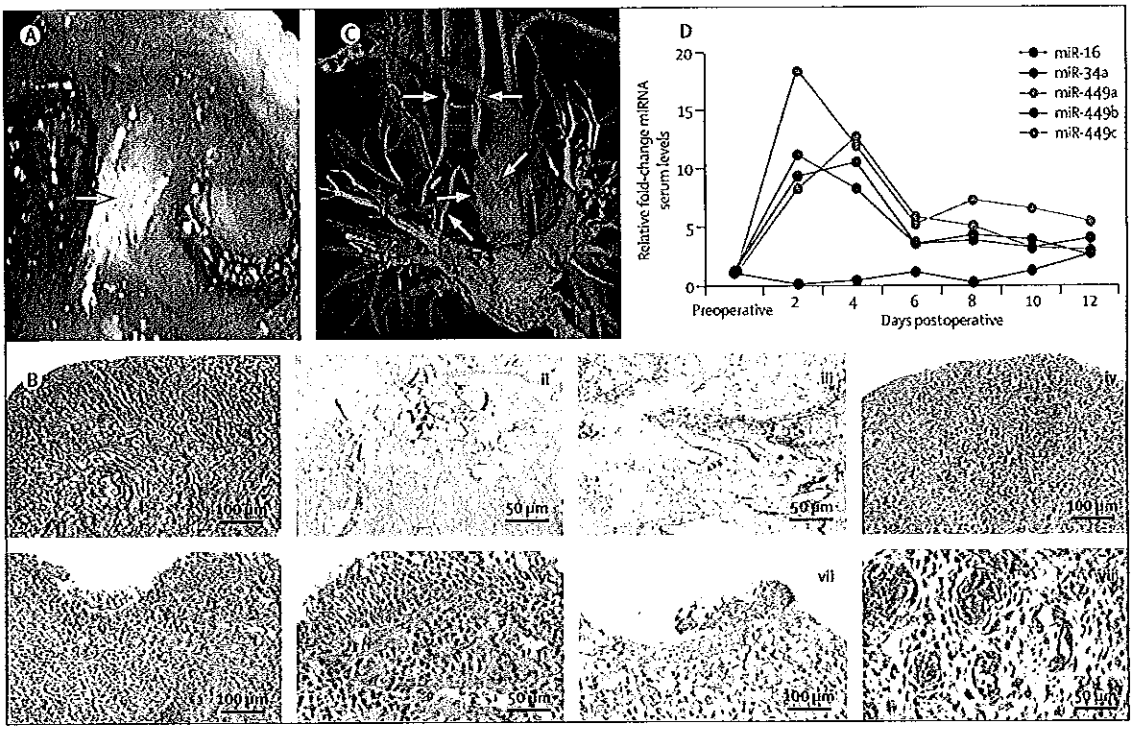

Figure 2: **Postoperative follow-up**

(A) Bronchoscopy image showing the transplanted bioengineered construct integrated with surrounding tissues. (B) Histological evaluation (Masson) of the first postoperatively obtained biopsy sample (at day 7) from the distal part of the graft showed necrotic connective tissue (i) with fungi contamination (periodic acid-Schiff stain; ii) but developed vascular structure (CD146 with Bond Polymer Refine Detection brown colour; NGFR with Bond Polymer Refine Red Detection red colour [without stained structures]; immunolabelling was done on Leica -Bond-Max automated immunostainer; iii). By contrast, the follow-up biopsy at 2 months (haematoxylin-eosin stain) showed ulceration with granulation tissue (iv) and still inflammation, but also respiratory epithelium with mucus secreting cells (haematoxylin-eosin stain; v and vi). Additionally, P63-DAB/CK17 staining showing detached metaplastic squamous epithelium (red; vii) and Mib1-DAB/Vimentin staining showing proliferating (brown) endothelial structures in capillaries. (C) Postoperative volume rendered (VR) image. Air in airways is shown in bright blue. Note that the VR technique displays only the factual air and not the scaffold material. Yellow arrows show borders for scaffold insertion. (D) Serum levels of miR-16, miR-34, miR-449b, and miR-449c were measured by quantitative PCR in serum samples gained at the indicated timepoints before and after surgery.

	May, 2011 (before surgery)	October, 2011 (4 months after surgery)
FVC (L)	3·80	2·63
FEV_1 (L)	1·52	1·95
FEV_1:FVC (%)	40·02%	74·37%

FVC=forced vital capacity. FEV_1=forced expiratory volume in 1 s.

Table: **Lung function tests**

Analyses by micro-RNA expression have shown that serum levels of miR-34 and miR-449 members are potential biomarkers for promotion of terminal differentiation of airway epithelium.[10] Compared with preoperative levels, we noted upregulation 2 days after transplantation, which gradually decreased (figure 2D). By contrast, serum levels of miR-16—a ubiquitous miRNA frequently used for normalisation of serum miRNA levels[11]—remained unchanged.

The autologous bone marrow MNCs were seeded on the synthetic graft and incubated in the bioreactor (webappendix p 14), resulting in a bioengineered tracheobronchial construct suitable for transplantation (webappendix p 17). Scanning electron microscopy of cells incubated in the bioreactor and confocal microscopy of live cells statically exposed to the biomaterial identified cells of different morphologies inside the scaffold, including long processes, filopodia, and lamellipodia (webappendix pp 16–17), whose formation requires anchorage to the scaffold. Although a shortage in material prevented us from undertaking a thorough analysis of cell division, some of the observed cells seemed to be newly divided (webappendix p 17) and cells exposed to the bioreactor aggregated in dense clusters, suggesting clonal expansion. Staining with the CD105 marker showed a subpopulation of cells of mesenchymal lineage (webappendix p 17). Flow cytometric phenotyping of the bioreactor medium showed a selective reduction of MSCs and haemopoietic stem cells (HSCs) after the reseeding process, with a particular decrease in CD90 high and CD59 dim cells (webappendix p 17), suggesting their preferential attachment and engraftment to the scaffold.

Monitoring of patient cell counts and plasma markers showed formation of typical acute phase reactants,

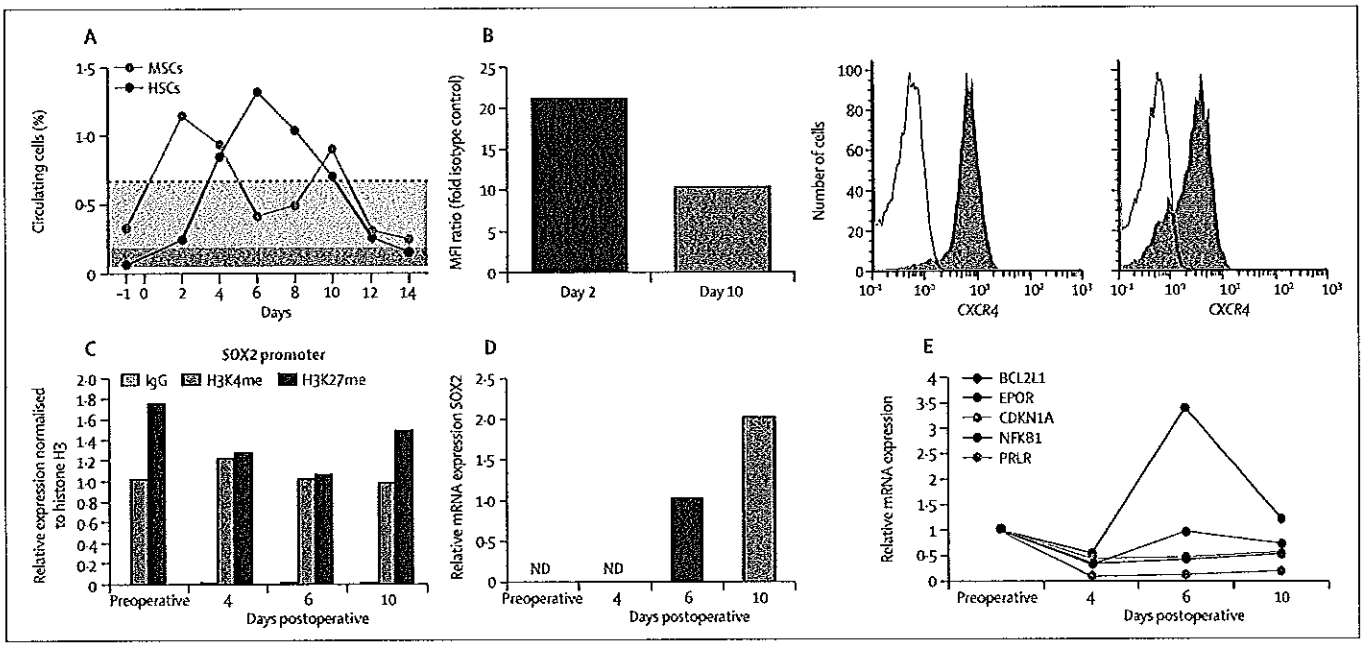

Figure 3: **Analysis of peripheral blood mononuclear cells after surgery (flow cytometry, gene expression, and epigenetic regulation)**
(A) Dynamics of circulating MSCs and haemopoietic stem cells (HSCs) as analysed by high-resolution flow cytometry. MSCs in circulation reached a peak level 2 days after surgery and subsequently decreased, and thereafter reached a secondary peak at day 10. The detection ranges from four healthy donors matched for age and sex (male donors aged from 32–39 years, randomly selected at the Karolinska Institutet, Stockholm, Sweden) are shown in light grey. The percentage of circulating HSCs increased and reached to a plateau at day 6 but then rapidly decreased to normal levels at day 14. Reference ranges assessed from four donors are shown in dark grey. (B) Expression of CXCR4 on circulating MSCs on days 2 and 10 as acquired by flow cytometry. Left panel: comparison of mean fluorescence intensity (MFI) ratios on days 2 and 10. Right and centre panels: red lines indicate isotype controls and green histograms indicate MSCs. (C) Quantitative PCR results after chromatin immunoprecipitation procedure using antibodies against histone H3 (for normalisation), trimethylated lysine 4 (H3K4me3), and trimethylated lysine 27 (H3K27me3) on histone 3 at the promoter regions of the gene SOX2. (D) Expression of the SOX2 gene relative to GAPDH, analysed by quantitative RT-PCR. (E) Fold change of genes with antiapoptotic function, relative to the preoperative condition, analysed by quantitative RT-PCR array. ND=not detectable.

wounding, tissue remodelling, and regenerative factors after surgery (webappendix pp 18–19). Webappendix p 19 shows results of a heat map analysis with the exact kinetics and numerical values for individual factors. Findings from a flow cytometric analysis of the peripheral blood showed an increase in HSCs at day 6, with a particular increase of the CD90+ subpopulation (webappendix pp 20–21). We noted an increased amount of circulating MSCs at day 2, to 15-fold higher levels than the age and sex matched healthy donor range (figure 3A), possibly as a result of the boosting therapy before surgery; this increase was followed by a three-fold decrease at day 4 and 6, to show a secondary two-fold increase at day 10. In line with these findings, the relative gene expression of homing-associated factor SDF-1 receptor CXCR4 was two-fold higher in MSCs at day 2 than at day 10 (figure 3B).

We then undertook a molecular analysis of the stem-cell phenotype. Chromatin immunoprecipitation showed that the *SOX2* gene, encoding a progenitor-associated transcription factor, showed stable concentrations of the H3K4me3 activity mark throughout the postoperative analysis. However, the H3K27me3 repressive mark was decreased in samples retrieved 4 and 6 days after surgery, showing an increased activity and decreased repression at these timepoints (figure 3C). Accordingly, this increased total activity preceded an induction of SOX2 gene expression at day 6 and a further increase at day 10 (figure 3D). Another progenitor-associated gene, GNL3, also displayed an increasing ratio of active and repressive marks H3K4me3 and H3K27me3 at day 6, correlating with increased gene expression (data not shown). These results on chromatin state and gene expression lend support to the flow cytometric analysis indicating a second wave of circulating MSCs (figure 3A, webappendix p 20).

We investigated the expression in PBMCs of genes involved in the JAK/STAT pathway—a major signalling transduction pathway activated by epoetin beta. Most genes showed a consistent trend of downregulation at day 4 postoperatively, compared with the preoperative condition, with subsequent progressive recovery of the expression levels at days 6 and 10 (webappendix p 22). Analysis of antiapoptotic genes showed a peak in the expression of BCL2L1 and EPOR at day 6, suggesting increased antiapoptotic activity in PBMCs at that time (figure 3E).

Discussion

Findings from this proof-of-concept case study show the feasibility of tracheal transplantation with an artificial nanocomposite reseeded with autologous stromal cells.

Panel: Research in context

Systematic review

We searched Medline and PubMed without date or language restrictions for articles with the following terms: "trachea", "tracheal replacement", "tracheal cancer", "tracheal surgery", "transplantation", "stem cells", "cell mobilization", "tissue engineering", "scaffold", and "synthetic material". We identified several relevant articles showing challenges and outcome of tracheal reconstruction and replacement, published between 1997 and 2011.[3,4,9,10,11,13,14,15] However, we could not locate any report showing the successful transplantation of a cell-seeded synthetic scaffold-based tracheal transplantation in human beings. Moreover, we identified no publication showing detailed insights into active stem-cell mobilisation in tracheal transplanted patients.

Interpretation

Our study is the first to describe a successful transplantation of a synthetic-based stem-cell seeded scaffold in a patient. Our data were collected from preoperative and postoperative in-vivo measurements and in-vitro studies. We applied complementary methods to confirm findings. Even though we now describe only one case of tissue-engineered tracheal transplantation, the magnitude of data and the validation of a specific mechanism suggest solid evidence. Our specific findings are verified and discussed extensively in relation to earlier findings from independent investigators. Moreover, our data provide novel insights into cellular pathways.

We have also shown the possibility of stem-cell mobilisation and the dynamic patterns and profile of mononuclear cells in peripheral blood circulation. Despite much progress in the clinical translation of tissue engineered organs and complex tissues,[12,13] no safe and suitable solution has been identified to successfully replace the trachea.[14,15] With a human decellularised tracheal matrix, repopulated with in-vitro expanded and differentiated autologous chondrocytes of MSC origin and autologous epithelial cells via a novel bioreactor system, the first-in-man completely tissue-engineered trachea replacement was successfully done.[5] This strategy, improved by intraoperative graft seeding with autologous cells (bone marrow MSCs and respiratory cells) and conditioning with differentiation and tissue-protective factors,[16] was subsequently successfully used in patients with both benign and malign airway diseases. However, this approach has limitations—eg, a long period for the decellularisation process (15–20 days), the need for different patient-specific sizes, the risks for altering long-term natural matrix mechanical properties, bacterial contamination during the in-vitro natural graft manipulation, and, most importantly, the absolute requirement of obtaining a donor organ.

The primary tumour of our patient involved the last 5 cm of the distal trachea along with the tracheobronchial bifurcation, which represents an absolute contraindication to any surgical resection. Because the patient had a tumour recurrence with severe stridor, despite 70 Gy of radiation therapy, and the waiting time for a donation would have been unpredictable, we decided to attempt a curative surgery by replacement of the resected airway with an artificial POSS-PCU-based nanocomposite combined with a novel pharmacological boosting strategy. This decision was based on the fact that the POSS-PCU is biocompatible, non-toxic, non-biodegradable, inert, and has negligible immunoreactivity.[17] Additionally, it displays mechanical properties, in-vivo chemical stability, and nanostructural features,[18,19] which approach the ideal for a bioengineered tracheal implant. And, it is patient specific, since it could be designed to replace not only the trachea but also the bronchi, or a combination of both. Lastly, it can be produced in a rapid and clinically appropriate timeframe.

Previous attempts to replace the airways of patients with tracheal cancer with synthetic materials have been unsuccesful because of graft's limited cell seeding, infection, migration, stenosis, necrosis, and ultimately death of the patients.[4] These drawbacks are clearly related to the fact that the trachea is not located in a mesenchymal environment, but is in direct contact with the breathing air, making infection and contamination more likely to occur. Thus we used a bioreactor environment to reseed the bioartifical scaffold with autologous mononuclear cells. Results showed that 36 h of dynamic incubation of the mononuclear cells in the bioreactor was sufficient for them to adhere to the biomaterial. 2 days after seeding, the cells exposed to the bioreactor formed dense clusters, whereas those statically incubated were more evenly distributed (webappendix p 17), indicating that the bioreactor might help nested cells to proliferate. Antibody labelling and morphological analysis showed the presence of proliferating CD105+ cells with mesenchymal but not haemopoietic phenotype within the graft. Although an extracellular matrix (ECM)-like structure was observed on the scaffold (webappendix p 17) after the reseeding and bioreactor process, whether this structure is related to the autologous serum or the production of ECM by engrafted cells is unclear.

The most frequently reported airway complications after lung transplantation are necrosis, dehiscence, and stenosis, probably related to ischaemia of the transplanted bronchus during the immediate period after transplantation.[20–22] In this report, an avascularised, Y-shaped nanocomposite was implanted and the initial fungal infection had resolved within 4 months from transplantation; later the endoluminal surface was partly lined with respiratory mucosa, at which we noted nearly healthy epithelium and proliferating endothelium. This finding provides evidence that a bioengineered synthetic tracheobronchial nanocomposite can be recellularised in vivo with site-specific cells to become a living and functional scaffold completely integrated into the adjacent tissues. The measured levels of miR-34/449

micro-RNAs, which have been proposed as potential biomarkers of terminal differentiation of airway epithelium,[19] suggest the presence of postoperative airway epithelial differentiation in the patient.[11]

One of the key issues in a synthetic transplantation setting is the recruitment of repair cells that promote the integration and remodelling of the newly transplanted material. The cellular components contributing to regeneration can be recruited either from local tissue or from circulating progenitor cells. We observed HSC mobilisation together with increased amounts of circulating MSCs, which contrasts with previous findings[23] of no mobilisation of MSCs, when G-CSF was used as mobilising agent alone. Indeed, surgery-induced inflammation and chemokine and anaphylatoxin release at the implantation site could be the reason for the observed MSC mobilisation in our patient. We detected release of a large array of soluble mediators associated with wound healing, which could promote MSC mobilisation, as previously reported by other investigators.[24,25] Additionally, G-CSF induced neutrophil expansion, and release of proteases, which we also detected, could have promoted progenitor mobilisation.[26] Progenitor mobilisation presumably occurs by weakening their anchoring within the niche, either by degradation of the anchoring ECM components or their retention factor SDF-1a itself.[26] Bone marrow progenitor cell activation, recruitment, tissue repair, and local immune suppression at the surgery site could be enhanced by blood activation products, such as C3a and thrombin,[26–28] which were formed upon scaffold implantation. We detected a strong systemic release of growth factors and matrix metalloproteinases, which are probably produced by recruited progenitor and other immune cells. Furthermore, we recorded a substantial and very early increase of the epoetin-receptor expression with simultaneous upregulation of antiapoptotic genes, such as *BCL2L1*. During inflammation, trauma cytokines are released which upregulate epoetin receptors but inhibit tissue protection by downregulation of local epoetin production and antiapoptotic downstream pathways, favouring cell apoptosis. To avoid this early postoperative absence of local epoetin production, we administered regenerative (500 UI/Kg) epoetin doses, aiming to favour and trigger early local tissue protection and regeneration.

Taken together, these results provide evidence that a successful organ regeneration strategy has been accomplished (panel). The successful overall clinical outcome of this first-in-man bioengineered artificial tracheobronchial transplantation provides ongoing proof of the viability of this approach, in which a cell-seeded synthetic graft is fabricated to patient-specific anatomical requirements and incubated to maturity within the environment of a bioreactor. Additionally, in-depth cellular biochemistry analyses have provided new insight into the mechanisms by which the so-called pharmacological boosting factors contribute to cell mobilisation, differentiation, and ultrastructural organisation of the fully engrafted tracheobronchial construct.

Contributors

PJ was responsible for the bioreactor-based cell seeding; assisted the surgery and with collection of secondary data; and wrote corresponding methods, results, and interpretation sections. EA and TS undertook all flow cytometry characterisation of the cells, interpreted the results, and wrote corresponding methods. SB provided preclinical data for human tracheal biomechanics, and helped to write the report. KLB, BN, and GM designed, undertook, and assessed the multiplex analyses and wrote corresponding methods. KLB undertook the bone-marrow isolation. PB organised and supervised standards at the good manufacturing practice facility. BB did histological evaluation. CC and AS designed and developed the three-dimensional nanocomposite trachea, and wrote corresponding methods. OE and TG are responsible for the clinical follow-up of the patient and provided biopsy material and blood samples; TG also participated in the surgery and wrote corresponding methods. K-HG and JL assisted the surgery. SLG and SS did all cell imaging and wrote corresponding methods. OH and TL undertook and assessed all epigenetic analyses and wrote corresponding methods. JEJ and GH assisted in the preoperative and postoperative care. BL did all radiological imaging, interpretation, and three-dimensional reconstruction, and wrote corresponding methods. TL and CR undertook and assessed the miRNA studies, and wrote corresponding methods. VL and AIT undertook and analysed gene expression experiments, and wrote corresponding methods. EW isolated the mononuclear cells. PM was the primary investigator and leading author of the report, indicated how to built the three-dimensional nanocomposite, was leading surgeon and was responsible for the preoperative and postoperative course, and oversaw the review process. All authors provided primary data for modelling scenarios, and assisted with interpretation of results and report revision.

Conflicts of interest

We declare that we have no conflicts of interest.

Acknowledgments

The European Commission (FP7 EU Project: 280584-2BIOtracheaCP-FPFP7-NMP-2011-SMALL-5), the Knut and Alice Wallenberg Foundation, Swedish Research Council, and the StratRegen funded preclinical and postoperative in-vitro studies, gene expression, cell characterisation, and imaging. The Vinnova Foundation, Radiumhemmet, and Clinigene EU Network of Excellence funded multiplex and flow cytometric analyses. The Swedish Cancer Society supported the epigenetic studies. The Centre for Biosciences, the Knut and Alice Wallenberg Foundation, and the Swedish Research Council supported the Live Cell imaging Unit at the Department of Biosciences and Nutrition, Karolinska Institutet, used for live cell imaging. ERC-2007-Stg/208237-Luedde-Med3-Aachen funded the miRNA studies. The UCL Business supported the development of the three-dimensional nanocomposite scaffold. We thank all the health professionals of the Karolinska University Hospital in Huddinge, Stockholm, Sweden, without whom the transplantation could not have been done; Harvard Apparatus (Hollison, MA, USA) and Hugo Sachs Elektronik-Harvard Apparatus GmbH (March-Hugstetten, Germany) for supporting us with the bioreactor and the supervision of its use; Peter Güntner, for image analysis and measurements for scaffold production, and Anders Svensson, for three-dimensional volume image rendering, both from the Department of Radiology, Karolinska University Hospital Huddinge, Stockholm, Sweden; all the staff of the Landspitali University Hospital in Reykjavik, for the excellent support with the preoperative and postoperative care of the patient; Alessandra Bianco and Costantino Del Gaudio from Department of Science and Chemical Technologies, Intrauniversitary Consortium for Material Science Technology (INSTM), Research Unit Tor Vergata, Rome, Italy, for bi-dimensional and three-dimensional mathematical model for tracheal lateral area assessment; Iyadh Douagi from the Center of Hematology and Regenerative Medicine, Department of Medicine, Karolinska Insitutet for his assistance with flow cytometry; and Ulrika Felldin from ACTREM, Karolinska Institutet for her assistance with cell isolation.

References
1 Macchiarini P. Primary tracheal tumours. *Lancet Oncol* 2006; 7: 83–91.
2 Gaissert HA, Burns J. The compromised airway: tumors, strictures, and tracheomalacia. *Surg Clin North Am* 2010; 90: 1065–89.
3 Grillo HC. Primary tracheal tumours. In: HC Grillo, ed. Surgery of the trachea and bronchi. Hamilton: BC Decker, 2004: 791–802.
4 Macchiarini P, Jungebluth P, Go T, et al. Clinical transplantation of a tissue-engineered airway. *Lancet* 2008; 372: 2023–30.
5 Go T, Jungebluth P, Baiguera S, et al. Both epithelial cells and mesenchymal stem cell derived chondrocytes contribute to the survival of tissue-engineered airway transplants in pigs. *J Thorac Cardiovasc Surg* 2010; 139: 437–43.
6 Sigurdsson MI, Sigurdsson H, Hreinsson K, Simonardottir L, Gudbjartsson T. Bronchiovenous fistula causing bleeding and air embolism: an unusual complication of bronchoscopic tumor resection. *Am J Respir Crit Care Med* 2011; 183: 681–82.
7 Ahmed M, Ghanbari H, Cousins BG, Hamilton G, Seifalian AM. Small calibre polyhedral oligomeric silsesquioxane nanocomposite cardiovascular grafts: influence of porosity on the structure, haemocompatibility and mechanical properties. *Acta Biomater* 2011; 7: 3857–67.
8 Baiguera S, Jungebluth P, Burns A, et al. Tissue engineered human tracheas for in vivo implantation. *Biomaterials* 2010; 31: 8931–38.
9 Macchiarini P, Altmayer M, Go T, et al. Technical innovations of carinal resection for nonsmall-cell lung cancer. *Ann Thorac Surg* 2006; 82: 1989–97.
10 Lizé M, Herr C, Klimke A, Bals R, Dobbelstein M. MicroRNA-449a levels increase by several orders of magnitude during mucociliary differentiation of airway epithelia. *Cell Cycle* 2010; 9: 4579–83.
11 Bihrer V, Friedrich-Rust M, Kronenberger B, et al. Serum miR-122 as a biomarker of necroinflammation in patients with chronic hepatitis C virus infection. *Am J Gastroenterol* 2011; 106: 1663–69.
12 Atala A, Bauer SB, Soker S, Yoo JJ, Retik AB. Tissue-engineered autologous bladders for patients needing cystoplasty. *Lancet* 2006; 367: 1241–46.
13 Pham C, Greenwood J, Cleland H, Woodruff P, Maddern G. Bioengineered skin substitutes for the management of burns: a systematic review. *Burns* 2007; 33: 946–57.
14 Behrend M, Kluge E, Von Wasielewski R, Klempnauer J. The mechanical influence of tissue engineering techniques on tracheal strength: an experimental study on sheep trachea. *J Invest Surg* 2002; 15: 227–36.
15 Gilbert TW, Gilbert S, Madden M, Reynolds SD, Badylak SF. Morphologic assessment of extracellular matrix scaffolds for patch tracheoplasty in a canine model. *Ann Thorac Surg* 2008; 86: 967–74.
16 Bader A, Macchiarini P. Moving towards in situ tracheal regeneration: the bionic tissue engineered transplantation approach. *J Cell Mol Med* 2010; 14: 1877–89.
17 de Mel A, Punshon G, Ramesh B, et al. In situ endothelialization potential of a biofunctionalised nanocomposite biomaterial-based small diameter bypass graft. *Biomed Mater Eng* 2009; 19: 317–31.
18 Seifalian AM, Salacinski HJ, Tiwari A, Edwards A, Bowald S, Hamilton G. In vivo biostability of a poly(carbonate-urea) urethane graft. *Biomaterials* 2003; 24: 2549–57.
19 Kannan RY, Salacinski HJ, Butler PE, Seifalian AM. Polyhedral oligomeric silsesquioxane nanocomposites: the next generation material for biomedical applications. *Acc Chem Res* 2005; 38: 879–84.
20 Kshettry VR, Kroshus TJ, Hertz MI, Hunter DW, Shumway SJ, Bolman RM III. Early and late airway complications after lung transplantation: incidence and management. *Ann Thorac Surg* 1997; 63: 1576–83.
21 Santacruz JF, Mehta AC. Airway complications and management after lung transplantation: ischemia, dehiscence, and stenosis. *Proc Am Thorac Soc* 2009; 6: 79–93.
22 Puchalski J, Lee HJ, Sterman DH. Airway complications following lung transplantation. *Clin Chest Med* 2011; 32: 357–66.
23 Pitchford SC, Furze RC, Jones CP, Wengner AM, Rankin SM. Differential mobilization of subsets of progenitor cells from the bone marrow. *Cell Stem Cell* 2009; 4: 62–72.
24 Mansilla E, Marin GH, Drago H, et al. Bloodstream cells phenotypically identical to human mesenchymal bone marrow stem cells circulate in large amounts under the influence of acute large skin damage: new evidence for their use in regenerative medicine. *Transplant Proc* 2006; 38: 967–69.
25 Hannoush EJ, Sifri ZC, Elhassan IO, et al. Impact of enhanced mobilization of bone marrow derived cells to site of injury. *J Trauma* 2011; 71: 283–91.
26 Marquez-Curtis LA, Turner AR, Sridharan S, Ratajczak MZ, Janowska-Wieczorek A. The ins and outs of hematopoietic stem cells: studies to improve transplantation outcomes. *Stem Cell Rev* 2011; 7: 590–607.
27 Schraufstatter IU, Discipio RG, Zhao M, Khaldoyanidi SK. C3a and C5a are chemotactic factors for human mesenchymal stem cells, which cause prolonged ERK1/2 phosphorylation. *J Immunol* 2009; 182: 3827–36.
28 Moll G, Jitschin R, von Bahr L, et al. Mesenchymal stromal cells engage complement and complement receptor bearing innate effector cells to modulate immune responses. *PLoS One* 2011; 6: e21703.

Informed Consent

I, Mr. born on the 20.06.1973 (Personal ID in Iceland: , and resident in Reykjavik, Iceland, patient from the Department of ENT of the Karolinska Hospital in Huddinge declare voluntarily that:

I have been extensively informed by Prof. Paolo Macchiarini about the possibility of a complete resection of my primary malignant tracheal tumor and its reconstruction with a synthetic polymer-based and completely biocompatible tracheal scaffold reseeded *ex vivo* with autologous mesenchymal stem cells and *in vivo* with upper respiratory cells. I understand that I have currently shortness of breath and was found to have a primary carcinoma (a mucoepidermoid carcinoma) of the trachea, judged inoperable with traditional airway surgery. The tracheal tumor extends across the right tracheobronchial angle over a length of 5 cm, confirmed by CT and PET scans. The PET-CT shows no distant spread.

I have read as well the protocol of the transplant procedure, written in English, and understand that this represents the only chance of survival I have. A trachea of corresponding length and size will be custom-made at the University College in London by Prof. Seifalian and that Prof. Macchiarini will take the scaffold to Stockholm. I would then undergo a redo median sternotomy (re-opening of the chest) to take of the tracheal tumor using classic surgical airway principles. Before surgery (on June 7th), 200 to 300 mL of bone marrow would be aspirated from my left or right iliac crest and processed by Prof. LeBlanc K so that undifferentiated mesenchymal stem cells would be used for the reseeding process (48-72 hrs) using the bioreactor described in the Protocol.

At the time of transplantation, islands of respiratory cells will be taken from the right and left nose, and used to resurface the internal layer of the graft to promote re-epithelialization. Once the primary tracheal tumor has been resected, the tracheal scaffold will be reseeded with the above mentioned cells (respiratory cells on the internal) within the native tracheal bed of my body. Once the reseeding has been made, the tracheal graft will be anastomosed proximally and distally to recreate a trachea and tracheobronchial bifurcation, and wrapped with the *omentus major* (vascularised fat from the big stomach curve) to provide vascularisation and protect against radiation therapy (usual manoeuvres in lung transplantation). To boost the regeneration process, a perioperative treatment with local injection of transforming growth factor-B1 (50µg) (transforms mesenchymal stem cells into chondrocytes), granulocyte-coloning stimulating factor (10 mg/kg) (recruits progenitor endothelial cells) and erythropoietin (10.000UI) (reduces apoptosis) will be given for 2 weeks only. These drugs will be given at "regenerative" doses and have no side-effects. I have also been informed that tissue engineered graft will not require any immunosuppression at any time, and especially its side-effects.

Anaesthesia will be general and through selective orotracheal tube, using arterial monitoring lines, urinary bladder catheter, epidural analgesia and cardiopulmonary by-pass stand-by. Complications from this transplant could be postoperative bleeding, left recurrent nerve palsy, respiratory infections, anastomotic complications, wound infections, respiratory insufficiency and requirement of mechanical ventilation.

I have been informed clearly about every single details, and my questions and doubts have been clarified without any restrictions. It is therefore that I liberally take the decision to authorize the above mentioned procedure with the understanding that I could retract this consent at any time. As proof of willingness, I sign this document.

Huddinge, 26 the June 2011

Doctor Signature

Prof. .....

Signature of the patient

Mr .....

Karolinska Universitetssjukhuset 11001412308
Thoraxkliniken, Solna
N14 Thorax-IVA
171 76 Stockholm
tel: 08-517 748 04 fax:08-517 757 44

Appendix 6

* 2011-06-09 09:12 Jan Liska, Läk S - N14/24 Thiva/Thima (låst)

OPERATIONSBERÄTTELSE

Preop. bedömn.

36-årig man, tidigare väs frisk, ursprungligen från Eritrea, boende på Island sedan 2 år tillbaka. För 19 månader sedan sökt p g a stridorös andning, utredning visade en tumör i distala delen av trachea med nästintill totalstopp. Man gjorde då akut kirurgi för att avlägsna tumören via bronkoskopi. I samband med denna åtgärd perforerades trachea och även en lungartärgren samt vena azygos. Tillståndet ledde till omedelbar exploration via sternotomi och man kunde laga skadan med hjälp av hjärt/lungmaskinstöd. Dessutom exstirperades tumören lokalt. Efter förlängd vårdtid återhämtade sig pat mycket bra. Har sedan dess haft ett recidiv som strålbehandlats, har också haft en episod med miliar tuberkulos som är utläkt nu. Tumören har recidiverat och är av lågt diff mykoepidermoid cancer och har nu återigen andningsbesvär. Utredning med CT och PET-CT samt bronkoskopi visar att tumören är recessabel och att det inte föreligger någon misstanke på metastasering. Han remitteras därför hit för åtgärd i form av trachealresektion inkluderande carina samt rekonstruktion med en polymerprotes som förbehandlats med pats egna stamceller och slemhinna.

Assistent

Tomas Gudjarsson (thoraxkirurg från Reykjavik)
Jan Liska (Thoraxkirurgkliniken, Karolinska Univ sjh)
Paolo Macchiarini
K-H Grinnemo

Diagnos enl ICD-10

C339 Malign tumör i luftstrupen

Operationsdatum

11-06-09

Operations- åtgärdskod

GBC06 Resektion och rekonstruktion av trakea med protes
GBC13 Resektion och rekonstruktion av carina med protes
GBB00 Trakeostomi

Operationsförlopp

Resternotomi med cirkelsåg, i samband med denna liten skada på vena anonyma som ombesörjs med en 4-0 Prolene. Fridissektion av högerhjärtat och aorta ascendens (Liska). Fridissektionen fortsätter sedan (Macciarini) av cava superior, vena anonyma samt trachea proximalt, när man kommer till baksidan av vena cava finns här framför allt adherenser från tidigare operation samt strålfibros. Det går inte att få fritt utan att man delar av cavan mot detta område

Karolinska Universitetssjukhuset 11001412308
Thoraxkliniken, Solna
N14 Thorax-IVA
171 76 Stockholm
tel: 08-517 748 04 fax:08-517 757 44

längst ned. Innan dess ligeras vena azygos intrapleuralt. När man delat cavan från det fibrotiska området kring trachea på längden kan man lätt sy över denna med fortlöpande 5-0 Prolene. Ingen lumeninskränkning på cavan. Fortsatt dissektion av arteria pulmonalis på höger sida och utmed trachea proximalt inga bekymmer. I samband med dissektion av bifurkationen får man en skada på arteria pulmonalis som delas över kärltänger på höger sida alldeles mot carinaområdet. Så småningom kan sedan både höger huvudbronk och vänster huvudbronk fridissikeras. Man ser ingen makroskopisk överväxt av tumörvävnad, däremot en hel del fibrösa förändringar till följd av tidigare operationsingrepp samt strålning. Trachea delas av cirka 4-5 cm ovan carina och höger huvudbronk alldeles intill ovanlobsbronkens avgång. Vänster huvudbronk delas av cirka 1,5 cm från carina. Makroskopiskt ingen tumörväxt vilket även verifieras vid fryssnitt. Under tiden som dr Macciarini preparerar trachealprotesen sutureras pulmonalisartären (Liska) medelst interposition av ett 9 mm:s Dacrongraft. Får en tillfredsställande och bra anastomos med gott flöde i pulmonalisartären. Pat ventileras omväxlande med syrgaskateter i vänster huvudbronk samt en endotracheal tub som läggs via operationssåret. Tillfredsställande syresättning. Stabil cirkulation. Något förhöjda koldioxidvärden, i övr u a. Dr Macciarini syr sedan ner trachealprotesen. Börjar med anastomosen mot höger bronk som är tämligen mödosam. Syr först en fortlöpande rad posteriort och därefter enstaka suturer i den anteriora delen med 3-0 Prolene. Övergår sedan till den vänstra bronkanastomosen som sys på samma sätt. I samband med att man satt de enstaka suturerna i den anteriora delen fås återigen en skada på pulmonalisartären. Efter att kärltänger placerats här får så småningom det tätt. Fortsätter nu att avsluta denna bronkanastomos. Syr sedan den proximala tracheala anastomosen på samma sätt som de tidigare anastomoserna d v s fortlöpande sutur i bakväggen och framtill med enstaka suturer. Anastomosen blir harmonisk och bronkoskopiskt föreligger fina förhållanden med öppna anastomoser, inget påtagligt luftläckage. Övergår sedan till att reparera lungartären återigen (Liska). Då vi försöker exponera området där kärltången har satts tidigare börjar det blöda ymnigt. Vi beslutar då att genomföra reparation av lungartären genom att anbringa en kärltång på cava inferior och banda cava superior d v s genom en inflödesocklusion då vi planerar att göra reparationen när högerhjärtat är tomt. Risk finns vid ECMO-behandling i samband med en ev reparation för luftläckage in oxynatorn vilket är delitärt varför vi beslutar ang denna tidigare nämnda processen. Under inflödesocklusionen får pat naturligtvis

Karolinska Universitetssjukhuset 11001412308
Thoraxkliniken, Solna
N14 Thorax-IVA
171 76 Stockholm
tel: 08-517 748 04 fax:08-517 757 44

lågt blodtryck då minimalt med blod går över till vänsterhjärtat men vi kan hålla ett systoliskt tryck kring 35-40 med en märkligt nog tämligen god saturation. När det är minimal blödning i lungartären till följd av denna åtgärd kan vi sedan reparera densamma med pledgeterade suturer, efter en process på 4-5 minuter kan vi återigen släppa på blodflödet till hjärtat och pat återhämtar sig mycket snabbt. Lägger Flo-Seal, Tiesel och Surgicel i det reparerade området. Ingen kvarstående blödning. Sedan fortsätter operationen med att först lägger upp oment kring anastomosområdet mellan trachea och protesen samt vid bifurkationen. Slutligen slutes sternum efter dränageläggning i etager liksom bukincisionen. Avslutningsvis läggs en tracheostomi (P Macchiarini). Pat överstår ingreppet väl och vid överflyttning till IVA har pat stabil cirkulation och tillfredsställande ventilation.

---------- slut utskrift ----------

FRÅN

STOCKHOLMS LÄNS LANDSTING

Karolinska Universitetssjukhuset
Karolinska Universitetslaboratoriet
Klin Pat/Cyt lab

Tfn

B: 11001-341-306
S: 11001-341-306
F: 11001-341-306
R: 1026-7510367-9
L: T12760-11

SVAR PATOLOGI/CYTOLOGI

Appendix 7

TILL

Karolinska Universitetssjukhuset
Thoraxkliniken, Solna
N 13/23 Thorax
171 76 Stockholm

Regnr
T12760-11

Provtagningstid:	2011-08-04 10:00	Remittent:	Karl-Henrik Grinnemo
Ankomstid lab:	2011-08-04	SNABBSVAR:	Tfn: 0700568440

Preparatets natur: Syntetisk trachea med inodlade autologa celler

Frågeställning: Strukturell översikt av det syntetiska graftet, extracellulära matrix proteiner? engraftade celler?

Anamnes: Det vi skickar för undersökning är samma graft (syntetisk trachea) som implanterades i pat i juni i år. Det här graftet är syntetiskt och har samodlats med autologa stamceller. Vi är därför intresserade att studera ur strukturen på graftet ser ut när det samodlats med celler och vill därfär ha följande analyser:
1) HTX 2) Giemsa 3) Mason Trichrome 4) Verhoeffs elastic staining. Materialet består av 3 olika olika delar: vä bronk, hö bronk samt trachea. Preparaten ska paraffininbäddas

Strålbehandlad: Nej

SVAR

UTLÅTANDE
2011-09-06 T12760/2011
2011-442098

I snitten från de insända tre rör syntetisk trachea som representerar vänster bronch, höger bronch samt trachea ses likartad bild av ej färgbart poröst material med dubbelbrytande karaktär. På ytan av detta syntetiska material kan endast ett fåtal smala mesenkymala celler förmodas. Något välutveckat cellager kunde ej identifieras.

Tillägg: Vid specialfärgning och i ytterligare utskurna bitar framkomer ej mer detekterbart material som vid ovan.

DIAGNOS
Se ovan.

BIOBANKSINFORMATION
Patienten vill inte att provet lagras, men svarstalong saknas eller har ännu ej registrerats. Provet lagras tills vidare i avvaktan på att svarstalong inkommer/registreras.

Bela Bozoky 2011-12-01

----------slut----------

Framställd
2011-12-01 11:58

STOCKHOLMS LÄNS LANDSTING

SVAR PATOLOGI/CYTOLOGI

Appendix 8a

FRÅN
Karolinska Universitetssjukhuset
Karolinska Universitetslaboratoriet
Klin Pat/Cyt lab

Tfn

B: 11001-341-306
S: 11001-341-306
F: 11001-341-306
R: 1026-7558235-1
L: T13253-11

TILL
Karolinska Universitetssjukhuset
Thoraxkliniken, Solna
N 13/23 Thorax
171 76 Stockholm

Regnr
T13253-11

Provtagningstid: 2011-08-16 08:00
Ankomstid lab: 2011-08-17

Remittent: Karl-Henrik Grinnemo
SNABBSVAR: Tfn: 0700568440

Preparatets natur: Tre biopsier från transplanterad trachea
Frågeställning: Ett frysblock skall snittas och analyseras. De andra två blocken skall endast snittas och förvaras i -80 C.

Anamnes: Dessa biopsier är från samma graft (syntetisk trachea) som implanterades i pat i juni i år. Analyser som skall göras på blocket är: Färgning för epitelceller och kärnfärgning; basallager; vaskularisering och mukosa.
HTX , Mason Trichrome

Vänligen kontakta Dr. Jungebluth (0700568440) angående upphämtning av de två snittade blocken som förvaras i -80 så snabbt som möjligt.
Strålbehandlad: Nej

SVAR

Tidigare preliminärt utlåtande
2011-08-22 T13253/2011
2011-442098

I snitten från ena insända biopsin framkommer en vävnadscylinder som består av eosinofilt material snarast som vid degenererad bindväv med granulocytär reaktion vid ena kanten av biopsin. Vid dubbelbrytande mikroskopisk undersökning kan kollagentrådar detekteras. Även trichromfärgning visar kollagentrådar. Ingen bevarad kärnfärgning vilket talar för avancerad degeneration - nekros. Fokalt kan basofil granulärt material påvisas. Den kan representera dystrofisk förkalkning.

Vid trichromfärgning kan vidare erytrocyter delvis till synes i skuggformer av kärlstrukturer delvis interstitiellt förmodas.

Vid PAS färgning kan svamp hyfer identifieras. Gram-färgning visar bakterikolonier.

Immunhistokemisk undersökning kommer att göras för att försöka identifiera vävnadsstrukturer i nekrotisk bindväv.
Tidigare diagnos
Preliminär:
Nekrotisk bindväv med svamp och bakterier. Se ovan.
BIOBANKSINFORMATION
Patienten vill inte att provet lagras, men svarstalong saknas eller har ännu ej registrerats. Provet lagras tills vidare i avvaktan på

Framställd
2011-08-26 08:36

FRÅN

Karolinska Universitetssjukhuset
Karolinska Universitetslaboratoriet
Klin Pat/Cyt lab

Tfn

B: 11001-341-306
S: 11001-341-306
F: 11001-341-306
R: 1026-7558235-1
L: T13253-11

Appendix 8b

TILL

Karolinska Universitetssjukhuset
Thoraxkliniken, Solna
N 13/23 Thorax
171 76 Stockholm

Regnr
T13253-11

att svarstalong inkommer/registreras.

KOMPLETTERANDE UTLÅTANDE
2011-08-26 T13253/2011
2011-442098

De övriga två djupfrysta biopsier är också inbäddade och nedsnittade. Ena visar likartad bild av nekrotisk bindväv med detekterbara svamphyfer som vid ovan.

Den andra utgörs av kapillärrik granulationsvävnad delvis med ulcererad yta, delvis med igenkännbar respiratorisk epitelbeklädnad som visar skivepitelmetaplasi.

Biopsier från transplanterad trachea med nekrotisk bindväv med svamp och bakterier samt kapillärrik granulationsvävnad.
DIAGNOS
Slutlig: Biopsier från transplanterad trachea med nekrotisk bindväv med svamp och bakterier samt kapillärrik granulationsvävnad.
BIOBANKSINFORMATION
Patienten vill inte att provet lagras, men svarstalong saknas eller har ännu ej registrerats. Provet lagras tills vidare i avvaktan på att svarstalong inkommer/registreras.
Bela Bozoky 2011-08-26
----------slut----------

Biomaterials 34 (2013) 4057–4067

Contents lists available at SciVerse ScienceDirect

Biomaterials

journal homepage: www.elsevier.com/locate/biomaterials

Verification of cell viability in bioengineered tissues and organs before clinical transplantation

Philipp Jungebluth [a,1], Johannes C. Haag [a,1], Mei L. Lim [a], Greg Lemon [a], Sebastian Sjöqvist [a], Ylva Gustafsson [a], Fatemeh Ajalloueian [a], Irina Gilevich [a], Oscar E. Simonson [b], Karl H. Grinnemo [b], Matthias Corbascio [b], Silvia Baiguera [a], Costantino Del Gaudio [c], Staffan Strömblad [d], Paolo Macchiarini [a,*]

[a] Advanced Center for Translational Regenerative Medicine (ACTREM), Karolinska Institutet, Huddinge, Stockholm, Sweden
[b] Department of Molecular Medicine and Surgery, Division of Cardiothoracic Surgery, Karolinska Institutet, Karolinska University Hospital, Solna, Stockholm, Sweden
[c] University of Rome "Tor Vergata", Department of Industrial Engineering, Intrauniversitary Consortium for Material Science and Technology (INSTM), Research Unit "Tor Vergata", Rome, Italy
[d] Center for Bioscience, Department of Biosciences and Nutrition, Karolinska Institutet, Huddinge, Stockholm, Sweden

ARTICLE INFO

Article history:
Received 5 February 2013
Accepted 20 February 2013
Available online 6 March 2013

Keywords:
Airway tissue engineering
Transplantation
Bioartifical trachea
Cell proliferation assay
Cell viability
Synthetic scaffold

ABSTRACT

The clinical outcome of transplantations of bioartificial tissues and organs depends on the presence of living cells. There are still no standard operative protocols that are simple, fast and reliable for confirming the presence of viable cells on bioartificial scaffolds prior to transplantation. By using mathematical modeling, we have developed a colorimetric-based system (colorimetric scale bar) to predict the cell viability and density for sufficient surface coverage. First, we refined a method which can provide information about cell viability and numbers in an *in vitro* setting: *i)* immunohistological staining by Phalloidin/DAPI and *ii)* a modified colorimetric cell viability assay. These laboratory-based methods and the developed colorimetric-based system were then validated in rat transplantation studies of unseeded and seeded tracheal grafts. This was done to provide critical information on whether the graft would be suitable for transplantation or if additional cell seeding was necessary. The potential clinical impact of the colorimetric scale bar was confirmed using patient samples. In conclusion, we have developed a robust, fast and reproducible colorimetric tool that can verify and warrant viability and integrity of an engineered tissue/organ prior to transplantation. This should facilitate a successful transplantation outcome and ensure patient safety.

1. Introduction

Bioengineered tissues and organs with simple architectures have recently been successfully transplanted in patients with end-stage organ failure or disease [1,2]. Among them are tracheal scaffolds, either as decellularized donor tissue [2] or as nanotechnology-based artificial materials [3]. For a positive outcome, it seems that interactions between natural or artificial scaffolds and autologous bone marrow stromal cells, using bioreactors, play pivotal roles for clinical tissue and whole organ regeneration [4,5]. In the near future, this tissue engineering (TE) strategy could also be transferred to more complex structures, such as the heart or lung, and promising experimental findings in these areas have been reported [6–8].

In a clinical transplantation, scaffolds are usually reseeded with cells in bioreactors and implanted into humans within a few hours [2,3]. During this period, timing is important for obtaining vital information about the cells on the graft prior to transplantation. There is a wide range of techniques available to image and quantify the number of cells that are viable and proliferating, such as flow cytometry, scanning electron microscopy, confocal microscopy, *etc.* Unfortunately, the time- and labor-intensive protocols and the need for trained staff to reliably evaluate data can delay results. This severely increases the risk of implanting re-seeded scaffolds with non-functional cells. Cell labeling prior to seeding on the scaffold can be an alternative useful tool for cell tracking, but ethical guidelines would limit this technology in patients as the incorporated cell marker may produce unpredictable side effects.

* Corresponding author. Advanced Center for Translational Regenerative Medicine (ACTREM), Division of Ear, Nose and Thoat (CLINTEC), Karolinska Institutet, Hälsovägen 7, Plan 6, Huddinge, SE-141 86 Stockholm, Sweden. Tel.: +46 760 503 213 (mobile); fax: +46 (0)8 774 7907.
E-mail addresses: paolo.macchiarini@ki.se, pmacchiarini@thoraxeuropea.eu (P. Macchiarini).
[1] Contributed equally to this work.

0142-9612/$ – see front matter © 2013 Elsevier Ltd. All rights reserved.
http://dx.doi.org/10.1016/j.biomaterials.2013.02.057

In this study, we aimed to produce a reliable method to evaluate the pre-implantation state of cell-seeded bioartificial scaffolds in real time, *i.e.* maximum 2–3 h. To deliver a safe, reproducible and non-laborious method to detect and validate the viability and proliferation rate of attached cells on bioartificial scaffolds, we modified the 3-(4,5-dimethylthiazol-2-yl)-2,5-diphenyltetrazolium bromide (MTT) overnight protocol to be effective within less than 3 h [9], and stained cells with Phalloidin to label intracellular F-actin Refs. [10], and 4′,6-diamidino-2-phenylindole (DAPI) to visualize nuclei by a fluorescent microscope. This structural analytical panel was validated in rat transplantation studies of unseeded and seeded tracheal grafts. On the basis of these data, we could further use mathematical models to develop a colorimetric-based system to predict graft/scaffold cell density with a corresponding surface coverage. This method can provide critical information to decide whether a graft is suitable for transplantation or if additional intervention, e.g. additional cell seeding, is necessary.

2. Materials and methods

Male Sprague Dawley rats ($n = 16$) were used as donors for mesenchymal stromal cell (MSC) isolation and as recipients in the *in vivo* transplantation model. All animals were treated in compliance with the "Principles of laboratory animal care" formulated by the National Society for Medical Research and the "Guide for the care and use of laboratory animals" prepared by the Institute of Laboratory Animal Resources, National Research Council, and published by the National Academy Press, revised 1996. Ethical permission was approved by the Stockholm South Ethical Committee (Sweden) (registration number S74-12).

2.1. Rat mesenchymal stromal cell isolation

Eight animals were used for the *in vitro* study. MSCs were isolated and processed as previously described [11]. Briefly, animals were sacrificed and the bone marrow was flushed out gently from both the femur and tibia with phosphate buffered saline (PBS, Invitrogen, Sweden). The obtained cells were centrifuged and the pellet was resuspended in Dulbecco's Modified Eagle Medium (DMEM, Invitrogen, Sweden) supplemented with 10% Fetal Bovine Serum (FBS, Invitrogen, Sweden) and 1% antibiotic-antimycotic (Invitrogen, Sweden). The cell suspension was seeded in culture flasks (Corning, USA) and cultured for 24 h (37 °C, 5% CO_2). Non-adherent cells were removed and culture medium was changed every three days. Rat MSCs from passages 2 to 5 were used in the study.

2.2. In vivo animal model

Animals ($n = 8$) were anesthetized with a mixture of ketamine and xylazine [ketamine: 100 mg/kg intramuscular (i.m.; Intervet, Boxmeer, Netherlands); xylazine 10 mg/kg (i.m.; Intervet)] injection as a bolus. Under sterile conditions, the tracheae of the recipient animals (200 g–300 g) were exposed *via* an anterior midline cervical incision. Thereafter, we divided the sternohyoid muscles and dissected the cervical fat lobe. The pre-tracheal fascia was opened, the cervical trachea mobilized and traction sutures were placed to retract trachea superiorly.

After that the animals' cervical tracheae were resected and 1 cm replaced by the synthetic based tracheal graft. We utilized a continuous 6-0 polypropylene (Prolene; Ethicon, Inc, Somerville, NJ) suture to anastomose the posterior trachea and 6-0 absorbable polygalactin (Vicryl, Ethicon) interrupted sutures for the anterior trachea. The anastomotic suture knots were then tied outside the lumen. During the entire surgery, the animals were maintained on spontaneous ventilation. After hemostasis, we closed the tissue and skin in a usual fashion and animals were allowed to recover on a heating pad. All animals were observed on a daily basis. Euthanasia was induced at the endpoint of the study (30 days), implanted tracheae were harvested and analyzed both macroscopically and microscopically.

2.3. Colorimetric cell activity assay

3-(4,5-dimethylthiazol-2-yl)-2,5-diphenyltetrazolium bromide (MTT)-assay (Roche, Sweden) is a colorimetric assay that was used to detect viable cells and evaluate the metabolic activity of cells. All samples were analyzed in triplicates. Media and scaffold only were used as negative controls. The MTT substrate (40 μl) was added to each well and were either incubated: 4 h (Protocol I and II) or 1 h (Protocol III) at 37 °C with 5% CO_2. Next, 10% sodium dodecyl sulfate (SDS) in 0.01 M HCl (400 μl) was added across all protocols (I-III) and further incubated overnight (Protocol I) or 1 h (Protocol II and III) at 37 °C, 5% CO_2. The samples were read on a spectrophotometer (SpectraMax 250, Molecular Devices, USA), the absorbance was measured at 570 nm.

2.4. Phalloidin and DAPI staining on seeded synthetic scaffolds

Pieces from the seeded scaffold were cut to an appropriate size with a 6 mm biopsy punch. Samples were fixed in formaldehyde 4% (Histolab, Sweden) for 5–10 min, washed and stained with Phalloidin (Molecular Probes, Sweden) diluted in PBS/0,1% Triton X-100 (2 U/ml) (Sigma–Aldrich, Sweden) and incubated for 30 min. Samples were washed and counterstained with 4′,6′-diamidino-2-phenylindole (DAPI, Sigma–Aldrich, Sweden). Stained cells were either visualized with a fluorescent microscope (Olympus BX-60, Japan) using a 4× (dry, numerical aperture 0,13; Olympus, Japan), 10× objective (dry, numerical aperture 0,3; Olympus, Japan) and 20× objective (dry, numerical aperture 0,5; Olympus, Japan) or on a confocal microscope (Nikon A1+, Japan) using a 10× objective (dry, numerical aperture 0,45; Nikon, Japan).

2.5. Color change evaluation

2.5.1. Cell coverage quantification

Using the DAPI stained samples, cell numbers were either manually counted with ImageJ 1.46R (NIH, Maryland, USA) or an automated software CellProfiler 2.0 (BROAD Institute, Massachusets, USA). The readouts were converted to surface densities, denoted σ having units cm^{-2}, by dividing by the area of the samples (circular pieces with diameter 6 mm). The counted cell densities on samples were plotted against the seeding density, where the error bars indicate the mean and standard deviation of triplicate samples. The cell densities were then converted into values indicating the degree of cell coverage of the surface, using $\theta = A_{cell}\,\sigma \times 100\%$ i.e. multiplying σ by the average area of a single cell, A_{cell}. The images of phalloidin-stained cells [11] were analyzed using the CellProfiler software package to determine the value $A_{cell} = 280\ \mu m^2$.

2.5.2. Color change analysis of laboratory samples

After applying the MTT test to the samples, but prior to solubilizing the formazan crystals, the media was temporarily removed from the wells. A single color digital picture, showing a uniformly illuminated top view of the well plate and the samples, was obtained and imported into MATLAB. The image was converted into a grayscale image by applying the formula $Y = 0.2989 \times R + 0.5870 \times G + 0.1140 \times B$ to the RGB values in the image (using the MATLAB function rgb2gray.m provided with the Image Processing Toolbox). This allowed a single grayscale value, Y, to be obtained for each pixel in the image. The regions of the image corresponding to the upper surface of each sample were selected manually using mouse and cursor input for further analyses. The numerical value of the color change of a seeded sample was calculated using Equation (1):

$$\Delta C = \frac{Y_c - Y_s}{Y_c - Y_m} \times 100\% \tag{1}$$

where Y_s is the average of the grayscale values of the pixels in the sample, Y_c is the average of the grayscale values of the pixels in control samples (unseeded), and Y_m is the average of the grayscale values of pixels of regions where there was maximum purple staining (seeded samples). Hence $\Delta C = 0\%$ corresponds to no color change in the sample relative to the control, and $\Delta C = 100\%$ corresponds to a sample that is completely stained dark purple. The color change values of the samples were calculated using equation (1). The average and standard deviations were calculated for all triplicate sets for the different seeding densities. In order to extrapolate higher values of cell coverage and density, equation (2) was formulated:

$$\theta = \exp\left(\alpha\left(\left(\frac{\Delta C}{100\%}\right)^{\beta} - 1\right)\right) \times 100\% \tag{2}$$

The parameters α and β were fitted using least squares (using the MATLAB function fminsearch.m) to the data of the cell coverage with respect to the color change, yielding $\alpha = 4.25$ and $\beta = 0.58$. The functional form of $\theta(\Delta C)$ was chosen based on the assumption that maximum color change i.e. $\Delta C = 100\%$ corresponds to full coverage of cells on the sample. Equation (2) was used to relate a linear scale of color change, with values in the range of $\Delta C = 0$–100%, to the corresponding cell coverage and cell density values.

2.6. Synthetic scaffolds

The scaffold was designed based on the patient's CT-scan performed 4 weeks prior to the transplantation. The scan was analyzed and then used to create an electrospun, nanofiber-based composite made from polyethylene terephthalate (PET)/polyurethane (PU) supplied by Nanofiber Solutions® (Columbus, OH). The utilized FDA-approved materials, PET and PU, (Regulations, U.S. FDA, 1998) are non-biodegradable polymers that are non-cytotoxic and retain mechanical properties [12].

2.7. Fiber alignment evaluation

Fiber alignment has been evaluated by a custom-made software. Scanning electron microscopy (SEM) images were firstly binarized and then rotated around its center in step of 2°. For each direction the fraction of bright pixels was computed and the resulting standard deviation calculated. Results were represented by means

of a unitary polar plot that is specific for each analyzed electrospun mat. As measurement index, the eccentricity of the fitting ellipse of the polar plot was computed as follows:

$$E = \frac{A_M - A_m}{A_M + A_m} \quad (3)$$

where A_M is the major axis and A_m the minor axis. According to this formulation; $E = 1$ indicates a straight line (unidirectional fiber alignment) and $E = 0$ indicates a perfect circle (randomly arranged fibers). Moreover, the orientation of the fitting ellipse is indicative of the average fiber alignment [11].

2.8. Patient mononuclear cell isolation and cultures

Under aseptic conditions, bone marrow (200 ml) was obtained by punctation of the right and left crista iliaca. Mononuclear cells were isolated though density gradient separation. White blood cells, mononuclear cells, CD34+ cells, colony forming unit-fibroblast, flow cytometric characterisation, viability and sterility analyses were performed. MNCs were resuspended in low-glucose DMEM (Invitrogen, Stockholm, Sweden), transferred at room temperature to Good Manufacturing Practice (GMP) facility (VECURA, Karolinska University Hospital, Huddinge, Sweden). Cells were seeded under sterile conditions with a specially designed bioreactor for 72 h at 37 °C/5%CO_2. Patient's consent was given for all analytical evaluations and publication.

2.9. Scanning electron microscopy

To evaluate cell adhesion and integration of the seeded synthetic tracheal scaffold from the transplanted patient, small pieces from the external and internal part were fixed with 2.5% glutaraldehyde (Merck, Germany) in 0.1 M cacodylate buffer (Prolabo, France) for 2 h at room temperature, rinsed in cacodylate buffer, and dehydrated though an ethanol gradient. Samples were dried overnight and gold sputtered. The samples were used for analysis by SEM (JSM6490, JEOL, Japan).

2.10. Histological analysis

Samples of synthetic trachea from rats or brushing sample from patient were fixed in 10% neutral buffered formalin solution in PBS (pH 7.4) at room temperature. They were washed in distilled water, dehydrated in graded alcohol, embedded in paraffin (Merck, Darmstadt, Germany), and sectioned at 5 mm thickness. Sections were stained with Hematoxylin and Eosin stain (H&E) (Merck, Darmstadt, Germany) and imaged with a microscope at 4× or 20× magnification (Olympus BX-60, Japan).

2.11. Statistical analysis

Results were expressed as mean ± standard deviation. GraphPad Prism 5 (GraphPad Software, California, USA) was used for all statistical analysis, with significance levels of $^*p \leq .05$, $^{**}p \leq .01$, $^{***}p \leq .001$ and $^{****}p \leq .0001$. All data were compared using either an unpaired *t*-test or two-way ANOVA analysis.

3. Results

3.1. Qualitative and quantitative evaluation of attached cells on scaffold

We designed an analytical method that provides rapid information about cell viability and/or cell proliferation on engineered tissues or organs prior to clinical transplantation. We first analyzed cells on scaffold with a commercially available MTT-assay using its standard protocol (4 h MTT and overnight incubation with SDS; Protocol I), and then applied two modified protocols with reduced incubation time: 5 h (4 h with MTT and 1 h SDS; Protocol II) and 2 h (1 h with MTT and 1 h SDS; Protocol III). This was to ensure that the processing time modifications did not alter the qualitative information as compared to the standard protocol. Rat MSCs from passages 2 to 5 were seeded at a density of 7500 cells/cm^2 on PET/PU fiber coated 24 well plates (2 cm^2 surface-area/well; Nanofiber solutions®) as previously described [11]. All samples were measured by absorbance and we obtained significantly differences for all three protocols as compared to unseeded scaffolds (control) (control *versus* protocols I: $p \leq .01$; II: $p \leq .001$ and III: $p \leq .0001$) (Fig. 1A). This showed that the modification in processing time did not alter the qualitative information as compared to the standard method. Therefore, we further evaluated Protocol III (2 h) for its quantitative data. We seeded different cell numbers (2500; 5000; 10,000; 50,000 or 100,000) on 96-well plates with PET/PU nanofiber inserts for 48 h to investigate if cell numbers corresponded to different absorbancy measurements. The higher absorbancy measurements corresponded with higher cell numbers (Fig. 1B,C).

3.2. Quantification of cell density and coverage on scaffolds using mathematical modeling

In order to simplify the readout of the MTT method, we wanted to investigate whether the formazan crystal color change could predict the approximate cell number and surface coverage. Thus, seeded scaffold samples were analyzed after 1 h with MTT without using SDS to solubilize the formazan crystals from the cells (Fig. 2A). Images were imported into MATLAB and RGB color triplets of each pixel in the imported image were converted to grayscale values. An empirical mathematical model was then used to relate cell density, which was calculated on confocal images (Fig. 2B) using Cellprofiler™ 2.0 software package (BROAD Institute, Massachusetts, USA), to the measured color change. The color change values of the samples were computed using equation (1). In Fig. 2C, cell coverage and cell density was plotted against the color change for five different cell numbers used (2500; 5000; 10,000; 50,000 or 100,000). The graph showed that the greater the color change, the greater the coverage and density of cells on sample. We used the obtained data to develop a colorimetric scale bar that can provide the essential information about cell viability, density and surface coverage for engineered tissues and organs.

3.3. Bioengineered graft evaluation in an animal model

Rat tracheal nanofibrous scaffolds made from electrospinning (with an average fiber dimension of internal 0.61 ± 0.25 μm and external 0.52 ± 0.37 μm) were seeded with rat MSCs for 48 h and then orthotopically implanted into male Sprague Dawley rats. Prior to transplantation, we used our optimized MTT method and applied the developed colorimetric scale bar to estimate the surface coverage of the scaffold (Fig. 3A,B). Based on the color changes we found that the scaffold surface coverage was 63.8 ± 9.2%. Throughout the observational period of 30 days post implantation, animals ($n = 5$) showed no signs of health impairment or breathing difficulties. The implanted tracheae were then harvested, and subsequent histological analyses revealed respiratory epithelialization on the internal surface of the implants (Fig. 3C). There were no signs of bacterial or fungal contamination. The external surfaces displayed no marks that would indicate ongoing inflammatory processes, and seemed to have integrated well into the surrounding connective tissue. However, when unseeded rat tracheal scaffolds were transplanted ($n = 3$), after 3 ± 1 days the animals had to be sacrificed due to dyspnea. Histological analyses of these grafts showed near-total luminal occlusions and signs of severe inflammatory responses (Fig. 3D).

3.4. A translational approach, development of a clinical tracheal graft

A 21-year-old female patient suffered from an iatrogenic induced severe tracheal damage that affected the entire organ. An immediate transplantation was necessary to replace the entire trachea with a synthetic based TE tracheal graft. This surgery took place in August 2012 at the Department of Cardiothoracic Surgery and Anesthesiology at the Karolinska University Hospital, Stockholm (Sweden).

From the patient's CT scan, a scaffold was customized using electrospun PET/PU nanofibers (Fig. 4A). The average diameter of the fibers was 1.97 ± 0.32 μm on the internal and 2.15 ± 0.41 μm on

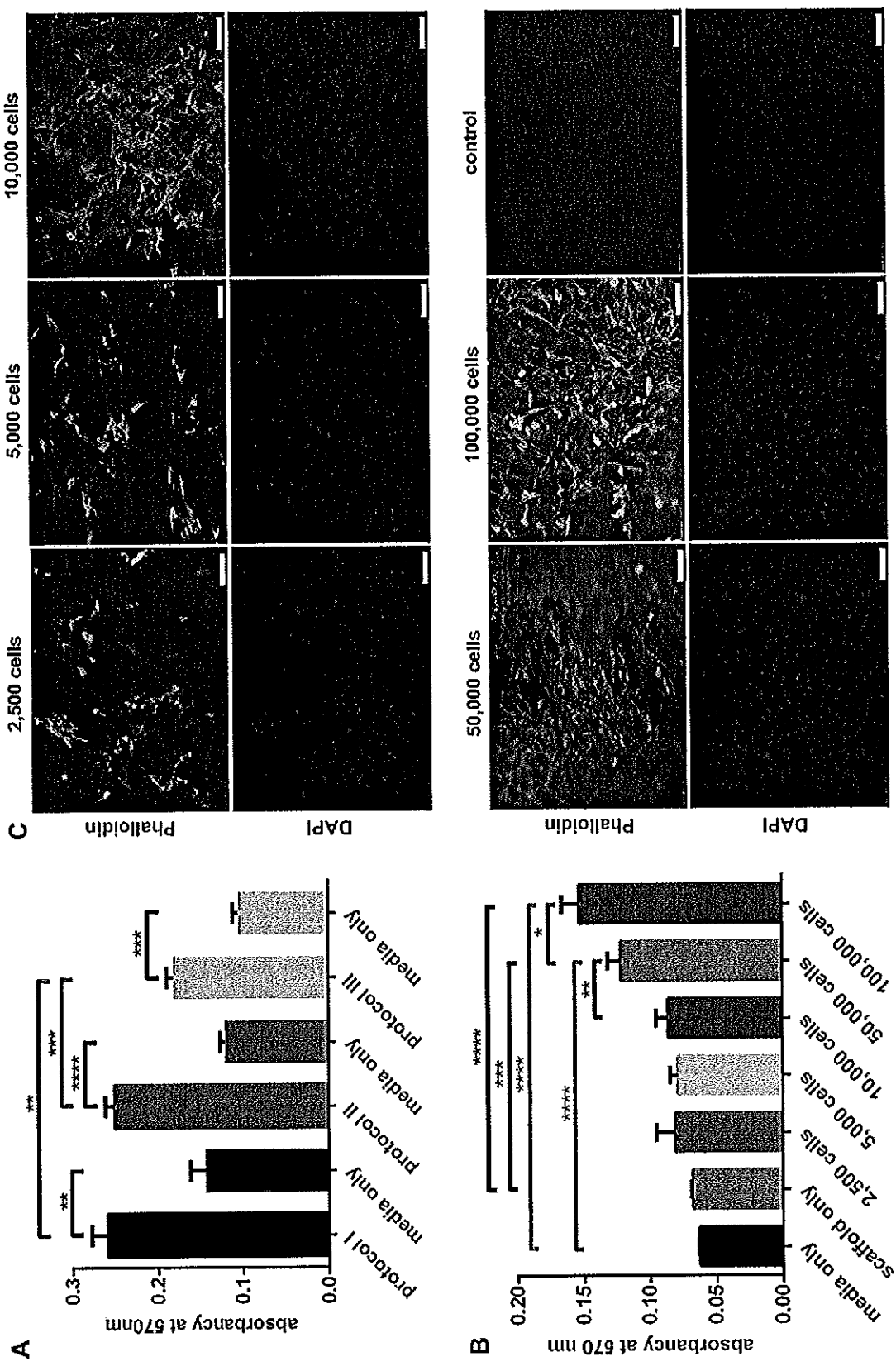

Fig. 1. Absorbance at 570 nm after having performed the colorimetric MTT-assay with the different protocols I-III on seeded PET/PU fiber coated plates after 48 h of culture compared to negative control i.e. media only (A). Absorbance at 570 nm after performing the colorimetric MTT-assay on reseeded pieces of the synthetic scaffold made of PET/PU with either 2500 cells; 5000 cells; 10,000 cells; 50,000 cells or 100,000 cells compared to negative controls i.e. media and scaffold only ($n = 3$) (B). Fluorescent images of seeded synthetic scaffolds with different cell numbers after 48 h culture stained with Phalloidin (green) and DAPI (blue). Magnification 10× scale bar representing 200 μm (C). (For interpretation of the references to colour in this figure legend, the reader is referred to the web version of this article.)

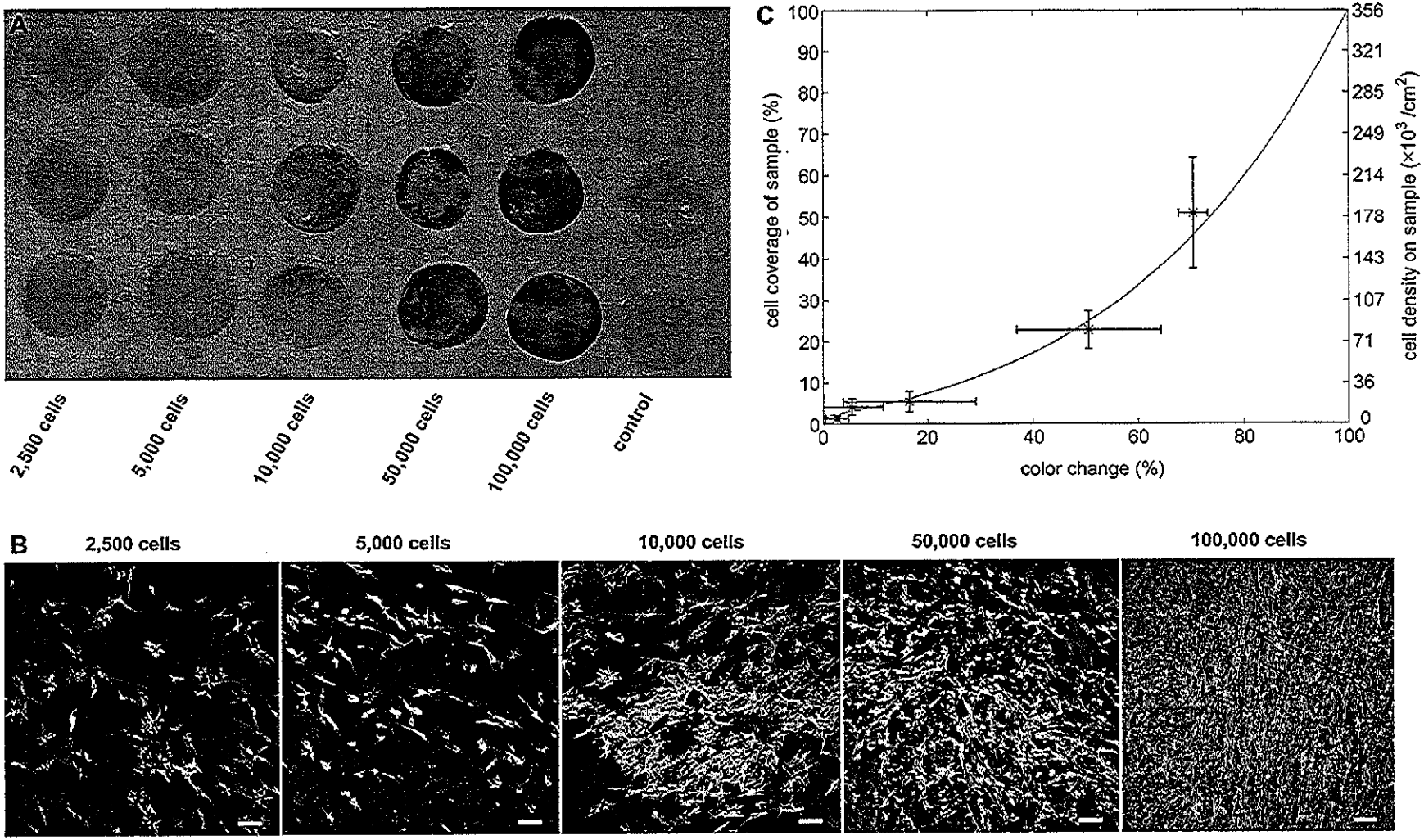

Fig. 2. Macroscopic pictures of seeded synthetic scaffolds with different cell numbers after 1 h incubation with the MTT-reagent (A). Confocal microscopy images on seeded pieces of the synthetic scaffold made of PET/PU with either 2500 cells; 5000 cells; 10,000 cells; 50,000 cells or 100,000 cells, stained with Phalloidin (green) and DAPI (blue). Maximum intensity images of the seeded scaffolds. Magnification 10×; scale bar representing 100 μm (B). Graph is showing cell coverage and cell density on the samples with respect to the color change (C). (For interpretation of the references to colour in this figure legend, the reader is referred to the web version of this article.)

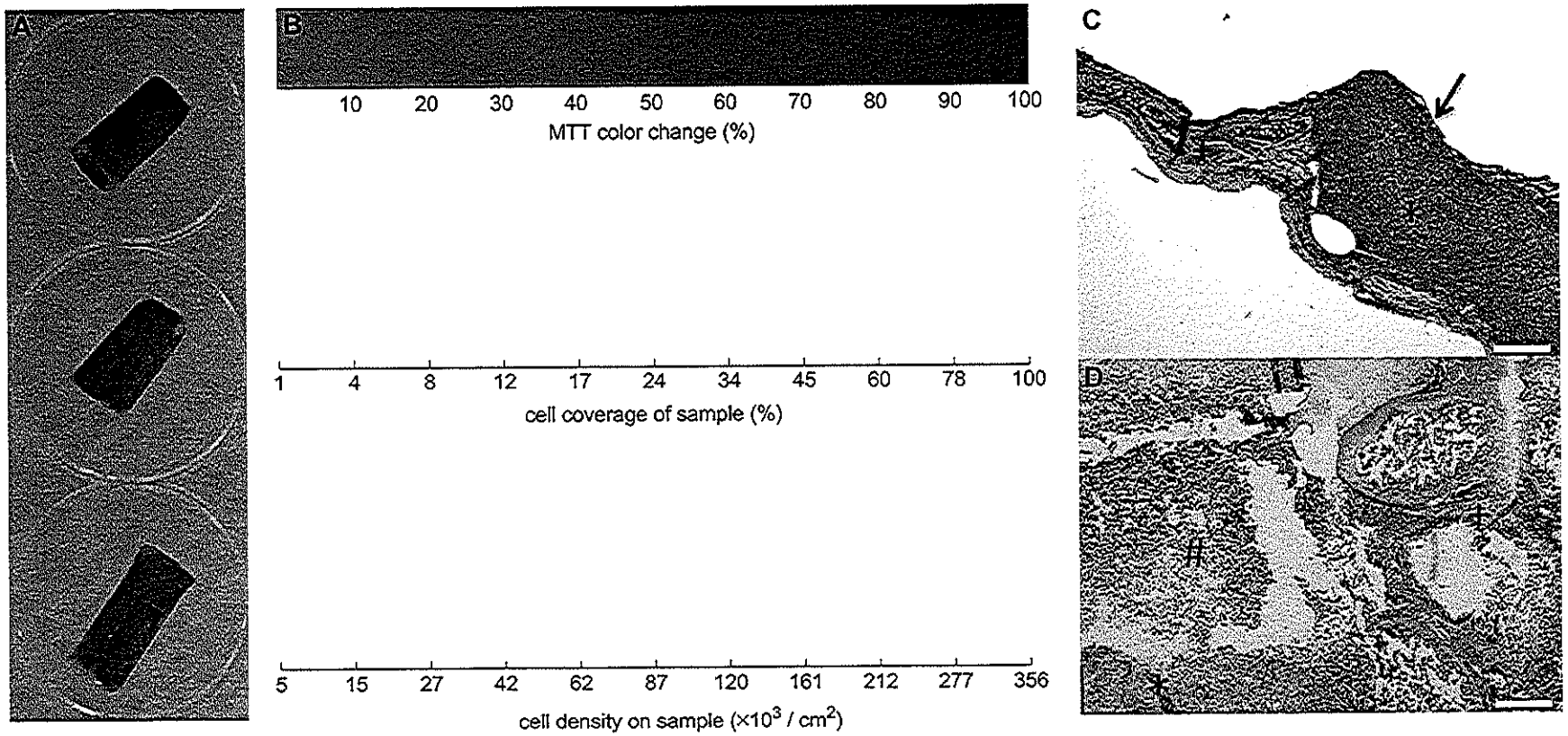

Fig. 3. Macroscopic images of MSCs seeded on synthetic grafts, analyzed with MTT by protocol III (A). Color scale bar is showing the cell coverage and cell density on a seeded sample corresponding to a given color change (B). Images of paraffin sections stained with H&E. Image shows synthetic graft seeded with rat MSCs at day 30 (post transplantation); asterisk indicates synthetic scaffold; + indicates the native trachea; arrow indicates epithelial layer. Magnification 4×; scale bar representing 500 μm (C). Image shows synthetic graft without MSCs on day 3 (post transplantation); asterisk indicates synthetic scaffold; + indicates the native trachea; # indicates increased number of granulocytes. Magnification 4×; scale bar representing 500 μm (D).

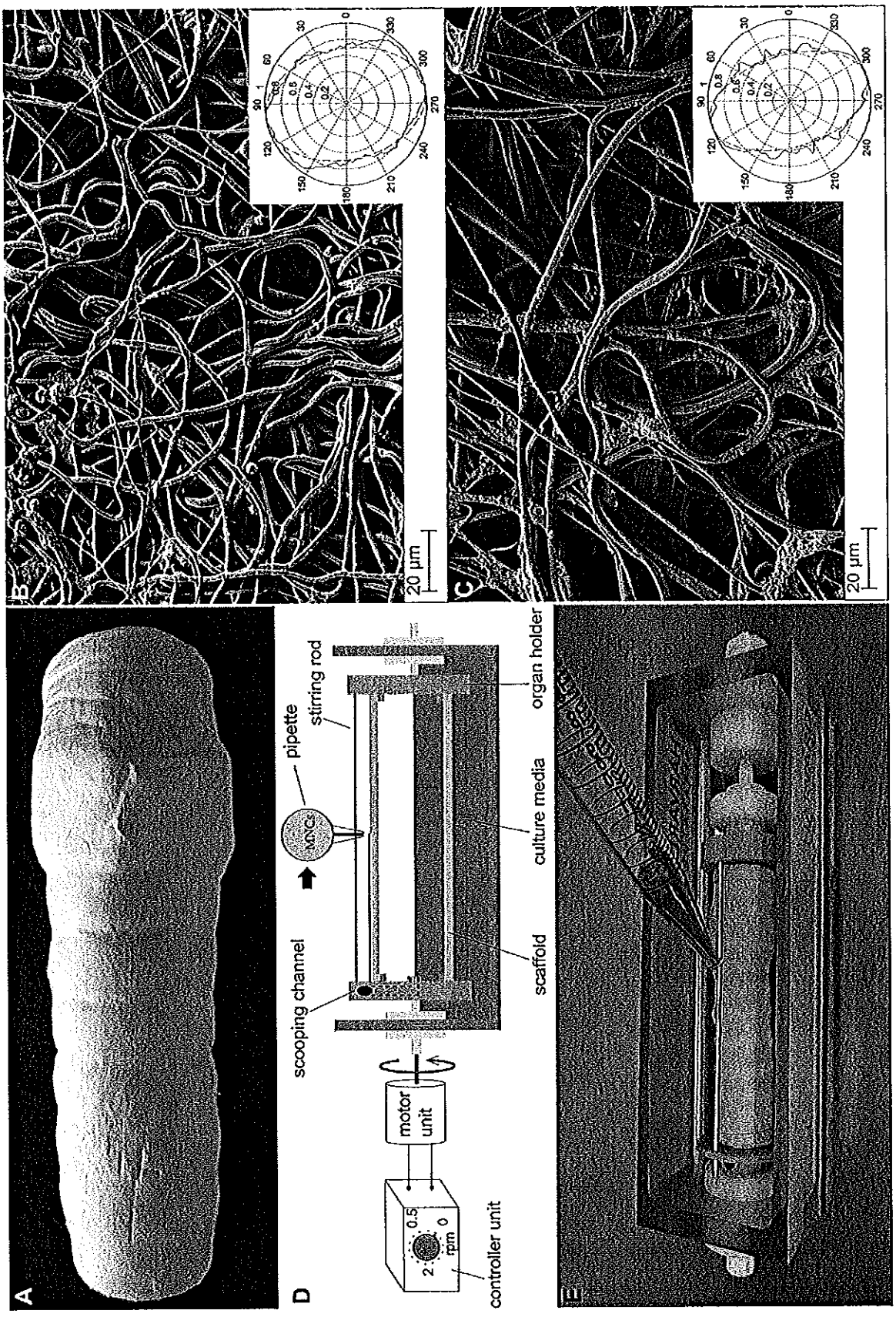

Fig. 4. Picture of a synthetic tracheal scaffold made of PET/PU-based nanofibers (A). SEM images of a synthetic scaffold showing the fiber network made of PET/PU, insets report the computed fiber alignment pattern. Magnification 1.500×: scale bar representing 20 µm (internal B; external C). Schematic drawing of the bioreactor culturing system composed of the bioreactor, motor unit and controller unit with a synthetic tracheal scaffold mounted inside with an organ holder (D). Image of the seeding process on the tracheal scaffold inside the bioreactor prior to transplantation (E).

the external side. The organization of the electrospun fibers mimics the fiber network of a native trachea. To determine the alignment of the transplanted scaffold, SEM images were evaluated on a custom-made image analysis software. The alignment of the fibers was measured at 0.29 ± 0.09 μm on the internal (Fig. 4B) and 0.27 ± 0.08 μm on the external side (Fig. 4C). The scaffold was seeded and cultured for 72 h at 37 °C/5%CO_2 with the patient's own MNCs isolated from bone marrow in a bioreactor as previously described (Fig. 4D,E) [3].

3.5. *Evaluation of the clinical samples, analytical panel with mathematical modeling*

Based on our experimental *in vitro* and *in vivo* results described above, we could develop a colorimetric scale bar and translate it to a clinical scenario of tissue engineered tracheal transplantation. Samples were collected from the tissue engineered tracheal graft prior to transplantation into the patient at two different time points: a) in the morning of the transplantation (samples 1) and b) during the operation when the graft was trimmed to the anatomical needs of the patient (sample 2). Autologous human MNCs stained with Phalloidin/DAPI were counted from three images taken from two clinical samples that yielded cell densities of 115 × 10^3/cm^2 and 148 × 10^3/cm^2. Simultaneous absorbancy readout using the 2h MTT protocol (Protocol III) showed significant differences between the seeded and unseeded control scaffolds (Figs. 5A and 6A). This suggested that the seeded graft contained cells that had attached and were viable and proliferating on both internal and external surfaces.

To investigate the value of our experimentally developed color scale bar, we analyzed the color changes on clinical samples and

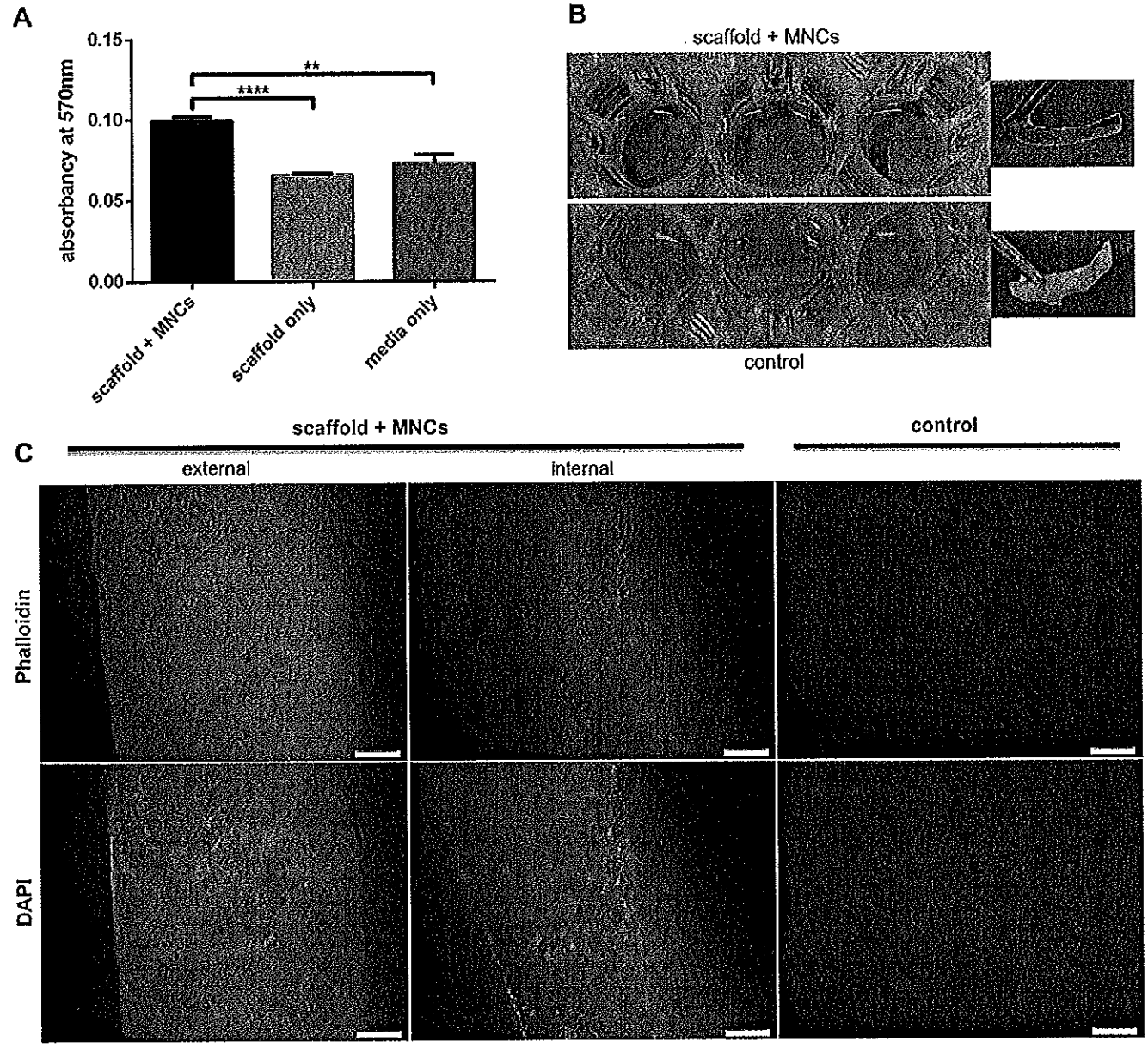

Fig. 5. Absorbance at 570 nm after having performed the colorimetric MTT-assay on sample I of the transplanted synthetic tracheal scaffold into patient (A). Macroscopic pictures of sample I reseeded with MNCs (upper part; $n = 3$) and control scaffolds without cells (lower part; $n = 3$), thin rings obtained from the distal part (graft-bioreactor fixation area) of the synthetic trachea (B). Fluorescent images of the internal and external part of the tracheal scaffold (sample I) stained with Phalloidin (green) or DAPI (blue). Unseeded pieces served as controls ($n = 3$). Magnification 10×; scale bar representing 200 μm (C). (For interpretation of the references to colour in this figure legend, the reader is referred to the web version of this article.)

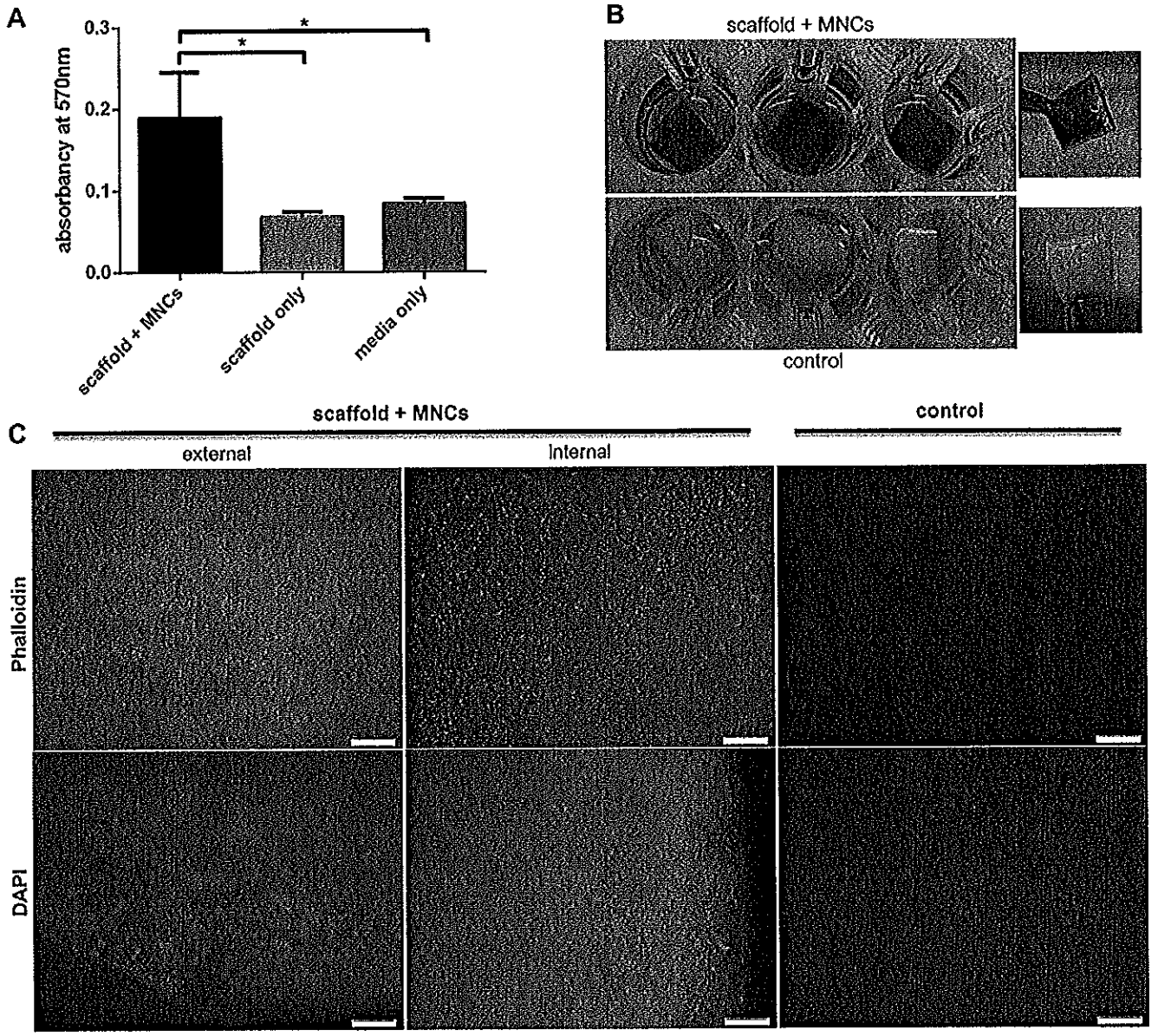

Fig. 6. Absorbance at 570 nm after having performed the colorimetric MTT-assay on sample II of the transplanted synthetic tracheal scaffold into patient (A). Macroscopic pictures of sample II reseeded with MNCs (upper part; $n = 3$) and control scaffolds without cells (lower part; $n = 3$), pieces from the distal part (obtained intraoperatively) of the synthetic trachea (B). Fluorescent images of the internal and external part of the tracheal scaffold (sample II) stained with Phalloidin (green) or DAPI (blue). Unseeded pieces served as controls ($n = 3$). Magnification 10×; scale bar representing 200 μm (C). (For interpretation of the references to colour in this figure legend, the reader is referred to the web version of this article.)

their corresponding cell numbers. Digital images of clinical samples stained with formazan crystals (Figs. 5B and 6B) were quantified for the color changes as described above. When applying equation 1 to the grayscale values of the pixels in the digital image, the values Y_c and Y_m were the same as those used in the laboratory samples. The result was $\Delta C = 67\%$, which was consistent with the measured cell density (Figs. 5C and 6C). The calibration curve (Fig. 2C) also showed that this corresponded to an average cell coverage on the entire samples of approximately 40%. However, when equations (1) and (2) were applied to each pixel in the image and the resulting histogram of the θ values was analyzed, it was found that 20% of the surface area of the sample had less than 25% cell coverage, whereas 20% of the area of the sample had greater than 75% coverage (Fig. 3B). This was confirmed by observations made from SEM images, which showed a wide variation in cell coverage ranging from an almost complete absence of cells (Fig. 7A) (the area where the scaffold was fixed to the bioreactor) to a full confluence (Fig. 7B). The early clinical evaluation revealed an initial graft epithelialization as judged from the 1-week post-operative brushing (Fig. 7C). The intermediate post-operative outcome (5 months) has shown a patent and non-contaminated graft without any signs of inflammation.

4. Discussion

The recent clinical successes of transplanting bioengineered tissues or organs suggest TE can potentially be routinely used in the very near future [1–3]. Hence, it is important to formulate ethical and clinical guidelines by establishing standard operating procedures that are both reproducible and reliable for TE. It is even

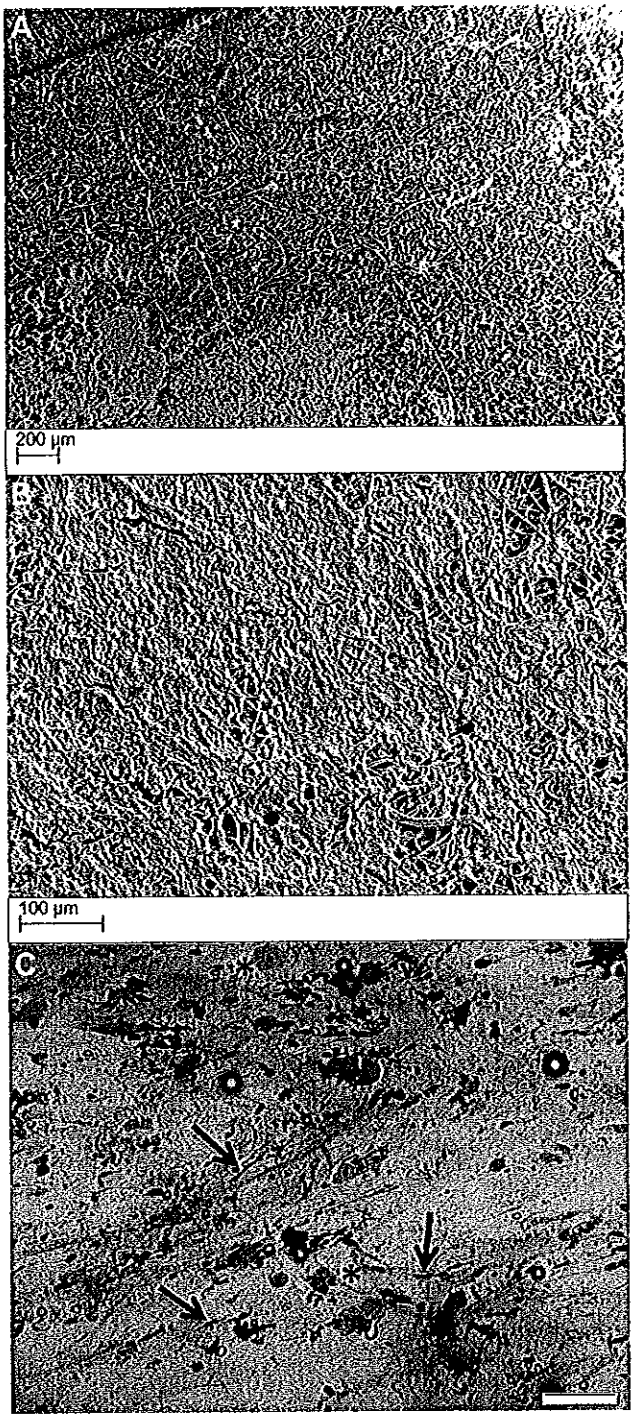

Fig. 7. Scanning electron microscopy images of the tracheal scaffold used in the clinical transplantation either showing the graft-bioreactor fixation area (Magnification 100×; scale bar representing 200 µm) (A) Or aside from this area (Magnification 400×; scale bar representing 100 µm) (B) Image shows a clinically obtained brushing sample of the patient's graft (H&E stained) at day 7 (post transplantation). Magnification 20×; scale bar representing 100 µm; arrows indicate epithelial cells, asterisks indicate basal cells (C).

more important to have qualitative and quantitative validations of the graft prior to transplantation, specifically concerning *i)* cell attachment, *ii)* cell viability, *iii)* proliferation rate, and *iv)* cell distribution while minimizing staff labor and laboratory equipment for performing the analyses. However, there is as yet no standardized analytical protocol that is applicable routinely in a clinical setting. Therefore, we set out to establish a reliable and simple evaluation panel that can give the most relevant information on graft features to the responsible clinicians and scientists involved. In order to meet the clinical requirements, analytical methods need to be time- and cost-effective, uncomplicated and simple with high reproducibility. We optimized an analytical panel, which includes a modified processing protocol (protocol III) from a commercially available MTT assay and fluorescence staining with Phalloidin/DAPI. We successfully proved the validity and reproducibility of this evaluation panel with both *in vitro* and *in vivo* studies. This was also transferred to a clinical setting during a recent trachea TE organ transplantation. The colorimetric MTT assay was first described by Mosman [9]. It is a well-accepted method to measure viability and proliferation of cultured cells. It is based on two substrates: the yellow tetrazolium salt MTT and SDS in 0.01 M HCl. MTT is cleaved to metabolically active cells to form purple formazan crystals, which provides a macroscopic indicator. The purple color change can be macroscopically recognized which makes this assay superior to many other marketed cell viability/proliferation assays such as Cell Titer Glo®, MTS (3-(4,5-dimethylthiazol-2-yl)-5-(3-carboxymethoxyphenyl)-2-(4-sulfophenyl)-2H tetrazolium) and XTT (2,3-bis-(2-methoxy-4-nitro-5-sulfophenyl)-2H-tetrazolium-5-carboxanilide) [13]. In the next step, the crystals are solubilized with SDS. The resulting color change is finally detected with a simple (ELISA-) spectrophotometer by measuring the absorbancy, which correlates with viability, proliferation and cell numbers [14]. Our data have demonstrated both experimentally (Figs. 1A and 2A) and clinically (Figs. 5A,B and 6A,B) that the reduced processing time to 2 h in the MTT assay could yield dual validation: i) macroscopic color change and ii) absorbancy readouts which correlated well with number of attached cells on the synthetic scaffolds.

We also show here that this simple and fast analytical panel can provide qualitative and quantitative data (cell viability, cell distribution) that are essential for clinical decision-making. We found that graft areas distal from the graft-bioreactor holder fixture had around 70% of the surface covered with cells, while nearly no cell adhesion was found in the holder fixture region. Similar observations were also found in transplantation studies carried out in animals here. Although the graft was not 100% seeded with autologous cells, the early clinical examination of the patient's graft did not show any bacterial or fungi contamination. Hence, we can assume that it may not necessarily be important to have a scaffold with confluent cell covering of the surface: around 70% coverage seems to be sufficient. However, although we have data on cell densities, we still do not know the patterns of proliferation and distribution of seeded cells on grafts *in situ*. Cell recruitment such as local resident and circulating stem and progenitor cells may also play a key role in regeneration [15]. Further studies could be performed to elucidate the different regulatory pathways or mechanisms involved during an *in situ* tracheal regeneration.

The complexity of TE and regeneration would remain a challenge because the restoration or creation of three-dimensional tissues and organs require a combination of stem cells, scaffolds and signaling molecules. Mathematical modeling is another approach, which we could make predictions of cliniscal outcomes from the evaluations. Here, we have successfully developed a mathematical model and converted it to a colorimetric scale bar that can predict cell coverage and different cell densities. This easy-to-use device can potentially be widely used and be well-accepted in a medical field to confirm the viability and integrity of the engineered tissue/organ directly prior to transplantation. The ability to acquire immediate visual information can certainly assist with the decisions about whether the tissue or organ is ready for implantation into a patient or a second bone marrow isolation and

reseeding is necessary with the postponement of transplantation. From an ethical point of view, it is most important to guarantee that the implanted tissue or organ graft is safe and does not jeopardize the patient's health. Within the fast growing field of TE and its clinical application, this analytical panel is an important and highly desired tool that can be implemented routinely to facilitate a successful and safe transplantation outcome.

5. Conclusion

We have developed a robust, fast and reproducible colorimetric tool that can verify and warrant viability and integrity of an engineered tissue/organ prior to transplantation. This should facilitate a successful transplantation outcome and ensure patient safety.

Acknowledgments

We would like to thank Prof. Alessandra Bianco for supporting the fiber alignment evaluation. Sylvie Le Guyader for assisting with confocal imaging. We thank all the health professionals of the Karolinska University Hospital in Solna (Sweden) without whom the transplantation could not have been done. We further want to thank all the staff of the Thorax Clinic of the Karolinska University Hospital in Solna for the excellent and outstanding support with the pre-, peri- and in particular the post-operative care of the patient.

The confocal imaging was performed at the Live Cell Imaging unit at the Department of Biosciences and Nutrition, Karolinska Institutet, supported by grants from the Knut & Alice Wallenberg foundation, the Swedish Research Council and the Center for Biosciences at Karolinska Institutet. This work was supported by European Project FP7-NMP- 2011-SMALL-5: BIOtrachea, Biomaterials for Tracheal Replacement in Age-related Cancer *via* a Humanly Engineered Airway (No. 280584–2), ALF medicine (Stockholm County Council): Transplantation of bioengineered trachea in humans (No. LS1101–0042.), The Swedish Heart-Lung Foundation: Trachea tissue engineering, Doctor Dorka Stiftung (Hannover, Germany): bioengineering of tracheal tissue. Mega grant of the Russian Ministry of Education and Science (agreement No. 11.G34.31.0065).

References

[1] Atala A, Bauer SB, Soker S, Yoo JJ, Retik AB. Tissue-engineered autologous bladders for patients needing cystoplasty. Lancet 2006;367(9518):1241–6.
[2] Macchiarini P, Jungebluth P, Go T, Asnaghi MA, Rees LE, Cogan TA, et al. Clinical transplantation of a tissue-engineered airway. Lancet 2008;372(9655):2023–30.
[3] Jungebluth P, Alici E, Baiguera S, Le Blanc K, Blomberg P, Bozóky B, et al. Tracheobronchial transplantation with a stem-cell-seeded bioartificial nanocomposite: a proof-of-concept study. Lancet 2011;378(9808):1997–2004.
[4] Ozeki M, Narita Y, Kagami H, Ohmiya N, Itoh A, Hirooka Y, et al. Evaluation of decellularized esophagus as a scaffold for cultured esophageal epithelial cells. J Biomed Mater Res A 2006;79(4):771–8.
[5] Lynen Jansen P, Klinge U, Anurov M, Titkova S, Mertens PR, Jansen M. Surgical mesh as a scaffold for tissue regeneration in the esophagus. Eur Surg Res 2004;36(2):104–11.
[6] Ott HC, Matthiesen TS, Goh SK, Black LD, Kren SM, Netoff TI, et al. Perfusion-decellularized matrix: using nature's platform to engineer a bioartificial heart. Nat Med 2008;14(2):213–21.
[7] Ott HC, Clippinger B, Conrad C, Schuetz C, Pomerantseva I, Ikonomou L, et al. Regeneration and orthotopic transplantation of a bioartificial lung. Nat Med 2010;16(8):927–33.
[8] Petersen TH, Calle EA, Colehour MB, Niklason LE. Bioreactor for the long-term culture of lung tissue. Cell Transplant 2011;20(7):1117–26.
[9] Mosmann T. Rapid colorimetric assays for cellular growth and survival: application to proliferation and cytotoxicity assays. J Immunol Methods 1983;65(1–2):55–63.
[10] Wulf E, Deboben A, Bautz FA, Faulstich H, Wieland T. Fluorescent phallotoxin, a tool for the visualization of cellular actin. Proc Natl Acad Sci U S A 1979;76(9):4498–502.
[11] Gustafsson Y, Haag J, Jungebluth P, Lundin V, Lim ML, Baiguera S, et al. Viability and proliferation of rat MSCs on adhesion protein-modified PET and PU scaffolds. Biomaterials 2012;33(32):8094–103.
[12] Grasl C, Bergmeister H, Stoiber M, Schima H, Weigel G. Electrospun polyurethane vascular grafts: in vitro mechanical behavior and endothelial adhesion molecule expression. J Biomed Mater Res A 2010;93(2):716–23.
[13] Goodwin CJ, Holt SJ, Downes S, Marshall NJ. Microculture tetrazolium assays: a comparison between two new tetrazolium salts, XTT and MTS. J Immunol Methods 1995;179(1):95–103.
[14] Hansen MB, Nielsen SE, Berg K. Re-examination and further development of a precise and rapid dye method for measuring cell growth/cell kill. J Immunol Methods 1989;119(2):203–10.
[15] Seguin A, Baccari S, Holder-Espinasse M, Bruneval P, Carpentier A, Taylor DA, et al. Tracheal regeneration: Evidence of bone marrow mesenchymal stem cell involvement. J Thorac Cardiovasc Surg 2012.. http://dx.doi.org/10.1016/j.jtcvs.2012.09.079.

Stem Cells 2

Engineered whole organs and complex tissues

Stephen F Badylak, Daniel J Weiss, Arthur Caplan, Paolo Macchiarini

End-stage organ failure is a key challenge for the medical community because of the ageing population and the severe shortage of suitable donor organs available. Equally, injuries to or congenital absence of complex tissues such as the trachea, oesophagus, or skeletal muscle have few therapeutic options. A new approach to treatment involves the use of three-dimensional biological scaffolds made of allogeneic or xenogeneic extracellular matrix derived from non-autologous sources. These scaffolds can act as an inductive template for functional tissue and organ reconstruction after recellularisation with autologous stem cells or differentiated cells. Such an approach has been used successfully for the repair and reconstruction of several complex tissues such as trachea, oesophagus, and skeletal muscle in animal models and human beings, and, guided by appropriate scientific and ethical oversight, could serve as a platform for the engineering of whole organs and other tissues.

Lancet 2012; 379: 943–52

See Comment page 877

See Perspectives page 886

This is the second in a Series of two papers about stem cells

McGowan Institute for Regenerative Medicine, Department of Surgery, University of Pittsburgh, Pittsburgh, PA, USA (Prof S F Badylak MD); Vermont Lung Center, University of Vermont College of Medicine, Burlington, VT, USA (D J Weiss MD); Center for Bioethics, University of Pennsylvania School of Medicine, Philadelphia, PA, USA (Prof A Caplan PhD); and Advanced Center of Translational Regenerative Medicine, Stockholm, Sweden (Prof P Macchiarini MD)

Correspondence to:
Prof Paolo Macchiarini, Advanced Center of Translational Regenerative Medicine (ACTREM), Division of Ear, Nose, and Throat, Department of Clinical Science, Intervention and Technology (CLINTEC) Karolinska Institutet, Alfred Nobel Allé 8, Huddinge, S-14186 Stockholm, Sweden
paolo.macchiarini@ki.se

Introduction

End-stage organ failure is a serious, growing, and costly issue. Every year in the USA alone, 120 000 people die from chronic lung disease,[1] 112 000 die from kidney failure,[2] 27 000 die from end-stage liver disease,[3] and 425 000 die from coronary heart disease.[4] At present, definitive treatment for end-stage organ failure is allogeneic transplantation. However, a combination of unremitting demand, expensive and potentially dangerous immunosuppression, and the requirement that donor organs be physiologically viable means that the clinical need will never be met and many patients on transplantation waiting lists will die before a donor organ becomes available. Patients fortunate enough to receive a donor organ endure life-long immunosuppressive therapy with its associated morbidity and also are at risk of acute or chronic organ rejection.[5]

Recent advances in tissue engineering and regenerative medicine have established a foundation on which the functional replacement of whole organs and complex tissues such as skeletal muscle, trachea, and oesophagus seems possible. The approach involves the use of naturally occurring extracellular matrix, obtained by the decellularisation of allogeneic or xenogeneic whole organs or tissues (figure 1). The ready availability of an off-the-shelf xenogeneic scaffold that could subsequently be recellularised with autologous cells is a potential solution to the donor shortage that exists for allogeneic whole-organ transplantation. In addition, this approach would obviate the need for immunosuppression. The matrix serves as an inductive three-dimensional biological template around which the recipient rebuilds functional tissue through recruitment or exogenous provision of endogenous replacement cells.[6–8] The appropriate spatial distribution of the cells and their functional and phenotypic maturation within a scaffold can occur in an ex-vivo bioreactor, in situ, or in a combination of these environments. A key advantage of this approach is the ready availability of an intact vascular network in the decellularised organs with appropriately sized inflow and outflow conduits for anastomosis to the recipient circulation and thus perfusion with nutrients and appropriate cues for cell behaviour.

The feasibility of a therapeutic strategy based on cellular repopulation of an intact extracellular matrix has evolved as a result of an improved understanding of cell–matrix interactions,[9,10] development of methods for isolation of tissue-specific and organ-specific native extracellular matrix with little change in native structure and composition,[11] rapid advancements of stem cell and progenitor cell biology (including the potential use of inducible pluripotent stem cells),[12,13] and the integration of the principles of developmental biology into regenerative medicine.[10] Although notable scientific and ethical challenges remain as this approach advances to clinical use, successful proof of principle for organs such as liver,[14,15] heart,[16] and lung[17–20] and complex tissues such as the trachea,[21] oesophagus,[22] and skeletal muscle[23] has been shown. Functional restoration of such tissues and organs with matrices might become a viable and practical therapeutic approach to meet future demand after organ failure.[14–13,21]

Search strategy and selection criteria

We searched the Cochrane Library, Medline, and Embase for articles published between Jan 1, 1970 and Jan 31, 2012, without language restriction, with the search terms "tissue engineering", "organ regeneration", "transplantation", "bioethics", and "regenerative medicine" in addition to tissue-specific terms. We mainly chose publications from the past 5 years, but did not exclude commonly referenced and highly regarded older publications. We also searched the reference lists of articles identified by this search strategy and included relevant articles. We included several review articles or book chapters because they provided comprehensive overviews that were beyond the scope of this Review. The reference list was modified during the peer-review process on the basis of comments from reviewers.

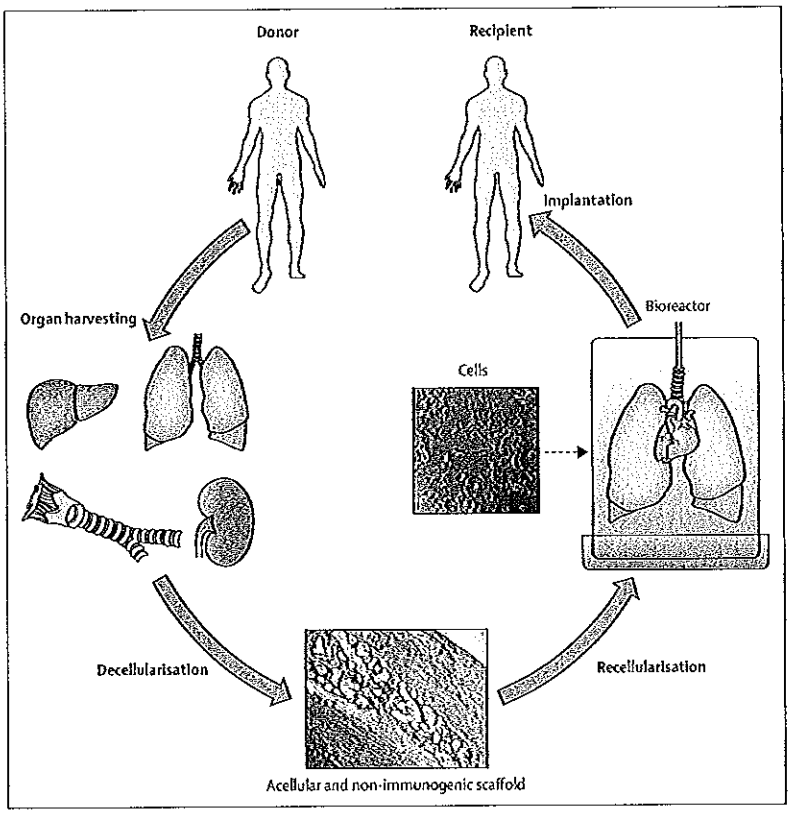

Figure 1: Organ and tissue bioengineering

We aim to review the state of the art for this technology and strategy and discuss the use of naturally occurring extracellular matrix as a biological scaffold and overview progresses made in individual organs and complex tissues.

Extracellular matrix

All tissues and organs are made up of cells and associated extracellular matrix—a secreted product of the resident cells consisting of a unique, tissue-specific three-dimensional environment of structural and functional molecules. Tissues and organs are usually regarded as cells with a supporting stroma. By contrast, the extracellular matrix is viewed in terms of its role in structural maintenance and three-dimensional shape of the respective tissue or organ. However, the extracellular matrix is actually in a state of dynamic reciprocity[24,25] with the resident cell population. The phenotype of the resident cells, including their active genetic profile, proteome, and functionality, is influenced by conditions of the microenvironmental niche including factors such as oxygen concentration, pH, mechanical forces, and biochemical milieu. In turn, resident cells secrete the appropriate molecules in which to survive, function effectively, and communicate with neighbouring cells. Through this reciprocal interaction, the extracellular matrix has an essential role in prenatal development and postnatal maintenance of healthy function.[9,10,25,27] In addition to the matrix's role in development and adult homoeostasis, it can be used as an inductive scaffold to promote a constructive tissue remodelling response after injury. Mechanisms of this response include release of cryptic peptides that are mitogenic and chemotactic for endogenous stem and progenitor cells,[28,29] modulation of the innate immune response,[30] and provision of tissue-specific molecular cues that support cell phenotype and function.[15,19,31–33] Thus, native extracellular matrix is a logical and ideal scaffold for organ and tissue reconstruction.

Intact three-dimensional extracellular matrix scaffolds from different allogeneic and xenogeneic tissues and organs have been manufactured effectively for regenerative medicine. Matrix scaffolds prepared by decellularisation of whole organs can maintain or promote site-appropriate cell phenotypes during the process of cell repopulation[15,18,19] through presentation of the ligands and bioactive molecules that are necessary for resident or migrant cell populations to self-assemble into functional groupings and—at least temporarily—show reasonably normal structure and partial function. These events are probably crucial for creation of a functioning organ that can respond effectively to the demands of a recipient after in-vivo implantation.

Structural and functional molecules in the extracellular matrix include glycosaminoglycans and the collagens elastin, fibronectin, laminin, and vitronectin. In general, these matrix molecules are highly conserved proteins in eukaryotic organisms,[34] which largely explains the absence of an adverse immune response after xenotransplantation. Much attention has been given to the galactose-α-1,3-galactose antigen (so-called Gal epitope), which is a cell-associated epitope responsible for rejection of whole-organ pig xenografts. Most xenogeneic sources of extracellular matrix scaffold materials contain the Gal epitope but convincing evidence[35] suggests that this antigen does not contribute to rejection or an adverse remodelling outcome. Thus, use of three-dimensional extracellular matrix organ or tissue scaffolds as a foundation for regeneration is a viable option for improvement of the continuing shortage of organ donors.

Principles and methods of decellularisation

Harvesting of extracellular matrix from an organ or tissue needs methods that can remove the cell population while restricting changes in structure, composition, or ligand background of the native matrix, including those components that provide the vascular and lymphatic networks. Removal of cells from their integrin-bound anchors and intercellular adhesion complexes while maintaining extracellular matrix surface topography and resident ligands is challenging. A combination of physical, ionic, chemical, and enzymatic methods are typically used to accomplish decellularisation and these

mechanisms are most efficiently delivered by perfusion of the already existing organ vasculature. Failure to effectively and thoroughly remove cellular remnants can cause a proinflammatory response in the recipient that interferes with the structure and function of the recellularised organ. Although complete removal of all cell remnants is not possible irrespective of the technique used, a combination of qualitative and quantitative strategies avoids such adverse responses. Quantitative criteria of decellularisation include the complete absence of visible nuclear material on histological examination (haematoxylin and eosin and 4′-6-diamidino-2-phenylindole [DAPI] stains), less than 50 ng of dsDNA per 1 mg dry weight of the extracellular matrix scaffold, and remnant DNA molecules shorter than 200 bp.[11] The appendix shows methods used for preparation of three-dimensional organ and tissue scaffolds made with extracellular matrix. Techniques vary strikingly and total procedure times for the decellularisation processes range from 5 h to 7 weeks.

Principles and methods of recellularisation

Strategies for repopulation of an extracellular matrix scaffold that has retained the native shape and structure of the original organ need to account for the unique characteristics of the parenchymal and non-parenchymal cell types of each organ. Because transplanted cells should ideally be autologous, a tissue biopsy from the patient is necessary if the starting cell population is expected to be fully differentiated. Such an approach assumes that enough healthy cells can be obtained from a patient who is a candidate for organ replacement. Alternatively, if remaining healthy differentiated tissue-specific cells are non-dividing, diseased, or poorly dividing and thus cannot be satisfactorily expanded ex vivo, endogenous organ-specific progenitor cells might be usable for repopulation of the extracellular matrix scaffold. Another possibility would be use of multipotent stem cells harvested from autologous bone marrow, adipose, or other tissues with subsequent directed differentiation along organ-specific or tissue-specific lineages. Examples of these cell populations include mesenchymal stromal cells or endothelial progenitor cells. Finally, autologous induced pluripotent stem cells that have been differentiated along selected pathways are a potential source of cells for scaffold repopulation. Use of any of these cell sources eliminates the need for immunosuppression after implantation in the host. Immunosuppression not only negatively affects quality of life but also introduces many unknown variables into the process of new organ maturation and development. Probably, a mix of different types of cells will be needed and these cell types will vary by the organs and tissues required; the appendix contains a summary of the advantages and challenges of various potential cell sources.

Irrespective of the cell source used, the method of reintroduction of the cells into a three-dimensional scaffold will take advantage of the retained vascular structures. Perfusion via the native venous or arterial circuitry provides the necessary route and infrastructure to deliver cells to all regions of the decellularised scaffold. Other organ-specific pathways (eg, airway delivery in the lung) might also be used. So far, the techniques used have not had the advantage of systematic studies assessing various cell concentrations in the perfusate, perfusion pressures, flow rates, or other variables that can affect cell survival. Despite the limitations of early attempts, an impressive distribution of viable cells in organs such as the lung,[18,20] liver,[14,15] and heart[16] have been reported. However, complete recellularisation of the three-dimensional scaffold is not the objective of the initial cell delivery effort. Rather, provision of an adequate number of cells with appropriate spatial distribution and contact with other cells and the underlying matrix will allow for subsequent self-assembly, proliferation, and differentiation.

See Online for appendix

Bioreactors

Bioreactors—sealed mechanical chambers providing suitable environmental conditions for cellular activity—are necessary for optimum physiological cellular repopulation of decellularised organ matrices. Design elements include provision of a flow of nutrient medium to the vasculature and physical and environmental stimuli to the cells in the repopulating matrix that mimic normal conditions specific to the growing organ (figure 2). Examples of physical stimuli include an air–liquid interface for tracheal regeneration,[17] breathing movements for lung regeneration, or electrical stimuli for cardiac regeneration. Bioreactors need to support sterile culture of parenchymal or stromal cells for several hours

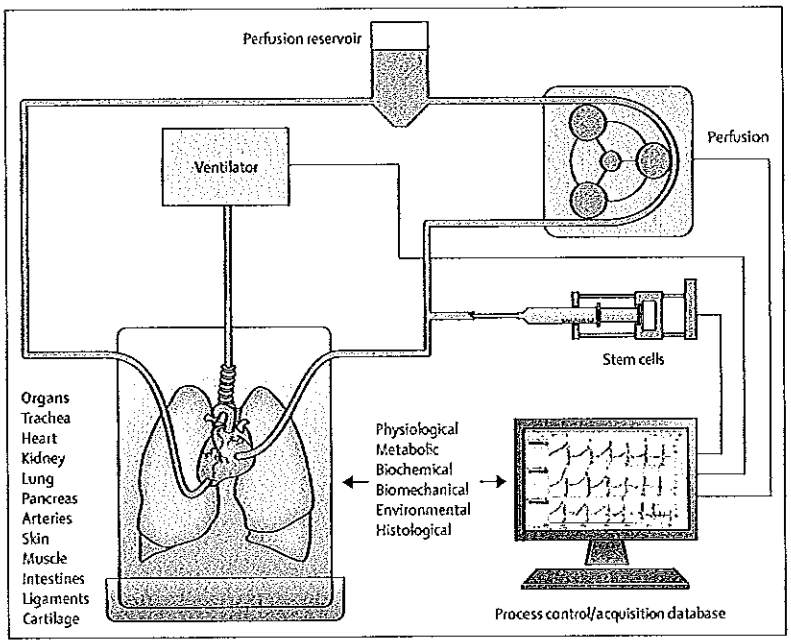

Figure 2: Key elements of an organ bioreactor

or even months,[37] and some dedicated commercial systems are already available.[17,21] However, very few bioreactor systems comply at present with good manufacturing process regulations. If recellularised organs are to become widely used, then closed bioreactor systems that are properly monitored, maintained, and made of sterilisable and disposable materials will be necessary.

Organ-specific examples

Skin

As with every organ or tissue system, skin has unique anatomical features, cell types, and physiological characteristics that need to be taken into account during the process of engineering replacement tissue. The main aim in skin replacement for large non-healing wounds is the restoration of the epidermal barrier to avoid infection and water loss. Although split-thickness autograft transplantation remains the standard of care, it cannot be provided to patients whose skin defects involve a large percentage of total body surface[38] because the shortage of donor dermis might result in severe scarring and contractures, and the native functional properties are usually not provided.[39] Ideally, a bioengineered skin graft would enable regrowth of a functional and physiological dermal layer of skin, including adnexal characteristics such as hairs or pigment. So far, skin restoration has been accomplished with artificial skin substitutes or cell-based therapies (or a combination of the two approaches).

New treatments range from novel formulations of naturally occurring biofunctional porous three-dimensional structures that act as extracellular matrix to in-situ delivery of epidermal stem cells.[40] Skin extracellular matrix supports cell engraftment, proliferation, and differentiation in vitro and in vivo, and provides collagen and other biological substances (eg, fibrin or hyaluronic acid) that assist wound healing and affect the development of scar tissue or reconstitution of the physiological architecture.[40] Several mature differentiated skin cell types have been investigated for use in grafts. Extracellular matrix can direct cells to their target region and supports growth and differentiation of local stem and progenitor cells that probably have a key role in wound healing and potentially provide scar-free healing.[41,42] Cells are necessary for complete wound healing but cells implanted alone without extracellular matrix survive poorly in the absence of their appropriate structural template. Cell therapy approaches for skin regeneration and grafting need to be improved in terms of the type of cells used (eg, keratinocytes alone do not result in fully functional skin), choice of autologous versus allogeneic cells (in-vitro cell culture or graft engineering can take weeks), and cell survival and functionality after in-situ delivery. Use of stem cells or progenitor cells and engineered scaffolds from preserved extracellular matrix may be the best solution but further development is necessary to provide a fully functional skin graft.

Respiratory system

Because trachea is a comparatively uncomplicated and hollow complex tissue, it was the ideal starting point for respiratory organ engineering. Moreover, synthetic degradable polymers or biomaterials have not been used successfully for clinical whole airway applications.[43] In 2008,[21] investigators repopulated a decellularised human windpipe in a bioreactor with cultured autologous respiratory epithelial cells and autologous chondrocytes of bone marrow-derived mesenchymal stromal cell origin, and used the resultant graft to replace a terminally diseased left main bronchus. At the time of publication, the patient was well, active and, most importantly, did not need immunosuppressive drugs. The procedure has been improved since 2008 by shortening the time required for decellularisation of the trachea and by use of the recipient's body as a bioreactor: the decellularised human tracheal scaffold is seeded intraoperatively with autologous respiratory epithelial and bone marrow-derived mononuclear cells.[44] This in-vivo tissue-engineered approach was used in a case series of nine paediatric and adult patients with benign and malignant diseases on a compassionate basis before it could obtain a full clinical trial authorisation from the Italian Ministry of Health. No graft-related mortality was reported after follow-up of 12–42 months, with all bioengineered grafts remaining vascularised and lined with healthy respiratory mucosa. However, partial collapse of the scaffolds was noted in three patients, and was unpredictable with regard to patients or within the same scaffolds. Reasons for this graft collapse are unknown but a number of improvements in decellularisation, recellularisation, biomechanical stabilisation, and implantation approaches for tracheal grafts are under investigation.[45–47]

In view of limitations of the use of natural matrices, including the absolute requirement of obtaining a suitable donor organ, an artificial tracheal and bronchial scaffold from a nanocomposite polymeric material with physical and mechanical properties equivalent to native tissue has been developed.[48] The artificial scaffold, which was seeded ex vivo with autologous bone marrow-derived stromal cells (in a bioreactor) and conditioned with pharmacological therapy, was implanted into a patient with a primary recurrent tracheobronchial tumour. The graft was patent, well vascularised, and lined with a well-developed healthy mucosa 8 months after transplantation.[49] Although more follow-up is needed, early clinical results suggest that a strategy based on optimally bioengineered materials combined with autologous cells and pharmacological intervention (to boost tissue regeneration and recruit or mobilise peripheral and local progenitor and stem cells) could provide a therapeutic option and eventual cure for patients with otherwise untreatable tracheal disorders (figure 3).

Provided that one side retains movement, most of the larynx can be removed with preservation of the airway and breathing functions. Therefore, a partial replacement

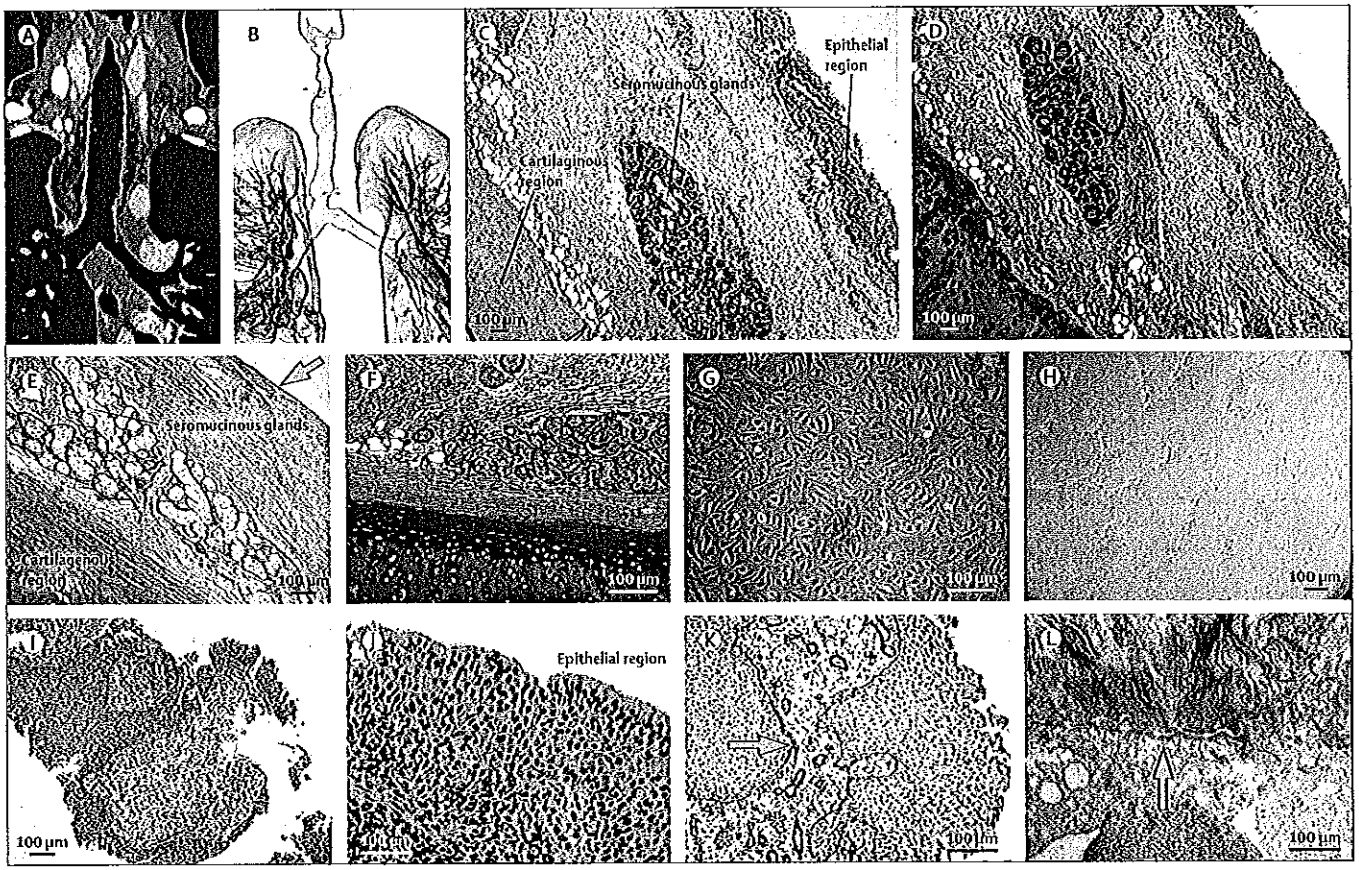

Figure 3: **Tissue-engineered tracheal transplantation**
CT scan of a patent tubular natural human scaffold implanted after removal of the native trachea for malignant disease (A; scan at 1 month) and benign disease (B; three-dimensional reconstruction based on a CT scan at 2 years). Haematoxylin and eosin stain of native (C) and decellularised (E) trachea; after application of 25 detergent-enzymatic cycles, the tracheal matrices were almost completely decellularised and only a few nuclei were still present in the cartilaginous region (arrow shows preserved basement membrane zones). Movat pentachromic staining (connective tissue staining) of the native (D) and decellularised (F) trachea; yellow-orange staining shows collagen and reticulum fibres, green shows mucins, blue-green shows ground substance, and red shows muscle. (G) Endothelial progenitor cells isolated from mobilised peripheral blood and expanded in vitro were able to organise into a meshwork of capillary-like tubules (H), suggesting the boosting effect of the regenerative therapy. Haematoxylin and eosin stain of decellularised trachea 1 year after transplantation (I), showing healthy tracheal epithelium (J). (K) Laminin immunostaining outlining the presence of a continuous layer of basal membrane (arrow) and small blood vessels (asterisks). (L) Transmission electronic micrograph showing the presence of the basal membrane (arrow).

of the larynx with a bioengineered construct would not need to exert any neuromuscular activity to achieve an acceptable functional result from an airway and breathing perspective, even if voice and swallowing functions are not perfect because of the absence of complete laryngeal architecture.[50] Decellularised human laryngeal scaffolds can be used as templates for remodelling of laryngeal tissue because they provide the precise anatomical reconstitution and native cartilaginous support. Akin to the trachea, decellularised scaffolds induce a strong in-vivo angiogenic response and could be used for partial or total implantation in human beings.[51]

Because of the complex three-dimensional architecture and structure–function relations of the lung, and the large number of differentiated cell types present, ex-vivo lung bioengineering is probably a difficult task compared with bioengineering of the trachea and larynx. Synthetic three-dimensional culture systems have been used as matrices for ex-vivo development of lung parenchyma and for the study of growth factors and mechanical forces on lung remodelling.[52–57] Human lung epithelial cells and capillary endothelial cells coated onto porous polydimethylsiloxane chips can mimic alveolar function.[58] This so-called lung-on-a-chip device was used to assess how nanoparticles and bacteria enter the lungs and will also be useful for high throughput screening of drugs. However, since these artificial scaffolds do not fully replicate the complexity of the lung architecture or function and cannot be implanted easily and anastomosed appropriately to the vascular and airway systems, investigations have concentrated on use of more natural models including nasal septa and decellularised whole lungs.[17–19,59,60] Several groups have shown the feasibility of production of acellular lung matrices, and have repopulated these matrices with various cell types and, after reimplantation, shown short-term survival in rats with some degree of gas exchange.[17–20,51,60] Notably, although there are several types of respiratory cells, a

carefully decellularised lung matrix seems to possess the appropriate ligands to direct attachment of epithelial cell subtypes to correct anatomical locations (figure 4).[19–20] Active areas of study include the effect of bioreactor cues (eg, negative pressure breathing, stretch, and oxygen tension) on epithelial differentiation and resultant barrier function and also whether stem or progenitor cells isolated from adult bone marrow, cord blood, or other sources (including the lung itself) can be used for functional lung regeneration in vivo.[20,52,61]

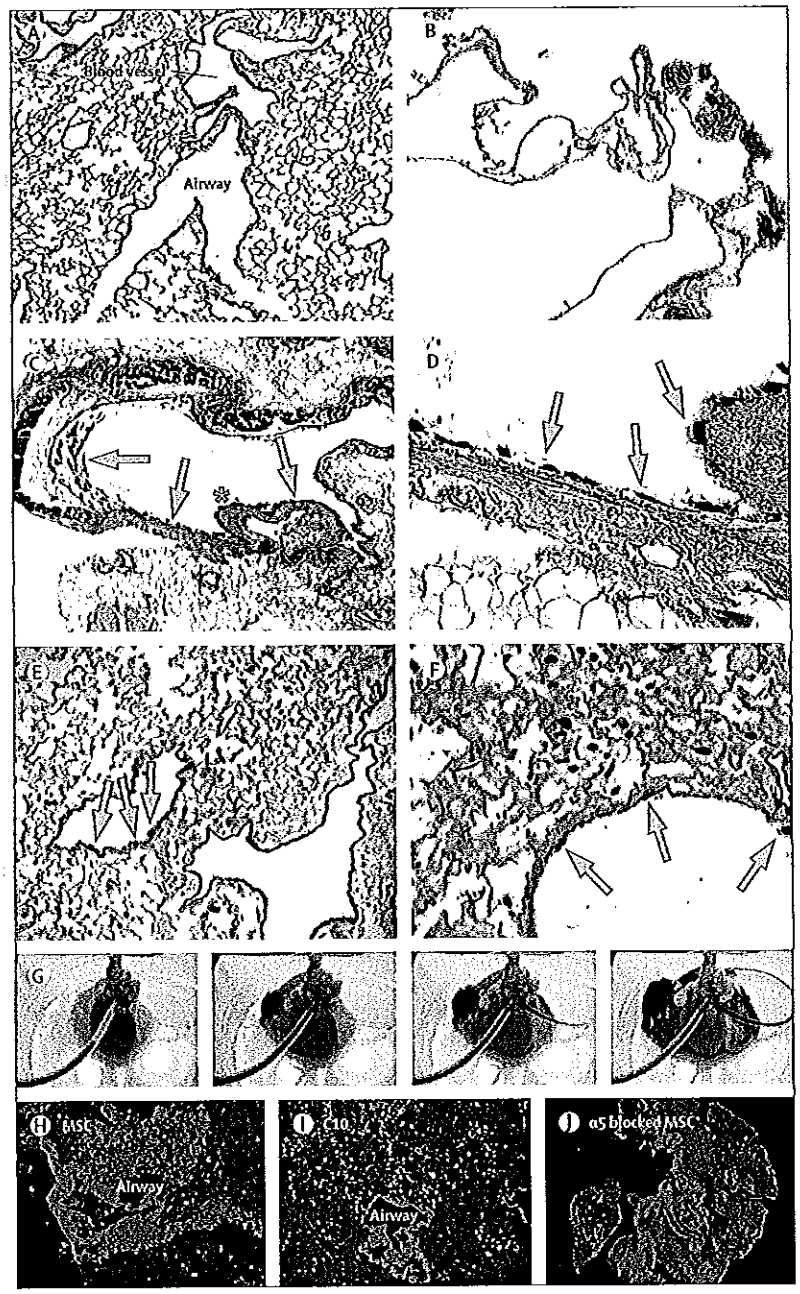

Liver

Retention of a healthy intact liver stroma after liver injury provides the necessary substrate to support full liver regeneration.[62] Decellularisation techniques vary substantially and which method is preferable to assure the appropriate ligand background for parenchymal and non-parenchymal cell attachment, differentiation, and function is unknown. Nonetheless, the ability to manufacture a three-dimensional liver scaffold made up of native liver extracellular matrix is both possible and practical.[14,15]

In-vivo transplantation of a recellularised whole liver scaffold is possible but haemorrhage and thrombotic complications have restricted long-term assessment.[14] The ability to sustain long-term in-vivo perfusion until a functional endothelialised vasculature can be formed is the limiting step at present in the whole-organ engineering approach, not just for liver but for all complex organs. Establishment of the optimal cell source for repopulation of liver scaffolds will require a substantial amount of work. Equally, the optimal abdominal circulatory system into which such a seeded scaffold would be placed has not been explored. The healthy liver has two blood supplies, including a high pressure, pulsatile hepatic artery source, and a low pressure, nutrient rich, non-pulsatile portal circulation. The extent to which the healthy circulatory environment needs to be present to encourage liver regeneration in an implanted engineered liver construct is unknown. Recent work suggests that even small numbers of transplanted hepatocytes have the potential to create new liver tissue in heterotopic sites.[63]

Kidney

New sources of organs are urgently needed for patients with end-stage renal disease.[64] One potential approach is the regeneration of damaged renal tissue through cell therapy with either progenitor or multipotent stem cells;[65,66] however, evidence suggests that cell therapy

Figure 4: **Tissue-engineered mouse lungs**
(A) Haematoxylin and eosin stain of a representative decellularised whole mouse lung and lung slices shows preservation of healthy architecture (magnification ×100). (B) Transmission electron micrograph images of alveolar septa in a representative decellularised whole mouse lung (magnification ×3000). (C–F) Intratracheally inoculated MSCs cultured to 1 month grow in parenchymal and airway regions of decellularised whole mouse lungs; representative photomicrographs (magnification ×100 in [C], ×400 in [D], ×400 in [E], and ×400 in [F]) show MSCs (arrows) in parenchymal lung regions and in airways. The asterisk in (C) shows the region magnified in (D). Vascular perfusion of a decellularised whole rat lung (G); after cannulation of the main pulmonary artery and the left atrium, 1·5% Evans blue dye was injected through the pulmonary artery. Rapid exiting from the left atrium was noted with simultaneous diffusion of dye throughout the lung parenchyma. Representative photomicrographs (magnification ×200) obtained 1 day after cell inoculation into decellularised whole mouse lungs (H–J); different cells localise to different regions of remaining extracellular matrix proteins. Specific fibronectin immunofluorescence is shown in red with 4′-6-diamidino-2-phenylindole (DAPI) nuclear staining in blue. MSCs inoculated into decellularised mouse lungs first localise to regions enriched in fibronectin (H). C10 mouse lung epithelial cells do not localise to regions enriched in fibronectin (I). Blocking the α5 integrin on MSCs with a neutralising antibody before cell inoculation results in MSCs localising in areas not enriched with fibronectin (J). MSC=mesenchymal stromal cell.

might be effective in acute kidney injury conditions but not in chronic renal failure. Therefore, whole-organ approaches, such as reseeding of extracellular matrix have been investigated. Ross and colleagues[67] successfully seeded rat renal extracellular matrix with mouse embryonic stem cells infused through the renal artery and the ureter, and showed proliferation and cell-specific differentiation of the stem cells within the glomerular, vascular, and tubular compartments. Acellular scaffolds with maintained expression patterns of native extracellular matrix proteins have been engineered and reseeded fromw cells obtained from donor kidneys of non-human primates and fetal kidney cells.[26] At present, much work needs to be done for ex-vivo kidney regeneration with extracellular matrix scaffolds and cell therapy approaches to become a viable clinical option.

Tissue-specific examples

Skeletal muscle

Skeletal muscle has a resident reserve cell population (called satellite cells) that retain the ability to regenerate damaged skeletal muscle. However, replacement of healthy functioning muscle without scar tissue in situations in which loss of muscle tissue exceeds 20% of the tissue mass is not possible. This factor is a key issue but preclinical studies have suggested that scaffolds composed of extracellular matrix from urinary bladder[68] or small intestinal submucosa[69] in pigs can aid the de-novo formation of large masses of functional skeletal muscle that are innervated and vascularised without substantial scar tissue formation. This approach allowed successful reconstitution of skeletal muscle in a patient with a volumetric loss of quadriceps muscle.[23] By contrast with reconstructive strategies that use decellularised whole organs such as lung, liver, or heart, the use of these acellular extracellular-matrix tissue scaffolds does not include an ex-vivo recellularisation step but rather relies on recruitment of endogenous stem or progenitor cells through naturally occurring cryptic peptides derived from the native extracellular matrix.[29,70,71] These cells subsequently proliferate and differentiate in situ in response to local microenvironmental cues.

Small intestine and urinary bladder

Use of extracellular matrix derived from pig small intestine (ie, small intestinal submucosa) and urinary bladder has been widely reported in both preclinical and successful clinical studies. Clinical applications have included the functional reconstruction of musculotendinous tissues,[23,69,72] lower urinary tract structures,[6] oesophagus,[22,73] cardiovascular structures,[74] and skin.[75] These scaffold materials are prepared by methods that largely retain their three-dimensional structure and composition. Non-homologous use of these materials suggests that factors in addition to site-specific or tissue-specific ligands have a key role in the reconstructive process. Unlike the whole-organ engineering approaches described previously, but akin to muscle replacement, these extracellular matrix scaffold materials are typically used without addition of a target organ cell population. Instead, these materials depend on endogenous recruitment of cells that have the capacity to form site-specific functional tissue. Degradation of extracellular matrix with release of bioactive cryptic factors is essential for recruitment of endogenous stem cells,[30,76-79] and modulation of the innate immune system towards a tissue rebuilding phenotype by extracellular matrix has a crucial role in constructive remodelling.[68] Although exogenous addition of cells to these scaffold materials might enhance their constructive properties, the regulatory, financial, and practical cost of such an approach is probably prohibitive for the incremental advantages it provides.

Bioethics

Numerous ethical challenges are raised by efforts to decellularise organs and tissues and repopulate the three-dimensional scaffolds that remain, inside or outside the body, with functioning cells. The pressure to advance this

	Donor sources	Decellularisation method	Seeded cell type	Source
Trachea[25]	Human donor trachea	DNase and deoxycholate	Autologous mesenchymal stromal cells and epithelial cells	30-year-old woman from Barcelona, Spain (2008)
Tracheal patch[83]	Pig jejunum	Mechanical removal, sodium acid solution, DNase, and desoxycholate	Autologous fibroblasts and muscle cells	58-year-old man from Hanover, Germany (2003)
Bladder[84]	Acellular scaffolds	--	Autologous urothelial and muscle cells	4-19-year-old children from Winston-Salem, NC, USA (2000-05)
Aortic root[85]	Human donor aortic root	Hypotonic solution, acids, and cryopreservation	Unseeded	31-80-year-old patients from Rochester, NY, USA (2002-03)
Heart valve[65]	Human pulmonary heart valve	Trypsin and EDTA	Autologous endothelial progenitor cells	11-13-year-old children from Chisinau, Moldova (2002)
Dermis[87]	Human dermis	Several commercial acellularisation protocols	Mostly unseeded	For example, hernia repair with human acellular dermal matrix after organ transplantation in Baltimore, MD, USA (2000-05)

DNase=deoxyribonuclease. EDTA=ethylenediaminetetraacetic acid.

Table: Clinical application of engineered tissues

technique, driven by demand, the race for prestige, and the potential for huge profits, mandates an early commitment be made to establish the safety of various strategies for decellularisation and recellularisation in the laboratory and in animals. The lesson such ethically challenging pressures exerted on promising techniques such as gene therapy[80] is a stark reminder of the ethical framework that must be in place for bioengineering efforts, particularly when there are so many potential patients and doctors who are desperate for any remedy that offers hope. Investigators working on bioengineering organs need to insist that clinical trials proceed only when sufficient evidence of safety and efficacy exists. The willingness of dying and desperate patients to be involved in innovative organ bioengineering experiments is no substitute for the competency of investigators, and the adequacy of their experimental infrastructure, full independent review of studies, ability to monitor patients, and intent to publish results. Research teams must be prepared to show sufficient experience with transplantation to confidently undertake these efforts. Transparency about the techniques involved, cell sources, financial costs to patients, strategies for dealing with experimental failure, and the ability to assist patients after initial treatment are ethically mandatory. To ensure that conflicts of interest do not arise, investigators with equity or financial interests in new techniques should not be involved directly with testing or assessing success of new treatments.[81]

Furthermore, because of the complexity and enthusiasm associated with efforts to bioengineer organs and complex tissues, institutional review boards and research ethics committees should insist that steps to ensure verified informed consent are in place and that study endpoints, recruitment strategies, plans for dealing with experimental failure, and conflict of interest controls are fully disclosed to potential participants. For clinical trials, due consideration needs to be given to who to recruit: suitable patients should be able to provide competent consent, have some amount of social support, have few comorbidities, and be willing to face a loss of privacy.[82] Once a minimum level of safety has been established, experimental efforts could be extended to children and other groups (table). Perhaps the strongest ethical duty the bioengineering community faces is the identification of criteria that constitute sufficient evidence of the evolution of an intervention from research to therapy. Such decisions should not be left solely to consumers, because they are easily exploited by unscrupulous individuals and groups,[83] or to third-party payers. Establishment of adequate safety and functional success will need input from investigators and key professional societies and organisations.

Conclusions

Use of three-dimensional extracellular matrix scaffolds populated with autologous cells is a promising approach for the replacement of complex tissues and whole organs. Early clinical successes with complex tissues in some individuals and preclinical studies have shown proof of concept. However, key barriers remain, including identification of the optimal cell source for different organs, an effective method for recellularisation of denuded vascular structures in whole-organ scaffolds, and identification of the appropriate population of patients. For these reasons, whole-organ transplantation is the treatment of choice at present. Because positive results have been reported with tissues once thought impossible to reconstruct, such as pancreas, brain, and eyes,[59,60] complex tissues and organs might become therapeutic targets if progress continues.

Contributors

PM devised the topic for systematic review, was lead author of the report, and oversaw the review process. SFB wrote sections of the report. AC and DJW extracted and categorised data for systematic review and helped to write the report and interpret results. All authors assisted with revision of the report.

Conflicts of interest

We declare that we have no conflicts of interest.

Acknowledgments

This review was supported by the Wallenberg Institute for Regenerative Medicine and Karolinska Institutet/SLL grants (Stockholm, Sweden) and grants from the US National Institutes of Health (RC4HL106625) and National Heart, Lung, and Blood Institute (R21HL094611). We thank Eve A Simpson, Philipp Jungebluth, and Silvia Baiguera for their excellent technical assistance with this report.

References

1 Centers for Disease Control and Prevention (CDC). Deaths from chronic obstructive pulmonary disease—United States, 2000–2005. *MMWR Morb Mortal Wkly Rep* 2008; 57: 1229–32.
2 United States Renal Data System (USRDS). Renal disease data 2009. http://www.usrds.org/ (accessed Oct 22, 2010).
3 Heron M, Hoyert DL, Murphy SL, Xu J, Kochanek KD, Tejada-Vera B. Deaths: final data for 2006. *Natl Vital Stat Rep* 2009; 57: 1–134.
4 Shin'oka T, Imai Y, Ikada Y. Transplantation of a tissue-engineered pulmonary artery. *N Engl J Med* 2001; 344: 532–33.
5 Orens JB, Garrity ER Jr. General overview of lung transplantation and review of organ allocation. *Proc Am Thorac Soc* 2009; 6: 13–19.
6 Chen F, Yoo JJ, Atala A. Acellular collagen matrix as a possible "off the shelf" biomaterial for urethral repair. *Urology* 1999; 54: 407–10.
7 Dahl SL, Koh J, Prabhakar V, Niklason LE. Decellularized native and engineered arterial scaffolds for transplantation. *Cell Transplant* 2003; 12: 659–66.
8 Badylak SF. The extracellular matrix as a biologic scaffold material. *Biomaterials* 2007; 28: 3587–93.
9 Barkan D, Green JE, Chambers AF. Extracellular matrix: a gatekeeper in the transition from dormancy to metastatic growth. *Eur J Cancer* 2010; 46: 1181–88.
10 Calve S, Odelberg SJ, Simon HG. A transitional extracellular matrix instructs cell behavior during muscle regeneration. *Dev Biol* 2010; 344: 259–71.
11 Crapo PM, Gilbert TW, Badylak SF. An overview of tissue and whole organ decellularization processes. *Biomaterials* 2011; 32: 3233–43.
12 Roomans GM. Tissue engineering and the use of stem/progenitor cells for airway epithelium repair. *Eur Cell Mater* 2010; 19: 284–99.
13 Takahashi K, Yamanaka S. Induction of pluripotent stem cells from mouse embryonic and adult fibroblast cultures by defined factors. *Cell* 2006; 126: 663–76.
14 Uygun BE, Soto-Gutierrez A, Yagi H, et al. Organ reengineering through development of a transplantable recellularized liver graft using decellularized liver matrix. *Nat Med* 2010; 16: 814–20.
15 Soto-Gutierrez A, Zhang L, Medberry C, et al. A whole-organ regenerative medicine approach for liver replacement. *Tissue Eng Part C Methods* 2011; 17: 677–86.

16 Ott HC, Matthiesen TS, Goh SK, et al. Perfusion-decellularized matrix: using nature's platform to engineer a bioartificial heart. *Nat Med* 2008; 14: 213–21.

17 Ott HC, Clippinger B, Conrad C, et al. Regeneration and orthotopic transplantation of a bioartificial lung. *Nat Med* 2010; 16: 927–33.

18 Petersen TH, Calle EA, Zhao L, et al. Tissue-engineered lungs for in vivo implantation. *Science* 2010; 329: 538–41.

19 Cortiella J, Niles J, Cantu A, et al. Influence of acellular natural lung matrix on murine embryonic stem cell differentiation and tissue formation. *Tissue Eng Part A* 2010; 16: 2565–80.

20 Daly AB, Wallis JM, Borg ZD, et al. Initial binding and recellularization of decellularized mouse lung scaffolds with bone marrow-derived mesenchymal stromal cells. *Tissue Eng Part A* 2012; 18: 1–16.

21 Macchiarini P, Jungebluth P, Go T, et al. Clinical transplantation of a tissue-engineered airway. *Lancet* 2008; 372: 2023–30.

22 Badylak SF, Hoppo T, Nieponice A, Gilbert TW, Davison JM, Jobe BA. Esophageal preservation in five male patients after endoscopic inner-layer circumferential resection in the setting of superficial cancer: a regenerative medicine approach with a biologic scaffold. *Tissue Eng Part A* 2011; 17: 1643–50.

23 Mase VJ Jr, Hsu JR, Wolf SE, et al. Clinical application of an acellular biologic scaffold for surgical repair of a large, traumatic quadriceps femoris muscle defect. *Orthopedics* 2010; 33: 511.

24 Bissell MJ, Hall HG, Parry G. How does the extracellular matrix direct gene expression? *J Theor Biol* 1982; 99: 31–68.

25 Boudreau N, Myers C, Bissell MJ. From laminin to lamin: regulation of tissue-specific gene expression by the ECM. *Trends Cell Biol* 1995; 5: 1–4.

26 Nakayama KH, Batchelder CA, Lee CI, Tarantal AF. Decellularized rhesus monkey kidney as a three-dimensional scaffold for renal tissue engineering. *Tissue Eng Part A* 2010; 16: 2207–16.

27 Murry CE, Keller G. Differentiation of embryonic stem cells to clinically relevant populations: lessons from embryonic development. *Cell* 2008; 132: 661–80.

28 Tottey S, Corselli M, Jeffries EM, Londono R, Peault B, Badylak SF. Extracellular matrix degradation products and low-oxygen conditions enhance the regenerative potential of perivascular stem cells. *Tissue Eng Part A* 2011; 17: 37–44.

29 Agrawal V, Tottey S, Johnson SA, Fruend JM, Siu BF, Badylak SF. Recruitment of progenitor cells by an ECM cryptic peptide in a mouse model of digit amputation. *Tissue Eng Part A* 2011; 17: 2435–43.

30 Valentin JE, Stewart-Akers AM, Gilbert TW, Badylak SF. Macrophage participation in the degradation and remodeling of extracellular matrix scaffolds. *Tissue Eng Part A* 2009; 15: 1687–94.

31 Sellaro TL, Ranade A, Faulk DM, et al. Maintenance of human hepatocyte function in vitro by liver-derived extracellular matrix gels. *Tissue Eng Part A* 2010; 16: 1075–82.

32 Nelson CM, Bissell MJ. Modeling dynamic reciprocity: engineering three-dimensional culture models of breast architecture, function, and neoplastic transformation. *Semin Cancer Biol* 2005; 15: 342–52.

33 Gassmann P, Enns A, Haier J. Role of tumor cell adhesion and migration in organ-specific metastasis formation. *Onkologie* 2004; 27: 577–82.

34 Exposito JY, D'Alessio M, Solursh M, Ramirez F. Sea urchin collagen evolutionarily homologous to vertebrate pro-alpha 2(I) collagen. *J Biol Chem* 1992; 267: 15559–62.

35 Daly K, Stewart-Akers A, Hara H, et al. Effect of the alphaGal epitope on the response to small intestinal submucosa extracellular matrix in a nonhuman primate model. *Tissue Eng Part A* 2009; 15: 3877–88.

36 Ott HC, Matthiesen T, Brechtken J, et al. A novel population of adult derived cardiac progenitor cells is capable of functional myocardial repair. *Circulation* 2005; 112: II-332.

37 Asnaghi MA, Jungebluth P, Raimondi MT, et al. A double-chamber rotating bioreactor for the development of tissue-engineered hollow organs: from concept to clinical trial. *Biomaterials* 2009; 30: 5260–69.

38 Lineen E, Namias N. Biologic dressing in burns. *J Craniofac Surg* 2008; 19: 923–28.

39 Auger FA, Lacroix D, Germain L. Skin substitutes and wound healing. *Skin Pharmacol Physiol* 2009; 22: 94–102.

40 Priya SG, Jungvid H, Kumar A. Skin tissue engineering for tissue repair and regeneration. *Tissue Eng Part B Rev* 2008; 14: 105–18.

41 Draheim KM, Lyle S. Epithelial stem cells. *Methods Mol Biol* 2011; 750: 261–74.

42 Guenou H, Nissan X, Larcher F, et al. Human embryonic stem-cell derivatives for full reconstruction of the pluristratified epidermis: a preclinical study. *Lancet* 2009; 374: 1745–53.

43 Grillo HC. Tracheal replacement: a critical review. *Ann Thorac Surg* 2002; 73: 1995–2004.

44 Laurence J. British boy receives tracheal transplant with his own cells. *BMJ* 2010; 340: c1633.

45 Curcio E, Macchiarini P, De Bartolo L. Oxygen mass transfer in a human tissue-engineered trachea. *Biomaterials* 2010; 31: 5131–36.

46 Gilbert TW, Stewart-Akers AM, Simmons-Byrd A, Badylak SF. Degradation and remodeling of small intestinal submucosa in canine Achilles tendon repair. *J Bone Joint Surg Am* 2007; 89: 621–30.

47 Baiguera S, Del Gaudio C, Jaus M, et al. Long-term changes to in vitro preserved bioengineered human trachea and their implications for decellularized tissues. *Biomaterials* (in press).

48 Baiguera S, Jungebluth P, Burns A, et al. Tissue engineered human tracheas for in vivo implantation. *Biomaterials* 2010; 31: 8931–38.

49 Jungebluth P, Alici E, Baiguera S, et al. Tracheobronchial transplantation with a stem-cell-seeded bioartificial nanocomposite: a proof-of-concept study. *Lancet* 2011; 378: 1997–2004.

50 Omori K, Tada Y, Suzuki T, et al. Clinical application of in situ tissue engineering using a scaffolding technique for reconstruction of the larynx and trachea. *Ann Otol Rhinol Laryngol* 2008; 117: 673–78.

51 Baiguera S, Gonfiotti A, Jaus M, et al. Development of bioengineered human larynx. *Biomaterials* 2011; 32: 4433–42.

52 Cortiella J, Nichols JE, Kojima K, et al. Tissue-engineered lung: an in vivo and in vitro comparison of polyglycolic acid and pluronic F-127 hydrogel/somatic lung progenitor cell constructs to support tissue growth. *Tissue Eng* 2006; 12: 1213–25.

53 Mondrinos MJ, Koutzaki S, Lelkes PI, Finck CM. A tissue-engineered model of fetal distal lung tissue. *Am J Physiol Lung Cell Mol Physiol* 2007; 293: L639–50.

54 Lin YM, Boccaccini AR, Polak JM, Bishop AE, Maquet V. Biocompatibility of poly-DL-lactic acid (PDLLA) for lung tissue engineering. *J Biomater Appl* 2006; 21: 109–18.

55 Choe MM, Sporn PH, Swartz MA. Extracellular matrix remodeling by dynamic strain in a three-dimensional tissue-engineered human airway wall model. *Am J Respir Cell Mol Biol* 2006; 35: 306–13.

56 Liu M, Post M. Invited review: mechanochemical signal transduction in the fetal lung. *J Appl Physiol* 2000; 89: 2078–84.

57 Andrade CF, Wong AP, Waddell TK, Keshavjee S, Liu M. Cell-based tissue engineering for lung regeneration. *Am J Physiol Lung Cell Mol Physiol* 2007; 292: L510–18.

58 Huh D, Matthews BD, Mammoto A, Montoya-Zavala M, Hsin HY, Ingber DE. Reconstituting organ-level lung functions on a chip. *Science* 2010; 328: 1662–68.

59 Antunes MB, Woodworth BA, Bhargave G, et al. Murine nasal septa for respiratory epithelial air-liquid interface cultures. *Biotechniques* 2007; 43: 195–96.

60 Price AP, England KA, Matson AM, Blazar BR, Panoskaltsis-Mortari A. Development of a decellularized lung bioreactor system for bioengineering the lung: the matrix reloaded. *Tissue Eng Part A* 2010; 16: 2581–91.

61 Shigemura N, Okumura M, Mizuno S, et al. Lung tissue engineering technique with adipose stromal cells improves surgical outcome for pulmonary emphysema. *Am J Respir Crit Care Med* 2006; 174: 1199–205.

62 Vracko R. Basal lamina scaffold-anatomy and significance for maintenance of orderly tissue structure. *Am J Pathol* 1974; 77: 314–46.

63 Hoppo T, Komori J, Manohar R, Stolz DB, Lagasse E. Rescue of lethal hepatic failure by hepatized lymph nodes in mice. *Gastroenterology* 2011; 140: 656–66.

64 Meguid El Nahas A, Bello AK. Chronic kidney disease: the global challenge. *Lancet* 2005; 365: 331–40.

65 Morigi M, Introna M, Imberti B, et al. Human bone marrow mesenchymal stem cells accelerate recovery of acute renal injury and prolong survival in mice. *Stem Cells* 2008; 26: 2075–82.

66 Morigi M, Rota C, Montemurro T, et al. Life-sparing effect of human cord blood-mesenchymal stem cells in experimental acute kidney injury. *Stem Cells* 2010; 28: 513–22.

67 Ross EA, Williams MJ, Hamazaki T, et al. Embryonic stem cells proliferate and differentiate when seeded into kidney scaffolds. *J Am Soc Nephrol* 2009; 20: 2338–47.

68 Brown BN, Valentin JE, Stewart-Akers AM, McCabe GP, Badylak SF. Macrophage phenotype and remodeling outcomes in response to biologic scaffolds with and without a cellular component. *Biomaterials* 2009; 30: 1482–91.

69 Valentin JE, Turner NJ, Gilbert TW, Badylak SF. Functional skeletal muscle formation with a biologic scaffold. *Biomaterials* 2010; 31: 7475–84.

70 Agrawal V, Johnson SA, Reing J, et al. Epimorphic regeneration approach to tissue replacement in adult mammals. *Proc Natl Acad Sci USA* 2010; 107: 3351–55.

71 Beattie AJ, Gilbert TW, Guyot JP, Yates AJ, Badylak SF. Chemoattraction of progenitor cells by remodeling extracellular matrix scaffolds. *Tissue Eng Part A* 2009; 15: 1119–25.

72 Borschel GH, Dennis RG, Kuzon WM Jr. Contractile skeletal muscle tissue-engineered on an acellular scaffold. *Plast Reconstr Surg* 2004; 113: 595–602.

73 Nieponice A, Gilbert TW, Badylak SF. Reinforcement of esophageal anastomoses with an extracellular matrix scaffold in a canine model. *Ann Thorac Surg* 2006; 82: 2050–58.

74 Bader A, Schilling T, Teebken OE, et al. Tissue engineering of heart valves—human endothelial cell seeding of detergent acellularized porcine valves. *Eur J Cardiothorac Surg* 1998; 14: 279–84.

75 Hodde JP, Ernst DM, Hiles MC. An investigation of the long-term bioactivity of endogenous growth factor in OASIS wound matrix. *J Wound Care* 2005; 14: 23–25.

76 O'Reilly MS, Boehm T, Shing Y, et al. Endostatin: an endogenous inhibitor of angiogenesis and tumor growth. *Cell* 1997; 88: 277–85.

77 Houghton AM, Grisolano JL, Baumann ML, et al. Macrophage elastase (matrix metalloproteinase-12) suppresses growth of lung metastases. *Cancer Res* 2006; 66: 6149–55.

78 Vlodavsky I, Goldshmidt O, Zcharia E, et al. Mammalian heparanase: involvement in cancer metastasis, angiogenesis and normal development. *Semin Cancer Biol* 2002; 12: 121–29.

79 Roy M, Marchetti D. Cell surface heparan sulfate released by heparanase promotes melanoma cell migration and angiogenesis. *J Cell Biochem* 2009; 106: 200–09.

80 Wilson JM. Medicine. A history lesson for stem cells. *Science* 2009; 324: 727–28.

81 Reynolds TA, Schriger DL, Barrett TW. Empiric antibiotic therapy for sepsis patients: monotherapy with β-lactam or β-lactam plus an aminoglycoside? *Ann Emerg Med* 2008; 52: 561–62.

82 Caplan A. Facing ourselves. *Am J Bioeth* 2004; 4: 18–20.

83 Biancosino C, Zardo P, Walles T, Wildfang I, Macchiarini P, Mertsching H. Generation of a bioartificial fibromuscular tissue with autoregenerative capacities for surgical reconstruction. *Cytotherapy* 2006; 8: 178–83.

84 Atala A, Bauer SB, Soker S, Yoo JJ, Retik AB. Tissue-engineered autologous bladders for patients needing cystoplasty. *Lancet* 2006; 367: 1241–46.

85 Zehr KJ, Yagubyan M, Connolly HM, Nelson SM, Schaff HV. Aortic root replacement with a novel decellularized cryopreserved aortic homograft: postoperative immunoreactivity and early results. *J Thorac Cardiovasc Surg* 2005; 130: 1010–15.

86 Cebotari S, Lichtenberg A, Tudorache I, et al. Clinical application of tissue engineered human heart valves using autologous progenitor cells. *Circulation* 2006; 114 (suppl): I132–37.

87 Brewer MB, Rada EM, Milburn ML, et al. Human acellular dermal matrix for ventral hernia repair reduces morbidity in transplant patients. *Hernia* 2011; 15: 141–45.

88 Caplan A, Levine B. Hope, hype and help: ethically assessing the growing market in stem cell therapies. *Am J Bioeth* 2010; 10: 24–25.

89 Eiraku M, Watanabe K, Matsuo-Takasaki M, et al. Self-organized formation of polarized cortical tissues from ESCs and its active manipulation by extrinsic signals. *Cell Stem Cell* 2008; 3: 519–32.

90 Eiraku M, Takata N, Ishibashi H, et al. Self-organizing optic-cup morphogenesis in three-dimensional culture. *Nature* 2011; 472: 51–56.